FILE COPY

REPORT DOCUMENTATION PAGE

Form Approved
OMB No. 0704-0188

1. AGENCY USE ONLY (Leave blank)	2. REPORT DATE	3. REPORT TYPE AND DATES COVERED
	14 May 1990	Final Report/1 Sep 85-31 Dec 89

4. TITLE AND SUBTITLE
Nonlinear Optical Studies of the Optical and Electronic Properties of Semiconductor Heterostructures

5. FUNDING NUMBERS
61102F/2301/A1

(2)

6. AUTHOR(S)
Duncan G. Steel

AD-A223 408

7. PERFORMING ORGANIZATION NAME(S) AND ADDRESS(ES)
University of Michigan
Depts Electrical Engineering
and Physics
Harrison M. Randall Laboratory of Physics
Ann Arbor MI MI 48109

8. PERFORMING ORGANIZATION REPORT NUMBER
AFOSR-TR- 90 0673

9. SPONSORING/MONITORING AGENCY NAME(S) AND ADDRESS(ES)
AFOSR/NP
Bolling AFB DC 20332-6448

DTIC
ELECTE
JUN 26 1990
S
D

10. SPONSORING/MONITORING AGENCY REPORT NUMBER
AFOSR-85-0280

11. SUPPLEMENTARY NOTES

12a. DISTRIBUTION/AVAILABILITY STATEMENT
Approved for public release; distribution is unlimited.

12b. DISTRIBUTION CODE

13. ABSTRACT (Maximum 200 words)
The following was accomplished. (1) First experimental observation of an interference effect in the nonlinear optical response in GaAs quantum well structures corresponding to a slow component in the nonlinear optical response. The interference effect is evidence that the exciton resonance frequency is shifted in the presence of the electron hole plasma produced by the ionized exciton. (2) Demonstration of frequency domain nonlinear optical spectroscopy methods for the direct measurement of the ambipolar diffusion coefficient and the lectron-hole recombination rate in GaAs quantum well structures. (3) Measure of the response time in strained quantum well structures where the heavy and light hole exciton overlap in energy. (4) Use of precision nonlinear optical spectroscopy methods for the study of phonon induced spectral diffusion of the heavy hole exciton at low temperature in GaAs quantum well structures.

14. SUBJECT TERMS
Nonlinear, Optical, Semiconductor

15. NUMBER OF PAGES
94

16. PRICE CODE

17. SECURITY CLASSIFICATION OF REPORT	18. SECURITY CLASSIFICATION OF THIS PAGE	19. SECURITY CLASSIFICATION OF ABSTRACT	20. LIMITATION OF ABSTRACT
UNCLASSIFIED	UNCLASSIFIED	UNCLASSIFIED	UL SAR

GENERAL INSTRUCTIONS FOR COMPLETING SF 298

The Report Documentation Page (RDP) is used in announcing and cataloging reports. It is important that this information be consistent with the rest of the report, particularly the cover and title page. Instructions for filling in each block of the form follow. It is important to **stay within the lines to meet optical scanning requirements.**

Block 1. Agency Use Only (Leave Blank)

Block 2. Report Date. Full publication date including day, month, and year, if available (e.g. 1 Jan 88). Must cite at least the year.

Block 3. Type of Report and Dates Covered. State whether report is interim, final, etc. If applicable, enter inclusive report dates (e.g. 10 Jun 87 - 30 Jun 88).

Block 4. Title and Subtitle. A title is taken from the part of the report that provides the most meaningful and complete information. When a report is prepared in more than one volume, repeat the primary title, add volume number, and include subtitle for the specific volume. On classified documents enter the title classification in parentheses.

Block 5. Funding Numbers. To include contract and grant numbers; may include program element number(s), project number(s), task number(s), and work unit number(s). Use the following labels:

C	- Contract	**PR**	- Project
G	- Grant	**TA**	- Task
PE	- Program Element	**WU**	- Work Unit Accession No.

Block 6. Author(s). Name(s) of person(s) responsible for writing the report, performing the research, or credited with the content of the report. If editor or compiler, this should follow the name(s).

Block 7. Performing Organization Name(s) and Address(es). Self-explanatory.

Block 8. Performing Organization Report Number. Enter the unique alphanumeric report number(s) assigned by the organization performing the report.

Block 9. Sponsoring/Monitoring Agency Names(s) and Address(es). Self-explanatory.

Block 10. Sponsoring/Monitoring Agency. Report Number. (If known)

Block 11. Supplementary Notes. Enter information not included elsewhere such as: Prepared in cooperation with...; Trans. of ..., To be published in .... When a report is revised, include a statement whether the new report supersedes or supplements the older report.

Block 12a. Distribution/Availablity Statement. Denote public availability or limitation. Cite any availability to the public. Enter additional limitations or special markings in all capitals (e.g. NOFORN, REL, ITAR)

DOD	- See DoDD 5230.24, "Distribution Statements on Technical Documents."
DOE	- See authorities
NASA	- See Handbook NHB 2200.2.
NTIS	- Leave blank.

Block 12b. Distribution Code.

DOD	- DOD - Leave blank
DOE	- DOE - Enter DOE distribution categories from the Standard Distribution for Unclassified Scientific and Technical Reports
NASA	- NASA - Leave blank
NTIS	- NTIS - Leave blank.

Block 13. Abstract. Include a brief (Maximum 200 words) factual summary of the most significant information contained in the report.

Block 14. Subject Terms. Keywords or phrases identifying major subjects in the report.

Block 15. Number of Pages. Enter the total number of pages.

Block 16. Price Code. Enter appropriate price code (NTIS only).

Blocks 17. - 19. Security Classifications. Self-explanatory. Enter U.S. Security Classification in accordance with U.S. Security Regulations (i.e., UNCLASSIFIED). If form contains classified information, stamp classification on the top and bottom of the page.

Block 20. Limitation of Abstract. This block must be completed to assign a limitation to the abstract. Enter either UL (unlimited) or SAR (same as report). An entry in this block is necessary if the abstract is to be limited. If blank, the abstract is assumed to be unlimited.

FINAL REPORT

SUBMITTED TO

THE AIR FORCE OFFICE OF SCIENTIFIC RESEARCH

BY
THE UNIVERISTY OF MICHIGAN
DEPARTMENTS OF ELECTRICAL ENGINEERING AND PHYSICS
HARRISON M. RANDALL LABORATORY OF PHYSICS
ANN ARBOR, MICHIGAN 48109

Duncan G. Steel, Principal Investigator
313-764-4469

Program Title: Nonlinear Optical Studies of the Optical and Electronic Properties of Semiconductor Heterostructures

Grant No.: AFOSR-85-0280

Summary of Recent Results

During the current grant period, experimental work emphasized demonstrating the use of high resolution frequency domain nonlinear laser spectroscopy for the study of materials, particularly semiconductor heterostructures. The work has demonstrated that cw four-wave mixing spectroscopy provides new information regarding the origin of the nonlinear optical response in semiconductor materials as well as new information about structure and relaxation. We have also begun measurements in the time domain using such methods as three pulse photon echoes, transient four-wave mixing, and two wavelength transient absorption in order to obtain additional information as well as to enable comparison between time domain and frequency domain measurements. This report summarizes our experimental and theoretical results obtained in GaAs/AlGaAs quantum well structures and CdSSe doped glasses.

A summary of the current progress shows:

- First experimental observation of an interference effect in the nonlinear optical response in GaAs quantum well structures corresponding to a slow component in the nonlinear optical response. The interference effect is evidence that the exciton resonance frequency is shifted in the presence of the electron hole plasma produced by the ionized exciton.

- Demonstration of frequency domain nonlinear optical spectroscopy methods for the direct measurement of the ambipolar diffusion coefficient and the electron-hole recombination rate in GaAs quantum well structures.

- Measurement of the response time in strained quantum well structures where the heavy and light hole exciton overlap in energy.

- Use of precision nonlinear optical spectroscopy methods for the study of phonon induced spectral diffusion of the heavy hole exciton at low temperature in GaAs quantum well structures.

- Demonstration of a large cw third order susceptibility in CdSSe microcrystallite doped glass.

- Demonstration of a temperature dependent slow component in the optical response of CdSSe microcrystallite doped glass due to the presence of defects. Using precision spectroscopy methods, we determined the activation energy for the trap along with the intensity dependence and the presence of an anomalous energy transport process.

- Demonstration of real time aberration correction through cw optical phase conjugation in CdSSe microcrystallite doped glasses. Demonstration of narrow band, tunable, wide angle field of view filter characteristics.

- Development of an analytical description for the general interpretation of the frequency domain nonlinear optical response in terms of systems which are quantum mechanically opened or closed.

- Use of modified optical Bloch equations to provide an interpretation of the interference profile observed in the four-wave mixing spectrum in GaAs quantum well structures.

- Use of modified optical Bloch equations to simulate the nonlinear optical spectrum obtained in GaAs quantum well structures at low temperature showing phonon assisted spectral diffusion.

For a more complete summary of the important results, please see the attached set of reprints and preprints.

Publication Summary

Journal Publications

H. Wang, M. Jiang, and D.G. Steel, "Measurement of phonon assisted migration of localized excitons in GaAs/AlGaAs multiple quantum well structures," to be submitted to Physical Review. (See attached preprint. Experiments were done on this program but the data was analyzed and the paper was written on the new AFOSR program.)

Hailin Wang, J.T. Remillard, M.D. Webb, D.G. Steel, J. Pamulapati, J. Oh, and P.K. Bhattacharya, "High resolution laser spectroscopy of relaxation and the excitation line shape of excitons in GaAs quantum well structures," Surface Science 228, pp69-73 (1990).

J.T. Remillard, H. Wang, M.D.Webb, D.G. Steel, "Frequency Domain Four-Wave Mixing Spectroscopy of Temperature and Optical Intensity Dependent Relaxation in CdSSe Doped Glass," to be published in J. Opt. Soc. Am. B, 1990.

J.T. Remillard, H. Wang, M.D. Webb, and D.G. Steel, "High Resolution Nonlinear Laser Spectroscopy of Room Temperature GaAs Quantum Well Structures: Observation of Interference Effects," Optics Letters 15, 1133 (1989).

J.T. Remillard, H. Wang, M.D. Webb, D.G. Steel, "Optical Phase Conjugation and Nonlinear Optical Band pass FIlter Characteristics in CdSSe Microcrystallite Doped Glass," IEEE J. Quant. Elec. QE-25, p408 (1989).

J.T. Remillard and D.G. Steel, "Narrow nonlinear optical resonances in CdSSe doped glass," Optics Letters 13, pp30-32 (1988).

D.G. Steel, J. Remillard, Jing Liu, S.C. Rand, "Effects of population pulsations on backward, nearly degenerate four-wave mixing spectroscopy and optical phase conjugation," J. Opt. Soc. Am. B 5. 171 (1988).

Duncan G. Steel and J.T. Remillard, "Resonant nearly degenerate backward four-wave mixing in open and closed systems," Phys. Rev. A 36, pp4330-4337 (1987).

Hailin Wang, J.T. Remillard, M.D. Webb, D.G. Steel, "High Resolution Spectroscopy and Photon Echoes of Excitons in Quantum Well Structures at Low Temperature", invited paper in Laser Spectroscopy IX, 1989.

J.T. Remillard and D.G. Steel, "Nonlinear laser spectroscopy studies of semiconductor materials," invited paper in Laser Spectroscopy VIII , Springer-Verlag, W. Persson and S. Svanberg, eds., pp264-266 (1987).

Conference Presentation with Proceedings

Invited Presentations

D.G. Steel, J.T. Remillard, Hailin Wang, M.D. Webb, J. Oh, J. Pamulapati, and P.K. Bhattacharya, "High Resolution Nonlinear Laser Spectroscopy of GaAs/AlGaAs Multiple Quantum Wells." OSA Topical Meeting on Quantum Wells for Optics and Optoelectronics, OSA Technical Digest 10, pp 62-65, (1989).

D.G. Steel, P.K. Bhattacharya, J.T. Remillard Hailin Wang, M.D. Webb, J. Pamulapati, J. Oh, "High Resolution Nonlinear Laser Spectroscopy of Excitons in GaAs Quantum Well Structures," Quantum Electronics and Laser Science Conference, OSA Technical Digest 12, MBB3 (1989).

D.G. Steel, J.T. Remillard, H. Wang, and M.D. Webb, "Application of 4-wave mixing spectroscopy to semiconductor material studies", Conference on Lasers and Electro-Optics, Technical Digest Series 7, pp260-261 (1988).

Contributed Presentations with Published Proceedings

H. Wang, J.T. Remillard, M.D. Webb, and D.G. Steel, "High Resolution Nonlinear Laser Spectroscopy and Efficient Optical Phase Conjugation in Semiconductor Microcrystallite Doped Glasses," to be published in the Technical Digest, Conference on Lasers and Electrooptics, OSA Technical Digest 11, pp156-157(1989).

H. Wang, J.T. Remillard, D.G. Steel, J. Oh, J. Pamulapati, and P.K. Bhattacharya, "High Resolution Laser Spectroscopy of Relaxation and the Excitation Line Shape of Excitons at Low Temperature in GaAs Quantum Well Structures," in the Proceedings of 4th International Conference on Modulated Semiconductor Structures, 1989. (See earlier citation in Surface Science above)

J.T. Remillard, H. Wang, M.D. Webb, and D.G. Steel, "Frequency domain four-wave mixing spectroscopy in semiconductor quantum wells and microcrystallites," International Conference on Quantum Electronics, Technical Digest, pp278-279, IQEC Tokyo (1988).

J.T. Remillard, J. Liu, and D.G. Steel, "Application of frequency domain 4-wave mixing spectroscopy to semiconductors: studies of semiconductor doped glasses," Proceedings of the International Workshop on High-Speed optical processes and Optoelectronic devices based on compound semiconductors, p F9, The University of Michigan, 1987.

Student Progress Summary

Five students have been supported by this program. Three of them have reached Ph.D. candidacy level. One student received his Ph.D. at the end of winter term, 1990. Two other students will complete their Ph.D. degree by the end of the 1990-1991 academic year. The program involves students from Applied Physics, Electrical Engineering, and Physics.

Resonant nearly degenerate backward four-wave mixing in open and closed systems

Duncan G. Steel and J. T. Remillard
Departments of Physics and Electrical Engineering, Randall Laboratory of Physics, The University of Michigan, Ann Arbor, Michigan 48109
(Received 11 February 1987)

This paper presents perturbation calculations using the density matrix to describe the nearly degenerate four-wave-mixing spectral response in resonant systems subject to state-specific reservoir coupling. The calculations provide physical insight into the origin of narrow resonances observed in recent experimental work in atomic sodium and ultranarrow resonances in crystals. The calculations are for systems which are homogeneously broadened as well as systems which are inhomogeneously broadened due to velocity effects or random crystal fields. The calculations show that it is possible to eliminate the effects of either kind of broadening and measure the decay rate of the dipole coherence as well as the decay rates of both states of the transition. Furthermore, the calculations indicate that the method of cross-correlated optical fields which was used to eliminate the effects of laser jitter in longitudinal relaxation rate measurements could be extended to the measurements of slow dephasing rates in crystals.

INTRODUCTION

The study of line shapes in nearly degenerate backward four-wave mixing (NDFWM) can provide important spectroscopic information about the relaxation of states or coherent superposition states due to reservoir coupling. A common example of this is spontaneous emission due to coupling to the vacuum radiation field. Spontaneous emission causes decay of a state as well as decay of coherence between the states of the radiating transition. There are also other important forms of coupling to a reservoir. In gas-phase systems, examples of reservoir coupling include state-changing, velocity-changing, or phase-interrupting collisions. In solids in addition to spontaneous emission, examples of reservoir coupling include phonon and impurity scattering. Decay of coherence can also be caused by fluctuating fields in a crystal.

Furthermore, NDFWM is of great practical importance. The NDFWM spectral response is related to the reflectivity bandwidth associated with optical phase conjugate mirrors produced in backward four-wave mixing. Such mirrors are of potential importance to real-time aberration correction in optical systems.

This paper describes the spectral response of backward NDFWM in a two-level system in the presence of state-specific reservoir coupling. The NDFWM response is defined as the line shape associated with the signal as a function of frequency of any of the three input beams. A number of line shapes are discussed for different cases of state-specific reservoir coupling. The model provides a simple physical explanation of the origin of collision-induced subnatural narrow resonances in Doppler-broadened gases[1,2] and the ultranarrow resonances in solids[3] observed in earlier experiments. The physics is shown to be similar to the origin of pressure-induced extra resonances in FWM (PIER4) first discussed by Bloembergen[4-8] (see also review by Rothberg[9]) and the narrow spectral holes and antiholes observed in modulation spectroscopy discussed in detail by Boyd.[10-14] These effects arise due to an incomplete cancellation of quantum-mechanical amplitudes.[15-17] We also extend the calculation to include the NDFWM spectral response in a medium inhomogeneously broadened by random crystal fields. We show that in some cases, it is possible to eliminate the effects of both inhomogeneous broadening and laser jitter in the measurement of the effective transverse and longitudinal relaxation rate.

MODEL

Nearly degenerate four-wave mixing is described by a third-order nonlinear optical susceptibility which can be evaluated using third-order perturbation theory and double-sided Feynman diagrams.[18-21] General expressions for all 48 terms of the third-order susceptibility have been given by many authors.[4,22,23] In this calculation, we rederive the third-order nonlinear optical susceptibility for a two-level system for backward NDFWM in order to obtain a physical understanding of the origin of NDFWM spectral profiles. The calculation takes into account spontaneous emission into the ground state along with decays of both states to the reservoir and pure dephasing of the dipole. Because of its generality to multilevel systems and its extension to the treatment of nonexponential decay coupling to the reservoir, we use the density-matrix approach first pioneered by Bloembergen and Shen[24] with a classical description of the radiation fields. While this calculation is based on assuming exponential decays for the different matrix elements, the density-matrix equations are particularly powerful since they can be generalized to a more complete quantum-mechanical transport equation.[25,26]

The specific form of the density-matrix equation is given as[27,28]

$$i\hbar\left[\frac{\partial}{\partial t}+\mathbf{v}\cdot\nabla\right]\rho=[H_0,\rho]+[V,\rho]-\frac{i\hbar}{2}\{\Gamma,\rho\}_+ +i\hbar\frac{d\rho}{dt}\bigg|_{sp}+i\hbar\frac{d\rho}{dt}\bigg|_{ph}+i\hbar\Lambda \quad (1)$$

where the $\mathbf{v}\cdot\nabla$ term accounts for motion and $\mathbf{v}$ is the classical velocity associated with the center of mass, H_0 is the Hamiltonian for the unperturbed system, V is the classical electromagnetic interaction of the form $-\mu\cdot\mathbf{E}$, where $\mathbf{E}=\frac{1}{2}\sum\mathbf{E}_a e^{i\mathbf{k}_a x-i\omega_a t}+\text{c.c.}$ is summed over all electromagnetic fields. Γ is the decay operator; Λ is the source term to account for incoherent pumping. The other two terms, $(d\rho/dt)|_{sp}$ and $(d\rho/dt)|_{ph}$, account for decay into a state due to spontaneous emission from a higher state and decay of coherence due to dephasing, respectively.

Unlike our earlier work, we do not include any source terms from the reservoir. For example, if we are describing a gas-phase system with collisions, the reservoir decay terms account for loss of an atom at velocity v due to a velocity-changing collision. However, we do not allow for the possibility of an atom in a given state at velocity v' to undergo a velocity-changing collision and have its velocity changed to v. This means we will fail to describe such important behavior as collision-induced velocity hole filling.

The polarization is given by $P=\text{Tr}(\mu\rho)$. If the system is a gas, then ρ is a function of velocity, and the polarization must be integrated over the velocity distribution. If the system is a solid and inhomogeneously broadened due to random crystal fields, the $\mathbf{v}\cdot\nabla$ does not contribute to the density-matrix equation, but the polarization must be integrated over the distribution describing the energy levels. This integration is a very important part of the problem and can greatly effect the results and physical interpretation.

To illustrate the physics observed in the experiments, we consider a simple two-level system shown in Fig. 1. The λ_i represent incoherent pumping into level i, and the corresponding operator in the Eq. (1) has the form $\langle i|\Lambda|j\rangle=\lambda_i\delta_{ij}$. The Γ are exponential decays to the reservoir due to spontaneous emission, inelastic collisions, or other nonradiative-type transitions. The operator has the form $\langle i|\Gamma|j\rangle=\gamma_{ij}\delta_{ij}$. Note that these decays contribute to the dephasing of the dipole. This is seen by noting that these terms contribute to the decay of the off-diagonal matrix element, the optical coherence ρ_{12}. In addition to this contribution, to the decay of the dipole coherence, there is additional dephasing. This term in the general equation is given by $\langle i|(\partial\rho/\partial t)|_{ph}|j\rangle=-\gamma_{ph}(1-\delta_{ij})$. This term represents so-called pure dephasing because the physical origin for this term does not contribute to any other decays. (It should be noted that in the earlier work,[1,2] velocity changing collisions and dephasing collisions arise from the same scattering event. Hence, the effects of velocity-changing collisions on the diagonal matrix elements, causing loss or generation of a state in a specific velocity group, and collision-induced dephasing, causing loss of dipole coherence and frequency shift of the resonance, is handled by a single operator. However, physically, the origin of the resonant response does not depend on these details.[29]) Finally, state 2 can decay by spontaneous emission back to 1. This is accounted for by a source term for state 1 given by

$$\left\langle 1\left|\frac{\partial\rho}{\partial t}\right|_{sp}\right|1\right\rangle=\gamma_{sp}\rho_{22}\ .$$

In the rotating-wave approximation (and noting $\rho_{ij}=\rho_{ji}^*$), the equations for the matrix elements become

$$i\hbar\left[\frac{\partial}{\partial t}+\mathbf{v}\cdot\nabla\right]\rho_{11}=[V_{12}\rho_{21}-\text{c.c.}]-i\hbar\gamma_1\rho_{11}+i\hbar\gamma_{sp}\rho_{22}+i\hbar\lambda_1\ , \quad (2)$$

$$i\hbar\left[\frac{\partial}{\partial t}+\mathbf{v}\cdot\nabla\right]\rho_{22}=-[V_{12}\rho_{21}-\text{c.c.}]-i\hbar\gamma_2^T\rho_{22}+i\hbar\lambda_2\ , \quad (3)$$

$$i\hbar\left[\frac{\partial}{\partial t}+\mathbf{v}\cdot\nabla\right]\rho_{12}=-\hbar\omega_0\rho_{12}+[V_{12}\rho_{22}-\rho_{11}V_{12}]-i\hbar\gamma_{ph}^T\rho_{12}\ , \quad (4)$$

where $\gamma_2^T=\gamma_2+\gamma_{sp}$ and $\gamma_{ph}^T=\frac{1}{2}(\gamma_2^T+\gamma_1)+\gamma_{ph}$. For level degeneracies, one must be more careful about correctly including the effects of source terms on coherences between degenerate states and correctly accounting for the vector nature of the interaction term $-\mu\cdot\mathbf{E}$.

Figure 1 also shows the optical beam configuration for backward NDFWM. There are three input fields, designated E_a, where $a=f$, b, or p for forward pump, backward pump, or probe, respectively. The nonlinear optical interaction of interest follows from a third-order nonlinear optical polarization of the form $P^{(3)}=\chi^{(3)}E_fE_bE_p^*$. The phase-matching conditions for the wave vectors result in the signal field, E_s, counterpropagating with respect to the probe beam, provided that the two pump beams are exactly counterpropagating. By energy conservation, if the pump beams are at frequency ω and the probe beam is at frequency

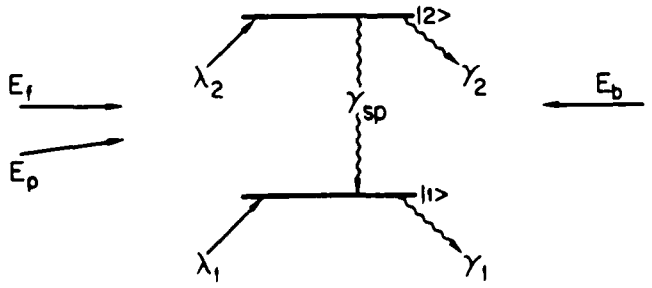

FIG. 1. Energy-level diagram for a general two-level system. For these calculations, the assumed experimental configuration is for backward NDFWM. Figure 1 shows the appropriate arrangement of incoming optical beams.

$\omega_p = \omega + \delta$, then the signal frequency is at $\omega - \delta$.

The equation of motion for the density operator is solved to third order in the electric field. Using Fig. 1, we can associate a simple physical interpretation for the origin of the signal wave. For a simple system such as this (in the absence of two-photon resonances), there are two important contributions to the signal. In the first case, the forward pump and probe interact to form an effective interference pattern which spatially modulates the ground-state and excited-state population. This spatial modulation of the population results in a spatial modulation of the absorption and dispersion. The "grating" spacing is $\lambda/[2\sin(\theta/2)]$, where θ is the angle between the forward pump and probe. If the backward pump is counterpropagating with respect to the forward pump, then it Bragg scatters off the grating in the direction counterpropagating with respect to the incoming probe. The second case is similar, except that the backward pump and probe interfere with a grating space of $\lambda/[2\cos(\theta/2)]$. In this case, the forward pump scatters from the spatially modulated population.

DISCUSSION

Initially, we consider a very simple homogeneously broadened system of two-level atoms with no motion. For a two-level system, we can ignore field polarization effects. The nonlinear polarization for the case of frequency degenerate pump beams at frequency ω, and probe beam at frequency $\omega_p = \omega + \delta$ is given by

$$P^{(3)} = -2N_0 \frac{\mu_{12}}{8} \chi_f \chi_b \chi_p^* e^{-i[(\omega-\delta)t + \vec{k}_p \cdot \vec{r}]} \{(\Delta + i\gamma_{ph}^T)^{-1} + [(-\Delta-\delta) + i\gamma_{ph}^T]^{-1}\}[(-\Delta+\delta) - i\gamma_{ph}^T]^{-1}$$
$$\times \left\{ \left[1 - \frac{\gamma_{sp}}{\gamma_2^T - \gamma_1} \right] (\delta - i\gamma_1)^{-1} + \left[1 + \frac{\gamma_{sp}}{\gamma_2^T - \gamma_1} \right] (\delta - i\gamma_2^T)^{-1} \right\} + \text{c.c.} \quad (5)$$

where Δ is the pump resonance detuning $\Delta = \omega - \omega_0$. χ_a is the Rabi flopping frequency $\mu_{12} E_a / \hbar$ associated with optical field E_a. N_0 is the equilibrium population difference:

$$(\rho_{11} - \rho_{22})_{eq} = \frac{\lambda_1}{\gamma_1} - \frac{\lambda_2}{\gamma_2^T} \left[1 - \frac{\gamma_{sp}}{\gamma_1} \right].$$

In the limit of weak coupling (no pump depletion and no coupling of energy to the probe beam) the field equations decouple and the frequency dependence (as a function of δ) of the signal intensity is obtained by looking at the absolute value squared of the polarization. Equation (5) shows a number of denominators with resonances as a function of δ. In general, there are resonances at $\delta = 0$ and $\pm\Delta$ with widths and amplitudes determined by the various state decays and dephasing.

In the first case, we examine Eq. (5) in the limit that the system is absolutely closed; i.e., $\gamma_1 = \gamma_2 = 0$ and there is no additional dephasing, $\gamma_{ph} = 0$ and $\gamma_{ph}^T = \gamma_{sp}/2$. In this case state $|1\rangle$ is the ground state, and we take $\lambda_1 = \lambda_2 = 0$ and $N_0 = (\rho_{11})_{eq}$. Figure 2(a) shows the NDFWM spectrum as a function of pump-probe detuning, δ. (In this discussion, all parameters are put in dimensionless form by normalizing with respect to the spontaneous emission rate.) There are two resonances. The first occurs when the probe frequency is coincident with the resonant frequency ω_0 at $\delta = -\Delta$. The second at $\delta = \Delta$ corresponds to the signal frequency being resonant with ω_0. The resonances are associated with the dipole coherence and the width of the resonances are determined by γ_{ph}^T. The resonances are expected at these values of δ because they correspond to the frequency of the probe where either the probe resonates with the dipole in absorption, or the signal resonates with the dipole in emission.

The individual time-ordered perturbation sequences are characterized by a resonance at $\delta = 0$ associated with population dynamics (seen in the second-order contribution to the perturbation sequence), though from Fig. 2(a) there is obviously no such resonance. The nonlinear response in the vicinity of $\delta = 0$ is determined in part by the dynamics of both the ground state and the excited state. The dynamics are determined by the rate at which a specific state decays. In this paper, we have restricted the discussion to a simple two-level system and are not considering excited-state or ground-state coherences. Hence, the tuning of δ can be interpreted as a temporal modulation of the populations. We first consider the origin of the resonance for each of the states separately

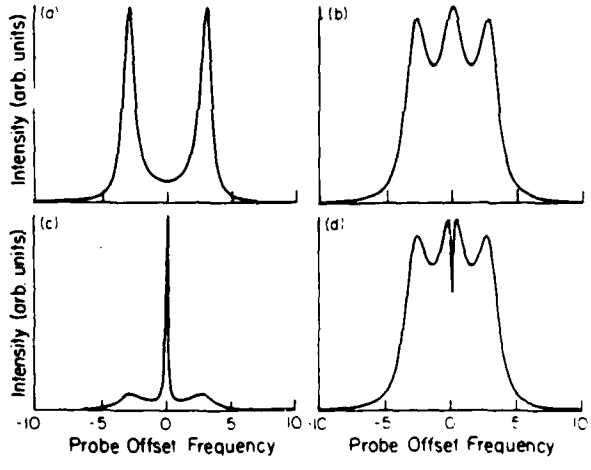

FIG. 2. NDFWM spectrum for $\Delta = 3$ for various decays. All frequencies and decays are normalized to the spontaneous emission rate. (a) The system is closed and there is no additional dephasing ($\gamma_1 = \gamma_2 = \gamma_{ph} = 0$). (b) Same as (a), except additional dephasing has been added, $\gamma_{ph} = 0.5$. (c) $\gamma_1 = 0.1$, $\gamma_2 = 1$, $\gamma_{ph} = 0$. (d) $\gamma_{ph} = 0.5$, $\gamma_1 = 0.1$, and $\gamma_2 = 0.05$. (See text for discussion.)

and then examine why in some cases, the resonance is not observed.

The perturbation of state $|2\rangle$ caused by the optical field exciting atoms from state $|1\rangle$ decays at a rate determined by the total decay rate out of state $|2\rangle$. The perturbation of state $|1\rangle$ caused by the optical field exciting atoms to state $|2\rangle$ decays with a rate determined by the net decay rate of state $|2\rangle$ back down to state $|1\rangle$ due to spontaneous emission (a "filling in" of state $|1\rangle$) plus the decay rate out of state $|1\rangle$. However, for $\gamma_1=\gamma_2$ (for a closed system, population is conserved and $\gamma_1=\gamma_2=0$,) the perturbation of state $|1\rangle$ decays at exactly the same rate as state $|2\rangle$; hence, there is no relaxation of the ground state determined by just γ_1: The resonance width determined by γ_1 is multiplied by an overall factor of zero [determined by $1-\gamma_{sp}/(\gamma_2^T-\gamma_1)$]. For a closed system, this result is physically expected since $\rho_{11}+\rho_{22}=N_0$ for all time (The case for different state decays is discussed below.)

For the excited state, the perturbation of state $|2\rangle$ is described by a resonant denominator with a width determined by the relaxation rate of state $|2\rangle$. The overall multiplier of this factor is not zero $[1+\gamma_{sp}/(\gamma_2^T-\gamma_1)]$. The resonance occurs at second order in the perturbation and is due to the fact that at second order the response of the system is determined by the dynamics of the diagonal matrix elements or population, in this case state $|2\rangle$. To understand, however, why this resonance is not observed under the conditions of Fig. 2(a), we note that formally, the numerator obtained by combining the two terms in the first set of square brackets is $-(\delta-2i\gamma_{ph}^T)$, and for a closed system, with no additional dephasing, $\gamma_{ph}^T=\gamma_{sp}/2$. In addition, $\gamma_2^T=\gamma_{sp}$, and the numerator exactly cancels the resonant denominator, thus accounting for the lack of resonance at $\delta=0$. This represents an interference of two different time-ordered perturbation sequences for the density matrix operator such as the type represented by Gustafson-Yee diagrams.

However, the strength of this interference is reduced in the presence of additional dephasing, γ_{ph}, or nonzero state decays. Hence, in a closed system, a third resonance at $\delta=0$ will be observed in the presence of additional dephasing. This behavior is shown in Fig. 2(b), and can be seen in the original equations of Bloembergen.[4] When these resonances are caused by the presence of pure dephasing, they are called dephasing-induced coherent emission resonances and have been discussed by Andrews and Hochstrasser.[30] However, the above description shows that these resonances can also be caused by state decay as well as "pure dephasing" and as the discussion below will show, the spectral response can be extremely narrow if $\gamma_1 \ll \gamma_2$. Finally, for a closed system in the presence of additional dephasing, the amplitude of the $\delta=0$ resonance is determined by γ_{ph} and the width is determined by the spontaneous emission lifetime.

We now consider the two-level system with state coupling to the reservoir; i.e., γ_1 and γ_2 are nonzero. For small γ_i and for $\gamma_1=\gamma_2$ there is little difference in the NDFWM line shape with Fig. 2(a) except for some slight additional broadening because of the additional dephasing due to the state decay, and some slight filling in around $\delta=0$ due to the fact that the interference between the first-order pump and probe interactions is no longer complete. However, Fig. 2(c) shows the NDFWM response when $\gamma_1<\gamma_2$. A very narrow resonance is observed with a width determined by γ_1. To understand the origin of this behavior, we note that as before, when the decays are equal, the resonant enhancement at $\delta=0$ due to the response of the upper-state dynamics is reduced by the interference between the two dispersive contributions. In addition, the ground-state dynamics are determined by the decay of the excited state back to the ground state in addition to the net decay out of the ground state. Hence, as before, there is no contribution from the dynamics associated with the pure decay of the ground state (the factor multiplying the ground state $\delta=0$ resonance is still zero). However, when $\gamma_1<\gamma_2$, the ground-state perturbation does not decay as fast as the upper state. Hence, there is a residual nonlinear contribution remaining due to the ground state. The dynamics of this nonlinear response is determined by γ_1, and we obtain a resonance at $\delta=0$ with a width given by γ_1. In the case of an experiment where the presence and magnitudes of the state-specific reservoir coupling rates is controllable from zero to some finite value, it would appear to be an extra resonance, of a type similar to PIER4 resonances referenced earlier.

However, when the dephasing is large, the sidebands associated with resonances at $\delta=\pm\Delta$ broaden and disappear altogether, leaving a single Lorentzian profile with a width given by γ_1. In the limit of very large dephasing ($\gamma_{ph} \gg \gamma_1,\gamma_2,\gamma_{sp}$), this response is very similar to the work in Cr: $YAlO_3$.[3] In that work, the model was a three-level system; however, the physical result of decay to a metastable state was to create a long-lived perturbation in the ground state with the ground-state dynamics determined by the decay of the metastable. We see, however, that these interactions are also viewed in terms of temporal modulations of the populations at frequency δ and, hence, are closely related to the population pulsation effects which give rise to spectral holes in the nonlinear absorption spectrum of homogeneously broadened material.[10,12]

In the discussion below, we will generalize the calculation to include the effects of velocity-induced inhomogeneous broadening; however, the physics of linewidth effects of reservoir coupling are not effected by this addition. In the earlier experiment,[1,2] we observed collision-induced line narrowing. For these experiments, we described the observations for $\Delta=0$ because of improved signal-to-noise ratio (the effects were also observed for finite Δ.) For $\Delta=0$, Eq. (5) predicts a single resonance, corresponding to the merging of the two resonances in Fig. 2(a), with the width determined by the spontaneous emission decay rate ($\gamma_1=\gamma_2=0$). In the presence of state-specific decay, however, where $\gamma_1<\gamma_2$, the line narrows to a linewidth given by γ_1 which would have been anticipated from Fig. 2 in the limit $\Delta\rightarrow 0$. (The physical origin of γ_i for these experiments is either velocity-changing or state-changing collisions.) We see from the analysis, however, that this resonance is the result of a

finite contribution from the ground-state dynamics. Hence, though this resonance appears as a narrowing of the spectral response, the physical origin is more correctly understood as arising from a resonance which is observed only in the presence of state specific reservoir coupling. This behavior is similar to the pressure-induced resonances mentioned earlier[4-8] if the physical origin of γ_1 and γ_2 is due to collisions. We note, however, that there is really no fundamental difference between this kind of resonance and the kind of resonance seen in solids such as Cr:$YA1O_3$.

It should be noted that in many experiments, one decay is significant compared to other decays resulting in line shapes which are often nearly Lorentzian. This is not seen in the figures shown because for the sake of illustration, the different decay rates were chosen to be comparable though different. A Lorentzian line shape is unusual for nonlinear spectroscopy signatures in homogeneously broadened systems, but was seen experimentally in the Cr:$YA1O_3$ measurements.[3] This is in contrast to the fully degenerate four-wave mixing response where the spectral profile (in the limit of weak pumps) is given by the cube of a Lorentzian.[31]

Finally, we consider the case where $\gamma_2 < \gamma_1$. In this case, we note that as a result of interference between ground-state and excited-state dynamics it is possible to produce a NDFWM spectra with a dip in the middle as shown in Fig. 2(d). The figure shows a NDFWM spectrum but with $\gamma_1 = 0.1$, $\gamma_2 = 0.05$, and $\gamma_{ph} = 0.5$.

We now consider the case where the atoms are moving, and we must consider Doppler effects and thermal washout described by $\mathbf{v}\cdot\nabla$. In this case, after velocity integration, we find that in the extreme Doppler limit[32] the polarization is given by (assuming a fully collinear geometry and a thermal velocity distribution)

$$P^{(3)} = \frac{N_0}{8ku_0}\mu_{12}\chi_f\chi_b\chi_p^* e^{-i[(\omega-\delta)t+\mathbf{k}_p\cdot\mathbf{r}]}\frac{2i\pi^{1/2}}{\delta-2\Delta-2i(\gamma_{12}+\gamma_{sp}/2+\gamma_{ph})} \times\left[\left[1-\frac{\gamma_{sp}}{\gamma_2^T-\gamma_1}\right]\frac{1}{\delta-i\gamma_1}+\left[1+\frac{\gamma_{sp}}{\gamma_2^T-\gamma_1}\right]\frac{1}{\delta-i\gamma_2^T}\right]+\text{c.c.} \tag{6}$$

In the Doppler limit, we have ignored the interference term between the backward pump and probe (small spacing grating) because this term is extremely small due to washout by thermal motion. In the limit that $\delta = 0$, the back grating effects are discussed very thoroughly by Lam and Abrams.[33] Physically, the thermal motion washout results when the transit time between fringes is small compared to the effective longitudinal relaxation rate. This motion has the effect of lowering the contrast ratio between the fringes that result between the backward pump and probe that spatially modulate the population difference, resulting in a reduced scattering efficiency for the forward pump.

In this case, we have considered the problem where the reservoir coupling may be due to velocity-changing or state-changing collisions. In the limit that we do not consider velocity-changing collisions into the resonant velocity group or consider collision-induced frequency shifts, we find that this equation follows directly from our earlier work.[1] The analytical description in the earlier analysis was more complete; however, the physical implications of state-changing collisions is not as easily seen. To illustrate the behavior, Fig. 3(a) shows the NDFWM spectral response as a function of pump-probe detuning for a system in the Doppler limit when $\gamma_1 = \gamma_2$. When the pump beam is tuned off resonance (with respect to the zero velocity group), we see that two resonances are observed. The first resonance occurs at $\delta = 0$ and has a width determined by the spontaneous emission rate. The second resonance occurs at $\delta = 2\Delta$ and has a width determined by the total dephasing rate. In the absence of state-specific reservoir coupling, these results are similar to those of Yariv and Nilsen.[34] Again, as we examine the polarization, we see that the resonance at $\delta = 0$ has a width given by γ_1 but does not contribute for the same reasons as given above. However, unlike the homogeneously broadened system, even when the system is closed, a resonance occurs at $\delta = 0$.

The physical origin of the two resonances is seen by considering the motion of the holes in velocity space as a function of pump-probe detuning. Figure 4 shows the ground-state velocity distribution assuming the pumps are detuned from resonance by an amount Δ. Assuming the pumps are degenerate, we find that they burn holes in the velocity distribution at velocities given by $\Delta - \mathbf{k}\cdot\mathbf{v} = 0$. Two holes are burned corresponding to velocities Doppler shifted into resonance for the backward and forward pump beams. The probe is detuned and burns a corresponding hole, according to the amount of detuning. If the probe is given by $\omega+\delta$, then by energy conservation, the signal is at frequency $\omega-\delta$. A corresponding hole is burned by the signal, but the signal $\mathbf{k}$

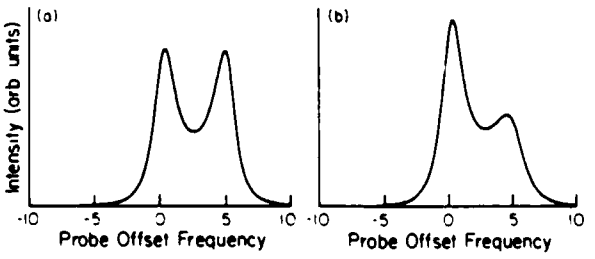

FIG. 3. NDFWM spectrum in a closed system inhomogeneously broadened by velocity effects at $\Delta = 2.5$. (All frequencies and decays normalized to γ_{sp}.) (a) Closed system with $\gamma_1 = \gamma_2 = \gamma_{ph} = 0$. (b) The same conditions as (a) except now $\gamma_{ph} = 0.25$. (See text for discussion.)

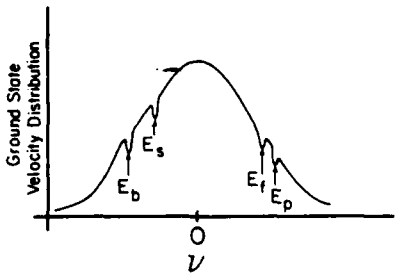

FIG. 4. A schematic of the origin of NDFWM resonances in Doppler-broadened material. This is a plot of the ground-state velocity distribution showing four velocity holes burned by the two frequency degenerate pumps, the probe beam, and the signal.

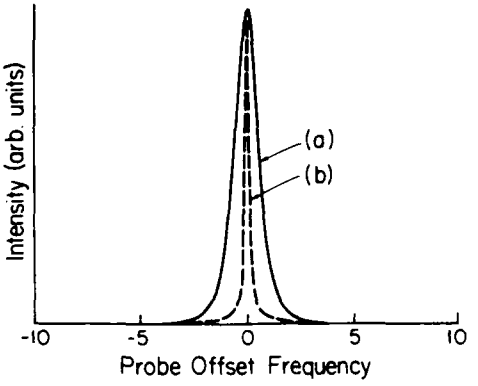

FIG. 5. (a) In order to show the apparent collisional narrowing observed in the atomic sodium experiments which were performed with $\Delta=0$, we show the predicted NDFWM spectrum under these conditions with no state-specific decay. (γ_i took on identical values corresponding to the transit time across the beam. The value is 0.001.) (b) In the presence of velocity or state-changing collisions, the γ_i become different ($\gamma_1=0.1$ and $\gamma_2=1$) resulting an apparent narrowing of the NDFWM spectrum. However, as shown from the analysis, this narrowing is really the appearance of a new resonance with a width due to the ground-state lifetime.

vector is shifted by a minus sign since the signal is propagating backward with respect to the probe (according to the phase-matching conditions). Resonances in the signal will then be observed when holes can be made to overlap. In this case, the probe hole can be adjusted. The two resonances described above are observed to occur when $\delta=0$ and $\delta=2\Delta$. The first corresponds to when the probe hole aligns with forward pump hole and the second corresponds to when the signal hole aligns with the forward pump hole. The remaining resonance at $\delta=-2\Delta$ corresponds to the probe hole aligning with backward pump hole, but is usually not observed inside the Doppler limit because of thermal washout described above. Hence, we see that the origin of the observed resonant structure can be interpreted in terms of velocity hole burning pictures.

We now consider the effect of reservoir coupling. First, as the system begins to experience additional pure dephasing, we see in Fig. 3(b) that, as expected, the second resonance begins to broaden. To examine the case of state specific reservoir coupling we consider the case for $\Delta=0$ (corresponding to experiments[1]). Curve (*a*) in Fig. 5 shows the NDFWM response, again with a width determined by the total dephasing for the case $\gamma_1=\gamma_2\simeq 0$ and $\gamma_{ph}=0$. As the state decay rates increase in the presence of state-specific reservoir coupling (due say to state- or velocity-changing collisions), we see in curve (*b*) the line narrows (for $\gamma_1<\gamma_2$). Nearly identical behavior is observed off resonance ($\Delta\neq 0$) in both the theory and experiment; however, in the experiment, the signal to noise becomes poor due to collision-induced optical pumping. Agreement between theory and experiment is excellent at low pressures. At high pressures this theory becomes inadequate, and it is necessary to correctly account for collisional processes that thermalize the effects of velocity hole burning.[1,17,35]

Finally, we consider NDFWM in material inhomogeneously broadened by random crystal fields. In this case, we simply assume a normal distribution in ω_0 and integrate Eq. (5) over ω_0. In the limit of extreme broadening,[32] the result for the polarization is

$$P^{(3)}=-\frac{N_0}{8W}\mu_{12}\chi_f\chi_b\chi_p^{*}\,e^{-i[(\omega-\delta)t+\vec{k}_p\cdot\vec{r}]}\frac{2i\pi^{1/2}}{-2\delta_{pf}-\delta_{fb}+2i(\gamma_{12}+\gamma_{sp}/2+\gamma_{ph})}$$
$$\times\left\{\left[1-\frac{\gamma_{sp}}{\gamma_2^T-\gamma_1}\right]\left[\frac{1}{\delta_{pf}-i\gamma_1}+\frac{1}{\delta_{pf}+\delta_{fb}-i\gamma_1}\right]\right.$$
$$\left.+\left[1+\frac{\gamma_{sp}}{\gamma_2^T-\gamma_1}\right]\left[\frac{1}{\delta_{pf}-i\gamma_2^T}+\frac{1}{\delta_{pf}+\delta_{fb}-i\gamma_2^T}\right]\right\}+\text{c.c}\,, \tag{7}$$

where W is the inhomogeneous width, and δ_{ij}, is $\omega_i-\omega_j$. In this polarization, we can identify two terms as *fp* [$1/(\delta_{pf}-\gamma_1)$ and $1/(\delta_{pf}-i\gamma_2^T)$] and two terms as *bp* [$1/(\delta_{pf}+\delta_{fb}-i\gamma_1)$ and $1/(\delta_{pf}+\delta_{fb}-i\gamma_2^T)$]. These terms describe the dynamics associated with either the ground state (state 1) or the excited state (state 2) and are associated with linewidths γ_1 or γ_2^T, respectively. The terms identified by *fp* are due to the interaction by the forward pump and probe, and hence are associated with the large spacing grating (in a nearly collinear interaction). The terms identified by *bp* are due to the interaction by the backward pump and probe and hence are associated with the small spacing grating. In the line shape discussions which follow, we do not include contributions from the terms identified by *bp* since these terms are usually small even in solids because of excita-

tion diffusion. Many times, these terms can be further reduced experimentally, however, by rotating the polarization of the backward pump. The magnitude of the backward pump and probe interaction is then determined by the strength of the alignment term which is often small.

For this problem, we notice that there is no dependence on the absolute resonance frequency (except by way of a Gaussian factor with a width determined by W; the broadening is assumed to be large, and the value of the exponential is taken as 1). This is because the strength of the interaction for any given atom is the same for all three input optical fields, independent of the field propagation direction. The only frequency group that has a strong interaction with the optical fields is the group in exact resonance with the fields. Hence there is no dependence on ω_0 except through the overall probability factor which determines how many atoms are in the specific resonance group. These results are similar to those obtained earlier for polarization spectroscopy techniques in condensed phases.[36]

To appreciate the effects of NDFWM in material inhomogeneously broadened by random fields, we first note that in degenerate four-wave mixing, the DFWM response in Doppler-broadened media is Doppler free. The line width as a function Δ (for $\delta=0$) is determined by the natural linewidth. Again, the reason is because it is only for the optical frequency corresponding to resonance for the zero velocity group for which a signal is observed. The equal but opposite Doppler shift for counter propagating beams eliminates the signal when the laser interacts with any other velocity group. This is not the case if the material is inhomogeneously broadened by random fields. The spectral width of DFWM would be determined by the total inhomogeneous width. However, if one of the optical beams is detuned in frequency, while the other beams are held fixed, it becomes possible to measure linewidths associated with fundamental decay processes, rather than a linewidth associated with the inhomogeneous width. In a typical system the probe frequency is detuned with respect to the pumps, then the linewidth is determined by the relaxation rates of states 1 and 2 as shown in Fig. 6(a) ($\delta_{fb}=0$). However, if the backward pump beam is detuned, then the linewidth is given by twice the dipole coherence relaxation rate, as shown in Fig. 6(b) (note the scale change on the x axis.) This kind of spectroscopy is clearly closely related to hole burning spectroscopy.[37] It is interesting to note that these results suggest a very powerful aspect to this kind of spectroscopy. Namely, using correlated fields, it should be possible to eliminate the effects of laser jitter on both transverse and longitudinal relaxation rate measurements. In the earlier work, we demonstrated that the longitudinal relaxation rate was measured as a function of δ_{fp}. Hence, if ω_f and ω_p are correlated (come from the same laser), then they have the same jitter, and δ_{fp} should be free of jitter, as we demonstrated.[3] We see now in the current calculation that the transverse relaxation rate is measured as a function of δ_{bf}, which if we use correlated fields, would also be free of laser jitter. The absence of laser jitter in these measurements is because the nonlinear response is independent of the absolute resonance frequency. Hence, the system does not sense changes in the absolute laser frequency, and it should be possible to measure very long dephasing times without resorting to the development of ultrastable lasers.

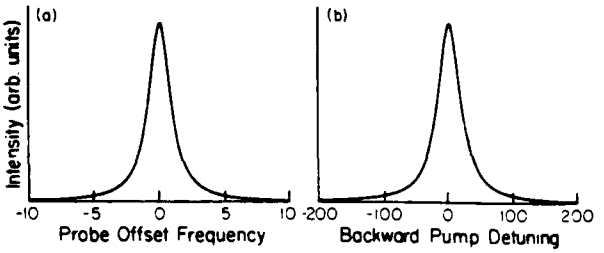

FIG. 6. NDFWM spectrum in a material which is inhomogeneously broadened by random crystal fields. In these curves, γ_{ph} was taken to be 10 times γ_{sp} and $\gamma_1=\gamma_2=0$. In these spectra, it is assumed that the grating formed by the backward pump and probe is small either because of excitation diffusion or because the polarization of the backward pump is rotated giving only a small alignment contribution. (a) The probe beam is scanned showing a width determined by γ_{sp}. (For both of these measurements, we took $\delta_{fb}=0$.) (b) The backward pump beam is scanned, showing a width determined by γ_{ph}.

SUMMARY

This paper describes the physical origin of many line shapes observed in frequency domain NDFWM. While there is considerable interest in using frequency domain four-wave mixing to study state specific reservoir coupling and ultrafast phenomena,[38] it is clear from this analysis that it may become difficult to interpret any given line shape without having considerable detailed information on the system from other experiments.

Note added in proof. Since this paper was first submitted, we have experimentally demonstrated the existence of narrow spikes and dips similar to Fig. 2 in collisionless systems. These narrow features are induced by radiative decay and are present when either population, alignment, or orientation is not conserved. Results for systems that do not conserve population are discussed in Ref. 39. Results and complete theory for systems that conserve population but not alignment and orientation will be discussed elsewhere.[40]

ACKNOWLEDGMENT

This work was supported by U. S. Air Force Office of Scientific Research Grant No. 85 0280.

[1]J. F. Lam, D. G. Steel, and R. A. McFarlane, Phys. Rev. Lett. **49**, 1628 (1982).
[2]J. F. Lam, D. G. Steel, and R. A. McFarlane, Phys. Rev. Lett. **56**, 1679 (1986).
[3]D. G. Steel and S. C. Rand, Phys. Rev. Lett. **55**, 2285 (1985).
[4]N. Bloembergen, H. Lotem, and R. T. Lynch, Indian J. Pure Appl. Phys. **16**, 151 (1978).
[5]N. Bloembergen, A. R. Bogdan, and M. W. Downer, in *Laser*

Spectroscopy V, edited by A. R. W. McKellar, T. Oka, and B. P. Stoicheff (Springer-Verlag, Berlin, 1981), p. 157.

[6]Y. Prior, A. R. Bogdan, M. Dagenais, and N. Bloembergen, Phys. Rev. Lett. **46**, 111 (1981).

[7]A. R. Bogdan, Y. Prior, and N. Bloembergen, Opt. Lett., **6**, 82 (1981).

[8]A. R. Bogdan, M. W. Downer, and N. Bloembergen, Opt. Lett., **6**, 348 (1981).

[9]L. Rothberg, in *Progress in Optics*, edited by E. Wolf (Elsevier Scientific, Amsterdam, 1987), pp. 39–101.

[10]L. W. Hillman, R. W. Boyd, J. Krasinski, and C. R. Stroud, Jr., Opt. Commun. **45**, 416 (1983).

[11]M. S. Malcuit, R. W. Boyd, L. W. Hillman, J. Krasinski, and C. R. Stroud, Jr., J. Opt. Soc. Am. B **1**, 73 (1984).

[12]R. W. Boyd and S. Mukamel, Phys. Rev. A **29**, 1973 (1984).

[13]M. A. Kramer, R. W. Boyd, L. W. Hillman, and C. R. Stroud, Jr., J. Opt. Soc. Am. B **2**, 1444 (1985).

[14]M. A. Kramer, W. R. Tompkin, and R. W. Boyd, Phys. Rev. A **34**, 2026 (1986).

[15]N. Bloembergen, in *Laser Spectroscopy IV*, edited by H. Walther and K. W. Rother (Springer-Verlag, New York, 1979), p. 340.

[16]G. Grynberg, J. Phys. B **14**, 2089 (1981).

[17]P. R. Berman, G. Khitrova, and J. F. Lam, in Proceedings of the Seventh International Conference on Spectral Line Shapes, Aussois, France, 1984 (unpublished).

[18]C. J. Borde, C. R. Acad. Sci. Ser. B **282**, 341 (1976).

[19]S. Y. Yee and T. K. Gustafson, Phys. Rev. A **18**, 1597 (1978).

[20]S. A. J. Druet and J. P. E. Taran, in *Progress in Quantum Electronics*, edited by T. S. Moss and S. Stenholm (Pergamon, Oxford, 1981), Vol. 7, No. 1, pp. 1–72.

[21]J. G. Fujimoto and T. K. Yee, IEEE J. Quantum Electron. **QE-19**, 861 (1983).

[22]S. A. J. Druet, B. Attal, T. K. Gustafson, and J. P. Taran, Phys. Rev. A **18**, 1529 (1978).

[23]J. L. Oudar and Y. R. Shen, Phys. Rev. A **22**, 1141 (1980).

[24]N. Bloembergen and Y. R. Shen, Phys. Rev. A **37**, 433 (1964). See also S. Stenholm, Phys. Rep. **43**, 151 (1978), and M. Sargent III, *ibid.* **43**, 223 (1978).

[25]P. R. Berman, in *New Trends in Atomic Physics, Les Houches, Session 38, 1982*, edited by G. Grynberg and R. Stora (North-Holland, Amsterdam, 1984), p. 451. This reference discusses gas-phase systems.

[26]P. R. Berman, J. Opt. Soc. Am. B **3**, 573 (1986). This reference discusses relaxation due to fluctuating fields in a solid or a gas.

[27]P. R. Berman, Phys. Rev. A **5**, 927 (1972).

[28]P. R. Berman, J. Opt. Soc. Am. B **3**, 562 (1986).

[29]To more accurately account for collisions, a general collision term is added to the right-hand side of the equation. In the optical region of the spectrum, collisions change the velocity and cause a broadening and shift of the resonance. The general description used in our earlier work was of the form: *for populations*

$$\left.\frac{d\rho_{ii}(\mathbf{r},\mathbf{v},t)}{dt}\right|_{\text{collision}} = -\Gamma_i\rho_{ii}(\mathbf{r},\mathbf{v},t) + \int_{-\infty}^{\infty} d\mathbf{v}' W_i(\mathbf{v}'\rightarrow\mathbf{v})\rho_{ii}(\mathbf{r},\mathbf{v}',t) ,$$

where W_i is the collision kernel for state i and

$$\Gamma_i = \int d\mathbf{v}' W_i(\mathbf{v}'\rightarrow\mathbf{v}) ,$$

and *for coherences*

$$\left.\frac{d\rho_{ij}(\mathbf{r},\mathbf{v},t)}{dt}\right|_{\text{collisions}} = -(\Gamma_{ij}+i\sigma_{ij})\rho_{ij}(\mathbf{r},\mathbf{v},t) .$$

For understanding the physical origins of the spectral response of NDFWM, including the above formalism helps to quantify agreement. Such behavior was discussed in the earlier work, and much more extensively, by G. Kitrova and P. Berman at the International Quantum Electronics Conference, San Francisco, 1986 (unpublished). However, the basic effect is to give rise to an apparent state specific reservoir coupling which, except for details of the frequency shift, and the velocity changing collision kernel, closely resembles the above discussion. It should be noted that one important difference between the current calculation and the more correct calculation for collision effects has been pointed out by Berman and Kitrova. Namely, that as the pressure increases, the magnitude of the γ's increase and the narrow resonance produced in the figures begins to broaden, without bound. However, when the correct collisional formulation is included, the linewidth is observed to broaden only to the natural linewidth. Physically, this appears to be due to the fact that at high pressure the system appears to be described by identical reservoir coupling for the excited state and the ground state.

[30]J. R. Andrews and R. M. Hochstrasser, Chem. Phys. Lett. **83**, 427 (1987).

[31]R. L. Abrams and R. C. Lind, Opt. Lett. **2**, 94 (1978); **3**, 205 (1978).

[32]The plasma dispersion functions that result from velocity or frequency integrals are approximated as $Z(a+ib)=i\sqrt{\pi}$ for $b>0$ in the limit for small argument. For $b>0$, the plasma dispersion function is defined as

$$Z(a+ib)=(\pi)^{-1/2}\int_{-\infty}^{\infty} dx \frac{\exp(-x^2)}{[x-(a+ib)]}$$

and

$$(\pi)^{-1/2}\int_{-\infty}^{\infty} dx \frac{\exp(-x^2)}{[x-(a-ib)]} = -Z(-a+ib) .$$

[33]J. F. Lam and R. L. Abrams, Phys. Rev. A **26**, 147 (1982).

[34]J. Nilsen and A. Yariv, J. Opt. Soc. Am. **71**, 180 (1981).

[35]G. Khitrova, PhD thesis, New York University, 1986.

[36]J. J. Song, J. H. Lee, and M. D. Levenson, Phys. Rev. A **17**, 1439 (1978).

[37]See, for example, L. E. Erickson, Phys. Rev. B **16**, 4731 (1977); R. M. McFarlane, R. M. Shelby, and D. P. Burum, Opt. Lett. **6**, 593 (1981), and references therein.

[38]See, for example, R. J. Trebino, C. E. Barker, and A. E. Siegman, IEEE Quantum Electron. **QE-22**, 1413 (1986), and included references.

[39]J. Liu, J. T. Remillard, and D. G. Steel, Phys. Rev. Lett. **59**, 779 (1987).

[40]P. R. Berman, D. G. Steel, G. Khitrova, and J. Liu (unpublished).

Reprinted from Optics Letters, Vol. 13, page 30, January 1988.

Narrow nonlinear-optical resonances in CdSSe-doped glass

J. T. Remillard and D. G. Steel

Harrison M. Randall Physics Laboratory, Departments of Physics and Electrical Engineering, The University of Michigan, Ann Arbor, Michigan 48109

Received May 12, 1987; accepted September 24, 1987

We describe frequency-domain spectroscopy studies of glasses doped with $CdS_{1-x}Se_x$ using low-power cw tunable dye lasers. The results show a narrow resonance (4.4 kHz at room temperature) in the backward nearly degenerate four-wave mixing spectrum, which we believe is determined by the phonon-mediated inverse lifetime of a deep level trap involved in the nonlinear response.

Semiconductor-doped glasses have been studied lately by numerous groups because of their large third-order nonlinear-optical susceptibility. Their properties are important to Q switches,[1] degenerate four-wave mixing (DFWM) and optical phase conjugation,[2–4] and optical bistability.[5] In addition, there is strong evidence that the semiconductor microcrystallites form by aggregation during the heating process of manufacture and that these microcrystallites have a size distribution of the order of 5 nm, which may make them interesting quantum-mechanical structures.[6–9]

A number of laboratories have begun experiments to characterize these materials in terms of their nonlinear response and the relevant relaxation times. Using pulsed lasers, Olbright and Peyghambarian[10] have measured n_2 by using a Twyman–Green interferometer. Olbright *et al.*[11] followed this work with an alternative approach based on pulsed-laser pump-induced changes in the absorption spectrum. The accompanying theory suggests that the nonlinearity arises because of band filling and screening. Similar results are obtained by Roussignol *et al.*[12] However, it is interesting to note that many of the groups are reporting different values for relaxation rates. Jain and Lind[2] reported grating relaxation times in DFWM shorter than 8 nsec, while Yao *et al.*[3] measured grating decay times of the order of 30 psec with a slow 9-nsec tail. In earlier work, using a short-pulse laser, Roussignol *et al.*[4] measured slow grating decay times of several tens of nanoseconds, and Danielzik *et al.*[13] measured relaxation times of the order of 2 nsec in a nonlinear Fabry–Perot configuration. In the more recent work,[12] Roussignol *et al.* ascribe some of the variations to aging effects in the glass filters to exposure to optical radiation. However, it is interesting to note that Cotter[14] and Nuss *et al.*[15] have reported decay times that are intensity dependent.

Here we describe nonlinear-optical measurements made based on four-wave mixing that show that at room temperature at low intensity the relaxation rate associated with the grating decay time is of the order of 72 μsec. The results show the lack of excitation diffusion, implying the potential for a large field of view for applications to optical phase conjugation, real-time holography, and tunable filters.

We used a standard backward four-wave mixing configuration for studying the DFWM and nearly degenerate four-wave mixing (NDFWM) response in Schott optical filter OG590, which is doped with $CdS_{1-x}Se_x$, where x is estimated to be 0.2. In these experiments, the probe frequency could be varied by using the method of cross-correlated optical fields[16] for measurements of bandwidths small compared with the laser jitter. A second tunable dye laser was used to measure the bandwidth associated with tuning of one of the pump frequencies. Phase-sensitive detection was used to facilitate low-pump-power measurements. Usually the forward pump beam was chopped.

First we measured the optical phase-conjugate reflectivity (defined as the ratio of the signal power to incident probe power) as a function of pump power. Figure 1 shows the data taken at $\lambda = 589$ nm, where the nonlinear response was large. For a weak nonlinear response, the reflectivity has a square-law dependence on the pump intensity.[17] The solid line has an $n = 2$ slope. From this line was can extract the nonlinear susceptibility since the reflectivity is given by $R = [(2\pi\omega/cn)\chi^{(3)}]^2(8\pi/cn)^2L^2I_fI_b$. At this wavelength, we infer that $\chi^{(3)} \approx 10^{-7}$ (esu) for $L = 0.3$ cm. (No local field corrections are included.)

A comparison of the DFWM response as a function of wavelength was made and compared with the absorption coefficient, as shown in the inset in Fig. 1. As expected, the nonlinear response decreases at short wavelength owing to an increase in pump absorption. At long wavelength, the nonlinear response decreases owing to reduction of the optical coupling.

To measure the grating relaxation rate, we measured the NDFWM relaxation rate using the method of cross-correlated optical fields to eliminate the effects of laser jitter. We measured the linewidth at low intensity (< 500 mW/cm^2) as shown in Fig. 2. Fitting a Lorentzian curve to the data, we infer a FWHM linewidth of 4400 kHz. We obtained the same linewidth independently of the pump intensity (below 5 W/cm^2). Furthermore, the linewidth is indepen-

0146-9592/88/010030-03$2.00/0

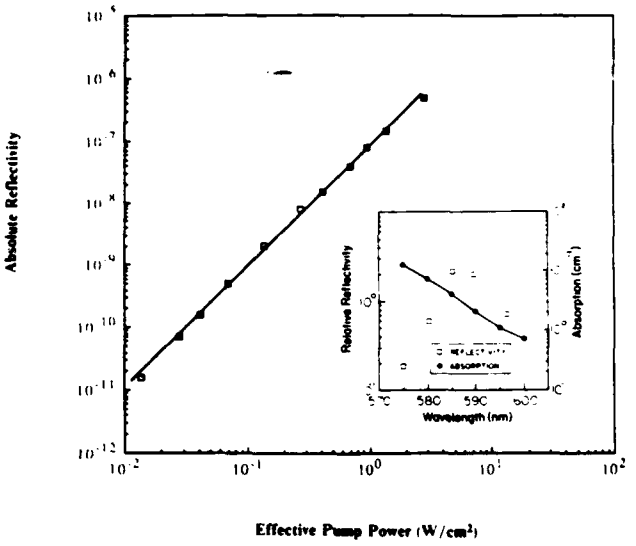

Fig. 1. The FWM reflectivity measured as a function of pump intensity. The straight line has a logarithmic slope of 2. The inset shows DFWM reflectivity as a function of wavelength at a constant pump intensity. The open points represent the absorption spectrum of the filter.

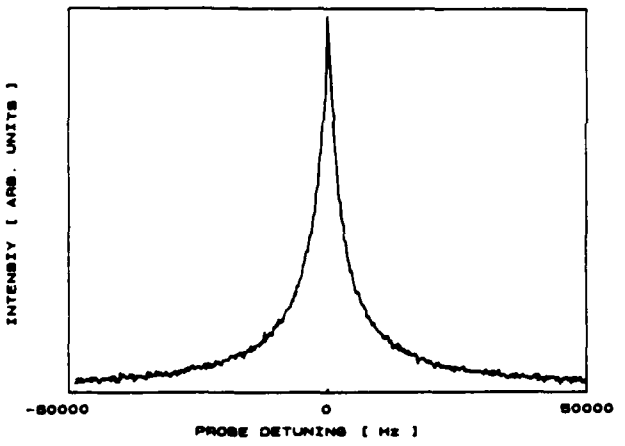

Fig. 2. The NDFWM spectrum observed at low pump intensity.

dent of the angle between the pump and probe, which shows that there is no excitation diffusion on this time scale.[18]

Finally, using a second dye laser, we examined the dependence of the nonlinear response on the frequency detuning of the backward pump. For simple two-level resonant systems, this bandwidth of the detuning would be associated with either the longitudinal or the transverse relaxation rate. However, in our measurements we determined that the nonlinear response was independent of the backward pump detuning as the laser was tuned into the red (limited by the laser to 620 nm). As we tuned the pump into the green ($\lambda < 590$ nm), the nonlinear response began to decrease, owing to absorption of the backward pump. We conclude from this that it is unlikely that the scattering of the backward pump beam is due to any resonant behavior.

Based on the above measurements, we believe that the large nonlinear response is due to the filling of deep level traps by the decay of the electron–hole excitation produced by the forward pump and probe. Figure 3 shows the energy-level diagram believed to model the interaction measured in our experiments. As indicated above, for the case of a copolarized forward pump and probe and a cross-polarized backward pump, the production of the electron–hole pair is proportional to the product of the field amplitudes ($\xi_f \xi_p^*$ + c.c.), resulting in a spatial modulation associated with the pair. The forward pump and probe are near resonance with the valence band-to-conduction band transition with energy difference $E_c - E_V$, as shown in the figure. As a result of the decay to the traps, the filled traps are also spatially modulated.

The signal results from a scattering of the backward pump off the resultant absorption and dispersion grating produced by the spatially modulated traps. The backward pump beam interacts with the traps through a dipole between the traps and a state in the continuum with energy E_c^*. This interaction is strong as long as the photon energy exceeds the photoionization energy of the trap. Earlier evidence of such traps has been reported.[12,19]

We take the nonlinear response to be due to trap filling and note that trap lifetimes are usually long compared with other state relaxation times. Figure 3 shows that the trap decays directly to the ground state, most likely by emitting a photon. If the trap decay is characterized by an effective net decay rate, γ_{TP}, the inverse NDFWM bandwidth provides the lifetime of the trap. To understand this, we note that the spatial modulation term, $\xi_f \xi_p^*$, has an exponential phase dependence given by $i(\omega_f - \omega_p)t - i(\mathbf{k}_f - \mathbf{k}_p)\mathbf{x}$. Hence

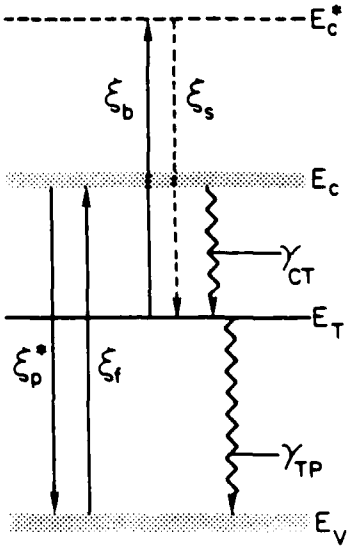

Fig. 3. Energy-level diagram associated with the NDFWM response. The decay rate associated with conduction-band excitation γ_{CV}, is not shown in this figure.

the trap excitation is temporally modulated at a rate $\delta = \omega_f - \omega_p$ as the interference fringes move through the medium. When $\delta < \gamma_{TP}$, the traps can follow the modulation. However, when $\delta > \gamma_{TP}$, the fringes wash out, lowering the scattering efficiency of the back pump.

In a simple rate-equation approximation using perturbation theory and ignoring coherences associated with band-to-band transitions (justified by the ultrafast dephasing time of this transition[20]) and saturation effects associated with trap filling or trap deexcitation by photoionization, the nonlinear polarization for backward NDFWM is given by

$$P^{(3)}_{NDFWM} = \frac{c}{16\pi}\frac{\alpha_0(\omega)}{\hbar\omega}\tilde{\chi}_T(\omega)\xi_f\xi_b\xi_p^* \times \exp[-i\mathbf{k}_p\,\mathbf{x} - i(\omega-\delta)t] \times \frac{1}{(i\delta + \gamma_{CV} + \gamma_{CT})}\frac{\gamma_{CT}}{(i\delta + \gamma_{TP})} + \text{c.c.},$$

where α_0 is the small-signal absorption coefficient for a transition between the valence band and the conduction band, $\tilde{\chi}_T$ is the linear susceptibility associated with a filled trap, γ_{CV} is the decay rate from the conduction band to the valence band, and γ_{CT} is the decay rate from the conduction band to the trap. In the limit that the decay rate from the conduction band is large compared with the decay from the trap, we see that the decay rate of the nonlinear response is dominated by the inverse trap lifetime, γ_{TP}. We see that the predicted NDFWM spectral response is Lorentzian [the signal is proportional to $|P^{(3)}|^2$] with a width determined by the inverse trap lifetime. (At very low intensity a NDFWM spectrum, such as that shown in Fig. 2, shows a non-Lorentzian behavior. The peak is sharper than expected for a Lorentzian and is thought to be the result of the presence of a distribution of trap lifetimes associated with different traps. At higher power, the curve broadens owing to photoionization of the trap, and the sharp peak vanishes.)

These experiments clearly present observations that are quite distinct from the earlier results obtained using pulsed dye lasers. The relaxation time reported in this Letter is considerably longer than that reported earlier. There are at least two possible reasons for this behavior. The first is that, on the time scale of the earlier measurements, the traps did not have time to fill. That is to say, the decay time from the conduction band to the traps is long compared with the measurement times. The other possibility is that, when high-power pulsed lasers are used, the traps completely fill, saturating this part of the nonlinear-optical response. Indeed, there is some evidence for the latter explanation in the recent work of Cotter.[14]

Such long-lived traps suggest that the trap lifetime is determined by a phonon-mediated process. Indeed, we have made preliminary measurements of temperature effects and have found that as we cool the material the NFDWM linewidth reduces considerably, implying an increased trap lifetime and reduced phonon-induced relaxation. Initial measurements of both the susceptibility and the relaxation rate show an exponential dependence on the inverse temperature, as expected for thermal deexcitation of the trap. The activation energy is estimated to be at least 93 MeV. However, the long lifetime suggests that these traps may be associated with the glass–semiconductor interface.

The authors gratefully acknowledge helpful discussion with Roberto Merlin, S. R. Hartmann, and Jasprit Singh. This research was supported by U.S. Air Force Office of Scientific Research grant 85-0280.

References

1. G. Bret and F. Gires, Appl. Phys. Lett. **4**, 175 (1964).
2. R. K. Jain and R. C. Lind, J. Opt. Soc. Am. **73**, 647 (1983).
3. S. S. Yao, C. Karaguleff, A. Gabel, R. Fortenbuery, C. T. Seaton, and G. Stegeman, Appl. Phys. Lett. **46**, 801 (1985).
4. P. Roussignol, D. Ricard, K. C. Rustagi, and C. Flytzanis, Opt. Comm.. **55**, 1431 (1985).
5. H. Gibbs, *Optical Bistability, Controlling Light with Light* (Academic, Orlando, Fla., 1985).
6. J. Warnock and D. D. Awscholom, Phys. Rev. B **52**, 5529 (1985).
7. A. I. Ekimov, A. L. Efros, and A. A. Onushchenka, Solid State Commun. **56**, 921 (1985).
8. L. Banyai and S. W. Kock, Phys. Rev. Lett. **57**, 2722 (1987).
9. N. F. Borrelli, D. W. Hall, H. J. Holland, and D. W. Smith, Jr., Appl. Phys. **61**, 5399 (1987).
10. G. R. Olbright and N. Peyghambarian, Appl. Phys. Lett. **48**, 1184 (1986).
11. G. R. Olbright, N. Peyghamarian, S. W. Koch, and L. Banyi, Solid State Commun. (to be published).
12. P. Roussignol, D. Rocard, J. Lukasik, and C. Flytzanis, J. Opt. Soc. Am. B **4**, 5 (1987).
13. B. Danielzik, K. Nattermann, and D. von der Linde, Appl. Phys. B **38**, 31 (1985).
14. D. Cotter, in *Digest of Fourteenth International Quantum Electronic Conference* (Optical Society of America, Washington, D.C., 1986), PD19-1.
15. M. C. Nuss, W. Zinch, and W. Kaiser, Appl Phys. Lett. **49**, 1717 (1986).
16. D. G. Steel and S. C. Rand, Phys. Rev. Lett. **55**, 2285 (1985).
17. A. Yariv and D. M. Pepper, Opt. Lett. **1**, 18 (1986).
18. For discussion of grating diffusion, see, for example, R. K. Jain and M. B. Klein, Appl. Phys. Lett. **35**, 454 (1979).
19. V. K. Mathur, P. S. Mak, and C. H. Lee, J. Appl. Phys. **51**, 4889 (1980).
20. S. R. Hartmann and F. Moshary, Department of Physics, Columbia University, New York, New York 10027 (personal communication of 60-fsec coherence relaxation rates in these glasses).

Reprinted from Journal of the Optical Society of America B, Vol. 5, page 171, January 1988

Effects of population pulsations on backward, nearly degenerate four-wave mixing spectroscopy and optical phase conjugation

D. G. Steel, J. Remillard, and Jing Liu

Department of Physics, Randall Laboratories, University of Michigan, Ann Arbor, Michigan 48109

S. C. Rand*

Hughes Research Laboratories, 3011 Malibu Canyon Road, Malibu, California 90265

Received June 5, 1987; accepted September 21, 1987

We discuss the effects of population pulsations on the spectral response of backward nearly degenerate four-wave mixing (NDFWM). We include the effects of state-specific decay and spontaneous emission on both two-level and inverted-V-type three-level systems. We compare the results with experiments in both the gas phase and the condensed phase that show ultranarrow resonances. In addition, we examine the response in the presence of strong pump fields. We show that in a simple two-level system, the NDFWM response results in an ac-Stark splitting of the spectral response, whereas in a simple three-level system with decay to a metastable state, a single narrow resonance is observed, which broadens in the presence of strong pumps.

1. INTRODUCTION

Consider an atom initially in level 1 in a optical electric field, $E = \mathcal{E} \exp[i(\mathbf{k}\cdot\mathbf{x} - \omega t)]$, of frequency ω nearly resonant with the transition at frequency ω_0 between level 1 and an excited state, level 2. The probability of the atom's being found in level 2 is proportional to EE^*. If E is not monochromatic, but is instead a sum of monochromatic fields, $E = \sum_i \mathcal{E}_i \exp[i(\mathbf{k}_i\mathbf{x} - \omega_i t)]$, then a typical population term is proportional to the real part of $\mathcal{E}_i\mathcal{E}_j^* \exp[i(\mathbf{k}_i - \mathbf{k}_j)\cdot\mathbf{x} - i\delta_{ij}t]$, where $\delta_{ij} = \omega_i - \omega_j$. For $i \neq j$, we then see in the rate-equation approximation that the population oscillates in time at frequency δ_{ij}.

Using the density-matrix description, such population pulsation effects in laser systems were first described by Lamb[1] as they pertained to multimode operation in lasers. The first observation of these effects appears to have been in a saturable absorber.[2] The first analysis of these effects outside a laser cavity was by Schwarz and Tan.[3] These effects were later examined for application to laser spectroscopy because the strength of the pulsation as a function of δ_{ij} was determined by relaxation rates associated with the eigenstates of the transition.[4] The results showed that, even in homogeneously broadened media, a hole could be observed in the absorption spectrum of a probe beam as a function of frequency in the presence of a saturating pump beam.

The first frequency-domain measurement of the hole was made using modulation spectroscopy in Cr:Al_2O_3 (Ref. 5) and was followed by additional experiments in alexandrite[6] and fluorescein,[7] along with extensive theoretical analysis pertaining to the basis of modulation spectroscopy.[8,9] In these experiments, a laser beam is resonant with a homogeneously broadened system. The optical beam is amplitude modulated at frequency δ, and the attenuation of the modulated signal is measured using phase-sensitive detection.

The physical origin of the response in modulation spectroscopy can be understood by considering the amplitude-modulated beam to be the sum of a central component, E_0, at frequency ω and two sidebands, $E_\pm$, at frequency $\omega \pm \delta$. When δ is large compared with the population-difference relaxation rate, T_1, the sidebands interact with the medium independently of the central component. The population terms that result between the interference of the central component and one of the sidebands oscillate at a frequency δ that is large compared with $1/T_1$. Hence the population difference cannot respond to this interference. However, for small δ, the population can respond to interference of the form $E_0E_\pm^* + E_0^*E_\pm$. The central component can then scatter from this population difference to give an induced polarization of the form $\beta_1 E_0 E_\pm^* E_0 + \beta_2|E_0|^2E_\pm$, where the terms oscillate at frequency $\omega \mp \delta$ and $\omega \pm \delta$, respectively. Both terms contribute energy to the corresponding sideband, resulting in an increased amplitude modulation and an apparent reduction in the attenuation of the modulated beam at low frequency. This effect is shown dramatically in Ref. 5. From this discussion, the detected response in modulation spectroscopy can be seen to be the result of a third-order nonlinear optical polarization and, hence, can be considered a form of forward four-wave mixing.

While the above work was being performed, there was also extensive work in the area of resonant backward degenerate four-wave mixing (DFWM) with particular interest in applications to laser spectroscopy and optical phase conjugation (OPC).[10] In OPC by DFWM, a probe beam interacts in a nonlinear material with two counterpropagating pump beams to produce a signal wave that is phase conjugate to the incoming probe wave. For a weak response, the signal is the

0740-3224/88/010171-09$02.00

result of an induced third-order nonlinear optical polarization. The input frequencies of the three input beams are the same (degenerate). The direction of propagation of the signal is determined by phase-matching conditions and is counterpropagating with respect to the probe beam. In resonant DFWM, the forward pump and probe beam interact to spatially modulate the population difference. This spatial modulation or hole burning produces a spatial modulation of absorption and dispersion. The result is similar to a volume hologram. The backward pump beam is counterpropagating with respect to the forward pump and scatters from this spatial modulation producing the signal wave. A spatial modulation of the absorption and dispersion also results because of the interaction between the backward pump and probe. The forward pump beam scatters from this modulation, producing an additional contribution to the signal.

To determine the relative pump–probe frequency-detuning bandwidth for applications to OPC in which the optical source for the pump beams might be different from the optical source for the probe beam, the nearly degenerate four-wave mixing (NDFWM) response is important. In this case, as the frequency of the probe beam is detuned from the pump beam, the interference fringes formed by the forward pump (backward pump) move through the medium in time, producing a traveling-wave-type excitation. The population difference becomes temporally modulated (as well as spatially modulated, as before). The temporal modulation is at a frequency $\delta = \omega_{\text{probe}} - \omega_{\text{pump}}$. In the limit of large dephasing (the total dephasing rate, $\gamma_{ph}T$, is large compared with all state relaxation rates, such as spontaneous emission), effects of coherences can be ignored, and the rate-equation approximation can be used. The signal strength as a function of δ is a maximum at $\delta = 0$ and falls off (as a Lorentzian) as δ becomes comparable with the population-difference-relaxation rate. Hence, in contrast to the work of modulation spectroscopy in which a hole is observed in a probe absorption spectrum, NDFWM produces a resonant emission in the response. In both cases, the width of the spectral feature can be narrower than the natural linewidth determined by dephasing. In some cases, the width of the spectral response can be narrower than the width associated with the spontaneous emission rate.

In Section 2 we will see that this simple explanation becomes much more complicated in the presence of state-specific reservoir coupling. Furthermore, for a closed or nearly closed quantum system, the effects of coherence become important and can result in interference effects that eliminate the observation of the central pump–probe detuning resonance at $\delta = 0$ associated with population pulsations.

Perturbation theory is adequate to describe the four-wave mixing interaction when the fields are weak. However, for efficient performance of a phase-conjugate mirror, pump intensities well in excess of the saturation intensity are required.[11] For a simple two-level system, this effect corresponds to having a Rabi flopping frequency, $\chi = \mu E/\hbar$, much larger than the natural linewidth determined by the total dephasing rate, $\gamma_{ph}T$. A large Rabi flopping frequency results in an apparent splitting of the atomic transition, called the ac-Stark effect. This effect is accompanied by a three-peaked fluorescence spectrum in resonant scattering.[12] This effect also leads to a splitting of the NDFWM response into a central peak along with two symmetric sidebands shifted by the Rabi flopping frequency[13–15] and necessitates a theoretical approach that accounts for the effect of the strong pumps on the energy levels. However, when optical pumping effects are present, as they can be in multilevel systems, four-wave mixing sidebands disappear and are replaced by a simple broadening of the NDFWM response that is *linear* in the pump intensity, as shown in Section 2.

2. DISCUSSION

A. Stationary Two-Level Atoms below Saturation

In the limit of low intensities, the third-order nonlinear optical susceptibility describing NDFWM can be evaluated using third-order perturbation theory. The experimental geometry is schematically shown in Fig. 1(a) (see Refs. 15 and 16 for a detailed discussion of the experimental setup) and consists of two counterpropagating pump beams designated $\mathbf{E}_f(\omega_f, \mathbf{k}_f)$ and $\mathbf{E}_b(\omega_b, \mathbf{k}_b)$ and a probe beam $\mathbf{E}_p(\omega_p, \mathbf{k}_p)$. For optical phase-conjugation experiments, we usually take $\omega_f = \omega_b = \omega$, $\mathbf{k}_f = -\mathbf{k}_b$, and $\omega_p = \omega + \delta$. The signal wave, $\mathbf{E}_s(\omega_s, \mathbf{k}_s)$, is then usually counterpropagating with respect to the probe beam with $\omega_s = \omega - \delta$. In this section, we examine the third-order nonlinear optical susceptibility for a two-level system for backward NDFWM to understand the NDFWM spectral profiles. The calculation considers spontaneous emission into the ground state along with decays of both states to the reservoir and pure dephasing of the dipole. Figure 1(b) shows the energy-level diagram. These calculations will deviate from expectations based on the traditional optical Bloch-vector formulation because we account for the specific decay of each state, which can lead to the noncancellation of quantum-mechanical amplitudes. The results will

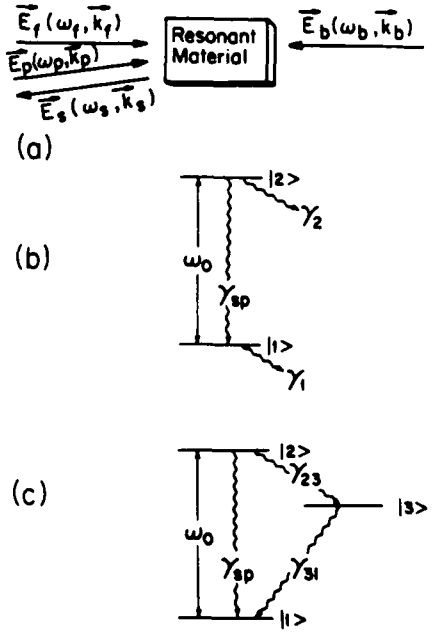

Fig. 1. (a) Geometry for backward four-wave mixing. (b) Two-level model with spontaneous emission and decay to the reservoir. (c) Closed three-level model. The input optical radiation interacts only with the transition between level 1 and level 2. Level 3 is assumed to be metastable with respect to transitions to the ground state.

also deviate from a rate-equation approach since we allow for the effects of interference between coherences induced by the different beams. We then extend the analysis to the simple three-level system shown in Fig. 1(c) and show how the theory for a two-level system anticipates the physics in the three-level system.

In this work, we perform a semiclassical calculation using classical fields and the equation of motion for the quantum-mechanical density-matrix operator presented by Bloembergen and Shen.[17] This calculation is based on a simple model for reservoir coupling, but the density-matrix description is convenient because a much more complete theory for reservoir coupling can be included.[18]

The specific form of the density-matrix equation is given as[19,20]

$$i\hbar\left(\frac{\partial}{\partial t}+\mathbf{v}\cdot\nabla\right)\rho=[H_0,\rho]+[V,\rho]-\frac{i\hbar}{2}[\Gamma,\rho]_+ + i\hbar\left.\frac{d\rho}{dt}\right|_{sp}-i\hbar\left.\frac{d\rho}{dt}\right|_{ph}+i\hbar\Lambda, \quad (1)$$

where the $\mathbf{v}\cdot\nabla$ term accounts for motion and $\mathbf{v}$ is the classical velocity associated with the center of mass, H_0 is the Hamiltonian for the unperturbed system, V is the classical electromagnetic interaction of the form $-\mu\cdot\mathbf{E}$, where $\mathbf{E}=(1/2)\sum\mathbf{E}_a\exp(i\mathbf{k}_a\cdot\mathbf{x}-i\omega_a t)+\text{c.c.}$ is summed over all electromagnetic fields. Γ is the decay operator that represents decay of any state to the reservoir. Terms of the form $-(i\hbar/2)[\Gamma,\rho]_+$ represent decay of a specific state due, for example, to spontaneous emission. Another example is the effect of a velocity-changing collision in a Doppler-broadened system where the atom is Doppler shifted out of resonance after the collision. Λ is the source term to account for incoherent pumping. The terms $d\rho/dt|_{sp}$ and $d\rho/dt|_{ph}$ account for decay into a state because of spontaneous emission from a higher state and decay of coherence due to dephasing, respectively.

Unlike in our earlier work,[21,22] we do not include any source terms from the reservoir, such as velocity-changing collisions that shift a velocity group into resonance. Thus we will fail to describe such important behavior as collision-induced velocity hole filling and Dicke narrowing. However, at low buffer-gas pressures, the present description is quite adequate to permit an understanding of the experimental observations.

The polarization is given by $P=\text{Tr}(\mu\rho)$. If the system is a gas, then ρ is a function of velocity, and the polarization must be integrated over the velocity distribution. If the system is a solid and is inhomogeneously broadened due to random crystal fields, the $\mathbf{v}\cdot\nabla$ does not contribute to the density-matrix equation, but the polarization must be integrated over the frequency distribution of energy levels.

To illustrate the physics observed in the experiments, we consider the two-level system shown in Fig. 1(b). The λ_i represent incoherent pumping into level i, and the corresponding operator in Eq. (1) has the form $\langle i|\Lambda|j\rangle=\lambda_i\delta_{ij}$. The Γ are exponential decays to the reservoir due to spontaneous emission, inelastic collisions, or other types of transitions. The operator has the form $\langle i|\Gamma|j\rangle=\gamma_{ij}\delta_{ij}$. Note that these decays contribute to the decay of the induced optical coherence, ρ_{12}. In addition, some dephasing caused by interactions with the reservoir does not cause transitions and is included in the general equation by setting $\langle 1|\partial\rho/\partial t|_{ph}|2\rangle=\gamma_{ph}\rho_{12}$. This term represents so-called pure dephasing because the physical origin for this term does not contribute to any other decays. Finally, state 2 can decay by spontaneous emission back to state 1. This decay is accounted for by a source term for state 1 given by $\langle 1|\partial\rho/\partial t|_{sp}|1\rangle=\gamma_{sp}\rho_{22}$. In the rotating-wave approximation (and noting that $\rho_{ij}=\rho_{ji}^*$), the equations for the matrix elements become

$$i\hbar\left(\frac{\partial}{\partial t}+\mathbf{v}\cdot\nabla\right)\rho_{11}=(V_{12}\rho_{21}-\text{c.c.})-i\hbar\gamma_1\rho_{11}+i\hbar\gamma_{sp}\rho_{22}+i\hbar\lambda_1, \quad (2)$$

$$i\hbar\left(\frac{\partial}{\partial t}+\mathbf{v}\cdot\nabla\right)\rho_{22}=-(V_{12}\rho_{21}-\text{c.c.})-i\hbar\gamma_2{}^T\rho_{22}+i\hbar\lambda_2, \quad (3)$$

$$i\hbar\left(\frac{\partial}{\partial t}+\mathbf{v}\cdot\nabla\right)\rho_{12}=-\hbar\omega_0\rho_{12}+(V_{12}\rho_{22}-\rho_{11}V_{12})-i\hbar\gamma_{ph}{}^T\rho_{12}, \quad (4)$$

where $\gamma_2{}^T=\gamma_2+\gamma_{sp}$ and $\gamma_{ph}{}^T=1/2(\gamma_2{}^T+\gamma_1)+\gamma_{ph}$. These equations are easily extended to multilevel-type systems, and multiple-photon effects (e.g., two-photon resonances) and level degeneracies are easily incorporated. For level degeneracies, the effects of source terms on coherences between degenerate states must be included, and the vector nature of the interaction term, $-\mu\cdot\mathbf{E}$, must be accounted for correctly.

The four-wave mixing interaction of interest here arises from a third-order nonlinear optical polarization of the form $P^{(3)}=\chi^{(3)}E_fE_bE_p^*$. The phase-matching condition for the wave vectors results in the signal field, E_s, propagating counter to the probe beam, provided that the two pump beams are exactly counterpropagating and have the same frequency. If the pump beams are at frequency ω and the probe beam is at frequency $\omega_p=\omega+\delta$, then the signal frequency is at $\omega-\delta$. The equation of motion for the density operator is solved to third order in the electric field. Furthermore, in the limit that the interaction is weak ($|E_s/E_i|^2\ll 1$, $i=f,b,p$), then the signal intensity is simply proportional to $[P^{(3)}]^2$.

To understand the physics, we first consider a simple homogeneously broadened system of two-level atoms with no motion. For a two-level system, we can ignore field-polarization effects. The nonlinear polarization for the case of frequency-degenerate pump beams at frequency ω and probe beam at frequency ω_p is given by

$$\begin{aligned}P^{(3)}=&-2N_0\frac{\mu_{12}}{8}\chi_f\chi_b\chi_p{}^*\exp[i(\mathbf{k}_f+\mathbf{k}_b-\mathbf{k}_p)\cdot\mathbf{x}-i(\omega-\delta)t]\\&\times\{(\Delta+i\gamma_{ph}{}^T)^{-1}+[(-\Delta-\delta)+i\gamma_{ph}{}^T]^{-1}\}\\&\times[(-\Delta+\delta)-i\gamma_{ph}{}^T]^{-1}\left[\left(1-\frac{\gamma_{sp}}{\gamma_2{}^T-\gamma_1}\right)(\delta-i\gamma_1)^{-1}\right.\\&\left.+\left(1+\frac{\gamma_{sp}}{\gamma_2{}^T-\gamma_1}\right)(\delta-i\gamma_2{}^T)^{-1}\right]+\text{c.c.},\end{aligned} \quad (5)$$

where Δ is the pump resonance detuning $\Delta=\omega-\omega_0$, χ_a is the Rabi flopping frequency ($\mu_{12}E_a/\hbar$) associated with optical field E_a, and N_0 is the equilibrium population difference:

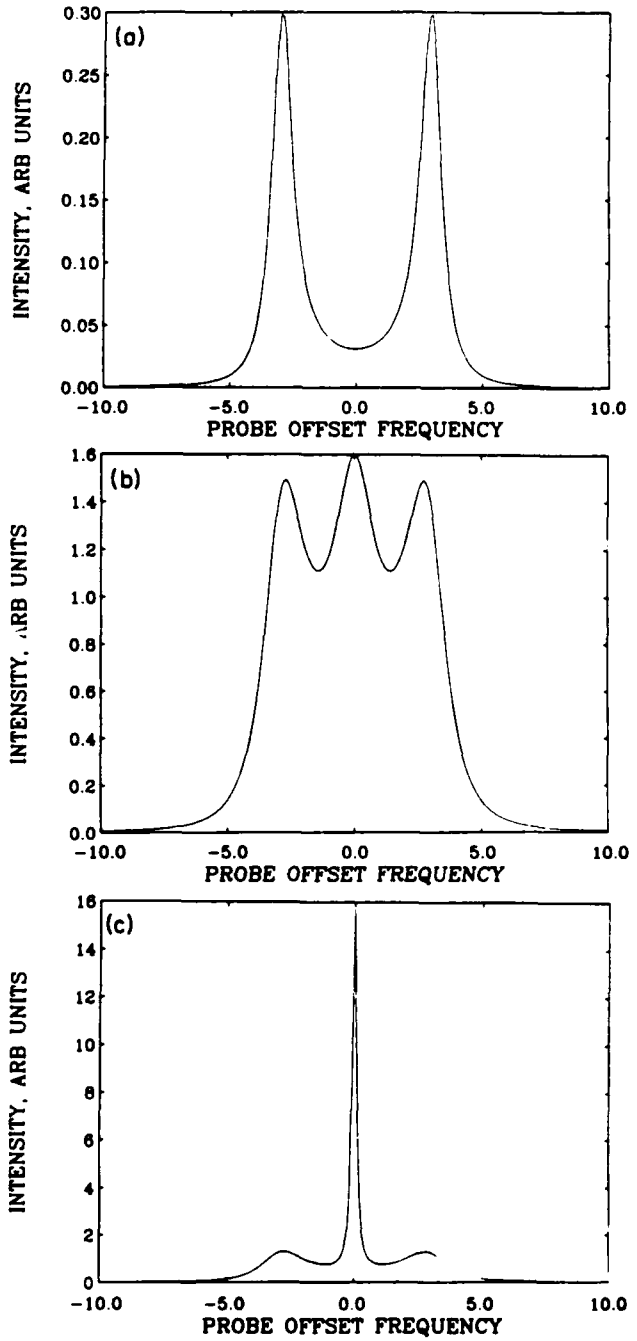

Fig. 2. (a) NDFWM spectrum for a completely closed system of stationary atoms with no additional dephasing. Interference effects eliminate the resonance at $\delta = 0$. (b) In the presence of additional dephasing, the interference is no longer complete, and a resonance at $\delta = 0$ is observed. (c) Both states decay to the reservoir, but $\gamma_1 < \gamma_2$. The narrow resonance has a width given by γ_1. (All frequencies are normalized to the spontaneous emission rate.)

$$N_0 = (\rho_{11} - \rho_{22})_{eq} = \frac{\lambda_1}{\gamma_1} - \frac{\lambda_2}{\gamma_2{}^T}\left(1 - \frac{\gamma_{sp}}{\gamma_1}\right). \tag{6}$$

Equation (5) shows a number of denominators with resonances as a function of δ. In general there are resonances at $\delta = 0$ and $\pm\Delta$ with widths and amplitudes determined by the various state decays and dephasing.

In the limit that the system is absolutely closed (i.e., $\gamma_1 = \gamma_2 = 0$ and the total population is conserved) and there is no additional dephasing ($\gamma_{ph} = 0$ and $\gamma_{ph}{}^T = \gamma_{sp}/2$), then state $|1\rangle$ is the ground state, and we take $\lambda_1 = \lambda_2 = 0$ and $N_0 = (\rho_{11})_{eq}$. Figure 2(a) shows the NDFWM spectrum as a function of pump–probe detuning, δ. (In this discussion, all parameters are put in dimensionless form by normalizing with respect to the spontaneous emission rate.) There are two resonances. The first resonance corresponds to the case when the probe frequency is coincident with the resonant frequency ω_0 at $\delta = -\Delta$ and represents the strong interaction that occurs when the input probe beam resonates with the dipole. The second resonance occurs when the signal frequency is coincident with the resonant frequency at $\delta = \Delta$. This second resonance is expected because it is the result of a dipole array's reradiating a wave at the natural frequency, ω_0. The resonances are associated with the dipole coherence, and the width of the resonances is determined by $\gamma_{ph}{}^T$.

The individual time-ordered perturbation sequences are characterized by a resonance at $\delta = 0$ associated with population dynamics (seen in the second-order contribution to the perturbation sequence), although Fig. 2(a) shows no such resonance. (This resonance does appear in a rate-equation approximation.) However, the resonance is not observed because of interference effects between two different coherent excitations of the populations. These interference effects completely eliminate contributions to the signal from population modulations. More precisely, this resonance is not observed because of an interference of two different time-ordered perturbation sequences for the density-matrix operator such as the type represented by Gustafson–Yee diagrams.[23] However, in the case when additional dephasing is present, the interference is no longer complete, and a central resonance, due to population modulation, is observed [see Fig. 2(b)]. The width of this resonance is determined by the relaxation rates associated with the populations. We note that in the past this resonance has been called a dephasing-induced coherence.[24] The basic behavior is included in the original work of Bloembergen *et al.*[25] However, the calculations show that this resonance would also be observed if γ_1 and γ_2 were nonzero, even if $\gamma_{ph} = 0$.

To consider the origin of the width of this resonance in more detail, the nonlinear response in the vicinity of $\delta = 0$ is determined by the dynamics of both the ground state and the excited state. The dynamics are determined by the rate at which a specific state decays. The perturbation of state $|2\rangle$ decays at a rate determined by the total decay rate out of state $|2\rangle$. However, for $\gamma_1 = \gamma_2$ the perturbation of state $|1\rangle$ decays with a rate determined by the net decay rate of state $|2\rangle$ back down to state $|1\rangle$ because of spontaneous emission (a filling in of state $|1\rangle$) plus the decay rate out of state $|1\rangle$, the perturbation of state $|1\rangle$ decays at exactly the same rate as state $|2\rangle$; hence there is no relaxation of the ground state determined by just γ_1, and the overall linewidth is determined by $\gamma_2{}^T = \gamma_{sp} + \gamma_2$. The resonance whose width is determined by γ_1 is multiplied by an overall factor of zero [determined by $1 - [\gamma_{sp}/(\gamma_2{}^T - \gamma_1)]$].

However, if there is state-specific reservoir coupling and γ_1 and γ_2 are not equal and not zero, then the spectral response may be greatly modified. In particular, if $\gamma_1 < \gamma_2$, then the decay of the ground-state perturbation by a filling in from the excited state is incomplete and is not offset by the ground-state decay to the reservoir, as it was earlier. In

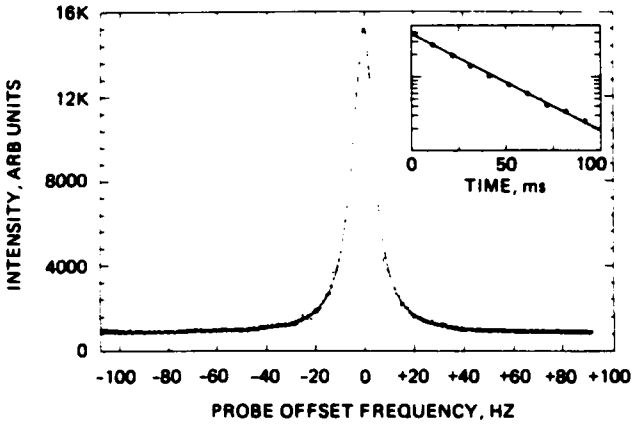

Fig. 3. NDFWM response in Cr:$YAlO_3$. The linewidth is 9.8 Hz. The inset is the fluorescence decay from the metastable state. The decay rate is 34 msec, in very good agreement with the ground-state lifetime inferred from the NDFWM linewidth.

this case, we expect to see a residual perturbation from the ground state with a width determined by γ_1. This result is shown in Fig. 2(c). When the presence and magnitudes of the state-specific reservoir coupling rates are able to be controlled experimentally from zero to some finite value, it could appear to be an extra resonance of a type similar to PIER4 resonances[26-29] in forward four-wave mixing or a narrowing of the response obtained in NDFWM when $\gamma_1 = \gamma_2$.[21,22] The calculations show that in fact the narrow response is the result of a *finite* contribution of an existing resonance.

When the dephasing is large, the sidebands associated with resonances at $\delta = \pm\Delta$ broaden and disappear altogether, leaving a single Lorentzian profile with a width given by γ_1. We see, however, that these interactions are also viewed in terms of temporal modulations of the populations at frequency δ and hence are closely related to the population pulsation effects that give rise to spectral holes in the nonlinear absorption spectrum of homogeneously broadened material just discussed.

B. Stationary Three-Level Atoms below Saturation

Now consider the NDFWM response of the three-level system in Fig. 1(c). The fields are resonant with the transition between the ground state and level 2. This system is closed, although the upper state of the optical excitation can decay to level 3, which may be metastable with respect to transitions to the ground state. If we consider the decay, due to optical excitation, of the excited-state perturbation (level 2), we note that it decays at the rate $\gamma_{sp} + \gamma_{23}$. However, the ground-state perturbation decays by a filling in by spontaneous emission from level 2 and a long-lived decay from level 3. If we take γ_{31} to be small compared with other decays, we expect to observe a NDFWM spectral response whose width is determined by the ground-state lifetime, γ_{31} (also the lifetime of the metastable).

This response is calculated by slightly modifying Eq. (1) and accounting for the equation of motion for ρ_{33}. Equation (2) is modified by adding a term $+\gamma_{31}\rho_{33}$ to the left-hand side. In Eq. (3), $\gamma_2{}^T = \gamma_{sp} + \gamma_{23}$. For a solid, we ignore the velocity effects. For ρ_{33}, we have $\dot{\rho}_{33} = \gamma_{23}\rho_{22} - \gamma_{31}\rho_{33}$. Because the system is closed, we take $\lambda_i = 0$ and note that probability is conserved in this system: $\rho_{11} + \rho_{22} + \rho_{33} = N_0$. For this system, the polarization is given by[16]

$$P^{(3)} = -2N_0 \frac{\mu_{12}}{8} \chi_f \chi_b \chi_p{}^* \exp[i(\mathbf{k}_f + \mathbf{k}_b - \mathbf{k}_p)\cdot\mathbf{x} - i(\omega - \delta)t]$$
$$\times \left[\frac{1}{\delta - i\gamma_2{}^T} + \frac{1}{\gamma_2{}^T - \gamma_{31}}\left(\frac{\gamma_{23}}{\delta - i\gamma_{31}} + \frac{\gamma_{sp} - \gamma_{31}}{\delta - i\gamma_2{}^T}\right)\right]$$
$$\times \left[\frac{1}{(-\Delta + \delta) - i\gamma_{ph}{}^T}\left(\frac{1}{\Delta + i\gamma_{ph}{}^T} - \frac{1}{(\Delta + \delta) - i\gamma_{ph}{}^T}\right)\right]$$
$$+ \text{c.c.} \tag{7}$$

We see in the limit that γ_{31} is much less than the other decays and that the response is dominated by the resonant denominator $\delta + i\gamma_{31}$, as we anticipated. Using the method of cross-correlated fields to eliminate the effects of laser jitter, we measured the NDFWM response in Cr:$YAlO_3$.[16] Figure 3 shows the measurement with a width of 9.8 Hz (γ_{31}/π). The solid line is a least-squares fit of a Lorentzian curve showing excellent agreement with the analysis. The inset shows the measured decay of the fluorescence from the metastable state. The decay is exponential with a decay time ($\gamma_{31}{}^{-1}$) of 34 msec, in good agreement with the NDFWM measurement.

C. Doppler-Broadened Two-Level Atoms below Saturation

We now consider the case in which the atoms are moving and we must consider Doppler effects and thermal washout described by $\mathbf{v}\cdot\nabla$. In this case, after velocity integration, we find that in the extreme Doppler limit[30] the polarization is given by (assuming a fully collinear geometry and a thermal-velocity distribution)

$$P^{(3)} = \frac{N_0}{8ku_0} \mu_{12}\chi_f\chi_b\chi_p{}^* \exp[-i[(\omega - \delta)t + \mathbf{k}_p\cdot\mathbf{x}]]$$
$$\times \frac{2i\pi^{1/2}}{\delta - 2\Delta - 2i(\gamma_{12} + \gamma_{sp}/2 + \gamma_{ph})}$$
$$\times \left[\left(1 + \frac{\gamma_{sp}}{\gamma_1 - \gamma_2 - \gamma_{sp}}\right)\frac{1}{\delta - i\gamma_1} + \left(1 - \frac{\gamma_{sp}}{\gamma_1 - \gamma_2 - \gamma_{sp}}\right)\right.$$
$$\left. \times \frac{1}{\delta - i(\gamma_2 + \gamma_{sp})}\right] + \text{c.c.} \tag{8}$$

In the Doppler limit, we have ignored the interference term between the backward pump and probe (small spacing grating) because this term is extremely small owing to washout by thermal motion. In the limit that $\delta = 0$, the backgrating effects are discussed thoroughly by Lam and Abrams.[31]

In this case, we have considered the problem in which the reservoir coupling may be due to velocity- or state-changing collisions or to spontaneous emission to another state. In the limit that we do not consider velocity-changing collisions into the resonant velocity group or consider collision-induced frequency shifts, we find that this equation is similar to our earlier work on collision effects.[21] The analytical description in the earlier analysis was more nearly complete. However, we have tried to emphasize a more general physical picture in this presentation.

To illustrate the behavior in the presence of atomic mo-

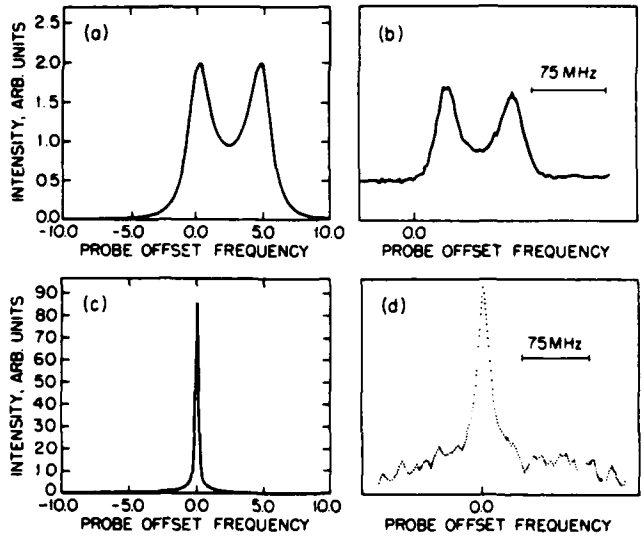

Fig. 4. (a) The NDFWM spectrum in Doppler-broadened material: $\Delta = 2.5\gamma_{sp}$. A fully collinear geometry is assumed. (b) The NDFWM spectrum measured in atomic sodium on the $F = 2 \rightarrow F = 3$ transition of the $D2$ line at 5890 Å. (c) The NDFWM spectrum in the presence of state-specific reservoir coupling with $\gamma_1 < \gamma_2$. (d) The NDFWM spectrum measured on the same transition as (b) but with 25 Torr of neon added. [The frequencies in curves (a) and (c) are normalized to the spontaneous emission rate.]

tion, Fig. 4(a) shows the NDFWM spectral response as a function of pump–probe detuning for a system in the Doppler limit when $\gamma_1 = \gamma_2$ and a fully collinear geometry (i.e., $\mathbf{k}_f = \mathbf{k}_p = -\mathbf{k}_b$). When the pump beam is tuned off resonance (with respect to the zero-velocity group), we see that two resonances are observed. The first resonance occurs at $\delta = 0$ and has a width determined by the spontaneous emission rate. The second resonance occurs at $\delta = 2\Delta$ and has a width determined by the total dephasing rate. Figure 4(b) is a comparison with experiments in atomic sodium on the $D2$ line [$^2S_{1/2}(F = 2) \rightarrow {}^2P_{3/2}(F = 3)$ transition]. (In these measurements, the angle between the pump and probe resulted in a residual Doppler width of the order of a few megahertz, which eliminated the observation of the effects of interference due to coherences between the magnetic substates.[32]) In the absence of state-specific reservoir coupling, the analytical results are similar to those of Nilsen and Yariv.[33] Again, as we examine the polarization, we see that the resonance at $\delta = 0$ that has a width given by γ_1 does not contribute for the same reasons as just given. However, unlike with the homogeneously broadened system, even when the system is closed a resonance occurs at $\delta = 0$.

We now consider the effect of reservoir coupling. As the system begins to experience additional pure dephasing, the second resonance begins to broaden and decrease in amplitude. In the presence of state-specific reservoir coupling where $\gamma_1 < \gamma_2$, we expect the $\delta = 0$ resonance to narrow. Because of the additional dephasing, the second resonance will broaden and weaken. Figure 4(c) shows the calculated NDFWM response for $\Delta = 0$ ($\Delta = 0$ was used in the experiments to give the best signal-to-noise ratio). To make the comparison experimentally, ground-state perturbers (such as neon buffer gas) were added to the cell of atomic sodium. In this case, cross sections for state- or velocity-changing collisions between the sodium atom and the perturber atom are larger for the $3p$ state than for the $3s$ state. Hence, in these experiments, the addition of buffer gas resulted in $\gamma_1 < \gamma_2$. Figure 4(d) shows the measured narrowing of the NDFWM response.[34]

On the basis of the work just discussed, such resonances should be observed if the upper state can decay to another state by spontaneous emission. One example is the $^2S_{1/2}(F = 2) \rightarrow {}^2P_{1/2}(F = 2)$ of the $D1$ line in sodium.[35] Dipole-selection rules allow the upper state to decay to the $F = 1$ ground state. In steady state, this would lead to optical pumping of the hyperfine split ground state. (This is not the case on the previous $F = 2 \rightarrow F = 3$ transition on the $D2$ line). In this case, even in the absence of any external reservoir coupling, the coupling to the vacuum radiation field, giving rise to spontaneous emission, is sufficient to make the interference effects incomplete, giving rise to a narrow NDFWM response on the $\delta = 0$ resonance. Figure 5(a) shows the calculated NDFWM response on this transition if decay to the $F = 1$ ground state is not allowed. If the decay is allowed (using the appropriate decay rates for this transition), Fig. 5(b) shows the expected narrow response; with the width being given by the transit time. To compare these results with experiment, it is necessary to account for the finite angle between the forward pump and probe, which

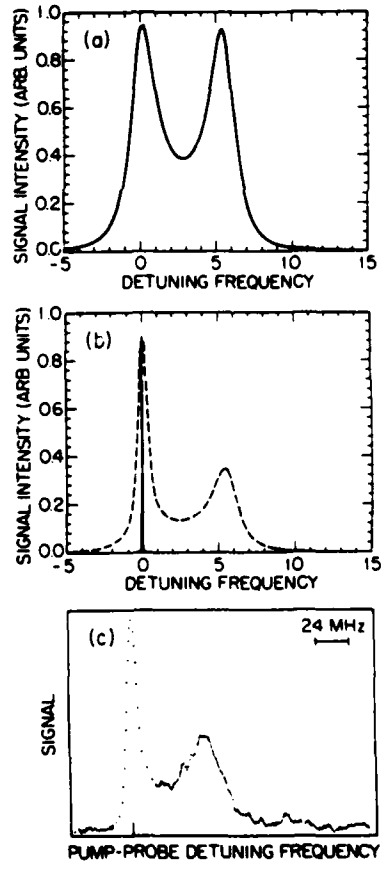

Fig. 5. The calculated NDFWM response in atomic sodium for the $F = 2 \rightarrow F = 2$ transition on the $D1$ line. For this calculation, spontaneous emission decay to the $F = 1$ ground state was not allowed. (The frequency is normalized to the spontaneous emission rate.) (b) The same calculation as in (a) except the $F = 2$ upper level is allowed to decay to the $F = 1$ ground state. The solid line is for a fully collinear geometry. The dashed line is the calculation allowing for the residual Doppler broadening of the $\delta = 0$ resonance owing to the finite angle between the forward pump and probe. (c) The experimental NDFWM showing the narrow $\delta = 0$ resonance. [This result should be compared with Fig. 4(b).]

results in a residual Doppler width associated with the $\delta = 0$ resonance. The dotted line in Fig. 5(b) shows the NDFWM response corrected for this effect. Figure 5(c) shows the experimental measurement. The second resonance has a width given by twice the total dephasing, as expected from Eq. (8). However, the $\delta = 0$ resonance is narrower and stronger than the second resonance, showing that the interference is incomplete and enabling the resonance associated with the ground-state lifetime to be observed.

D. Stationary Two- and Three-Level Atoms above Saturation

In a simple two-level system in the presence of strong resonant optical excitation, the levels appear to split because of the ac-Stark effect, resulting in a three-peaked fluorescence spectrum.[12] The ac-Stark effect is also directly observable as a splitting of the NDFWM spectrum.[13-15] The criterion for observing the splitting in any kind of experiment is that the Rabi flopping frequency $\mu E/\hbar$ must exceed the natural linewidth determined by the total dephasing rate, $\gamma_{ph}{}^T$. In a simple closed two-level system, this condition corresponds exactly to the requirement that the optical intensity must exceed the system saturation intensity. However, in a three-level system with a metastable third level, the saturation intensity (which is observed as a reduction in the absorption coefficient) can be reduced several orders of magnitude because of optical pumping-induced depletion of the ground state. In this case, there is no direct relationship between the ratio of the Rabi flopping frequency to the total dephasing rate and the ratio of the intensity to the saturation intensity. *Hence we expect to see saturation effects in the NDFWM spectrum without observing ac-Stark splitting.*

Assuming strong pumps and a weak probe beam, we solved the equation of motion for the density-matrix operator by using the same approach discussed in earlier work on saturable absorbers (see Refs. 11, 36, and 37).

We use Eq. (1) with the above modifications to describe Fig. 1(c) and write V as $V^0 + V^1$, where V^0 is the interaction potential due to the strong counterpropagating pump waves and V^1 is the interaction potential due to the weak probe wave. (We ignore the effects of the signal wave since we are assuming that the nonlinear response is sufficiently weak to result in a phase-conjugate reflectivity far less than unity.) The density-matrix equations can now be written as a set of zero-order equations because of the strong pumps:

$$i\hbar\dot{\rho}^0 = [H_0, \rho^0] + [V^0, \rho^0] + i\hbar \left.\frac{\partial \rho^0}{\partial t}\right|_{sp.em.} - \frac{i\hbar}{2}[\Gamma, \rho^0]_+ - i\hbar \left.\frac{\partial \rho^0}{\partial t}\right|_{ph}. \quad (9)$$

and a set of equations that includes the effects of perturbation by a weak probe:

$$i\hbar\dot{\rho}^1 = [H_0, \rho^1] + [V^0, \rho^1] + [V^1, \rho^0] + i\hbar \left.\frac{\partial \rho^1}{\partial t}\right|_{sp.em.} - \frac{i\hbar}{2}[\Gamma, \rho^1]_+ - i\hbar \left.\frac{\partial \rho^1}{\partial t}\right|_{ph}. \quad (10)$$

The first set of equations is solved exactly. Then the results are inserted into the second set, which is solved perturbatively. From the solution, we solve for the polarization given by $P = \mathrm{Tr}(\mu\rho)$, where μ is the dipole-moment operator. (The precise set of terms to be included in the polarization is determined by the phase-matching conditions that give rise to a signal counterpropagating with respect to the input probe.) We find that the polarization is given by

$$P = -2N_0 \frac{1}{8}\mu\chi_f{}^0\chi_b{}^0(\chi_p{}^1)^* \frac{(\Delta - i\gamma_{ph}{}^-)(\delta - i2\gamma_{ph}{}^T)}{\Delta^2 + (\gamma_{ph}{}^T)^2\left[1 + \frac{|\chi_R{}^T|^2}{\gamma_{ph}{}^T\gamma_2{}^T}\left(1 + \frac{\gamma_{22}}{2\gamma_{31}}\right)\right]} \frac{1}{(\delta - i\gamma_{ph}{}^T)} \times \frac{\exp[i(\mathbf{k}_f + \mathbf{k}_b - \mathbf{k}_p)\cdot\mathbf{x} - i(\omega - \delta)t]}{\dfrac{(\delta - i\gamma_{31})(\delta - i\gamma_2{}^T)([\Delta + \delta] - i\gamma_{ph}{}^T)(-[\Delta - \delta] - i\gamma_{ph}{}^T) - |\tilde{\chi}_R{}^T|^2/2}{2(\delta - i\gamma_{ph}{}^T)[\delta - i\gamma_{31} - i(\gamma_{23}/2)]}} + \text{c.c.}, \quad (11)$$

Assuming strong pumps and a weak probe beam, we solved the equation of motion for the density-matrix operator by using the same approach discussed in earlier work on saturable absorbers (see Refs. 11, 36, and 37).

We use Eq. (1) with the above modifications to describe Fig. 1(c) and write V as $V^0 + V^1$, where V^0 is the interaction potential due to the strong counterpropagating pump waves and V^1 is the interaction potential due to the weak probe wave. (We ignore the effects of the signal wave since we are assuming that the nonlinear response is sufficiently weak to result in a phase-conjugate reflectivity far less than unity.) The density-matrix equations can now be written as a set of zero-order equations because of the strong pumps:

where χ_i is the Rabi flopping frequency ($\mu E_i/\hbar$) associated with field E_i, $\chi_R{}^T = \chi_f \exp(i\mathbf{k}_f\cdot\mathbf{x}) + \chi_b \exp(i\mathbf{k}_b\cdot\mathbf{x})$, $\gamma_{31}{}^T = \gamma_{23} + \gamma_{sp}$, $\gamma_{ph}{}^T = \gamma_2{}^T/2 + \gamma_{ph}$, δ is the pump–probe detuning, and Δ is the pump-resonance detuning.

To predict the macroscopic nonlinear response, however, we must insert the polarization into the wave equation and perform a spatial average of the polarization since the term $\tilde{\chi}_R{}^T$ is spatially varying (because of the standing wave between the forward and backward pumps). We defer discussion of this full solution and simply discuss the physical behavior described by the polarization.

The signal is proportional to the square of the polarization, and, to simplify the discussion below, we set the cross term in $|\chi_R{}^T|^2$ to zero. (This is a serious error if one is attempting to predict absolute phase-conjugate efficiencies,[11] but unless one is trying to make quantitative lineshape measurements it does not qualitatively affect the NDFWM spectral response.)

First we note that in the limit of $\gamma_{ph} = \gamma_{23} = 0$, two resonances are expected as a function of δ at $\delta = \pm\Delta$. As the intensity is increased and saturation is observed, the levels undergo ac-Stark splitting, and three resonances are expected at $\delta = 0$ and $\delta = \pm|\chi_R{}^T|$. Figure 6(a) shows the expected behavior, in agreement with the discussion in Ref. 14.

However, in the limit of large dephasing ($\gamma_{ph} \gg \gamma_2{}^T$), finite γ_{23}, and a long-lived metastable, we expect a single narrow resonance with a width given by the metastable lifetime if the pump intensities are much less than the three-level saturation intensity. As the intensity increases above saturation, even though the ac-Stark splitting is still small compared with the width of level 2, as anticipated above, we expect the NDFWM spectral response to broaden. This effect is the result of Fig. 6(b). Most importantly, we note that, from the analytical description, we expect the saturated width to broaden linearly with the pump intensity.

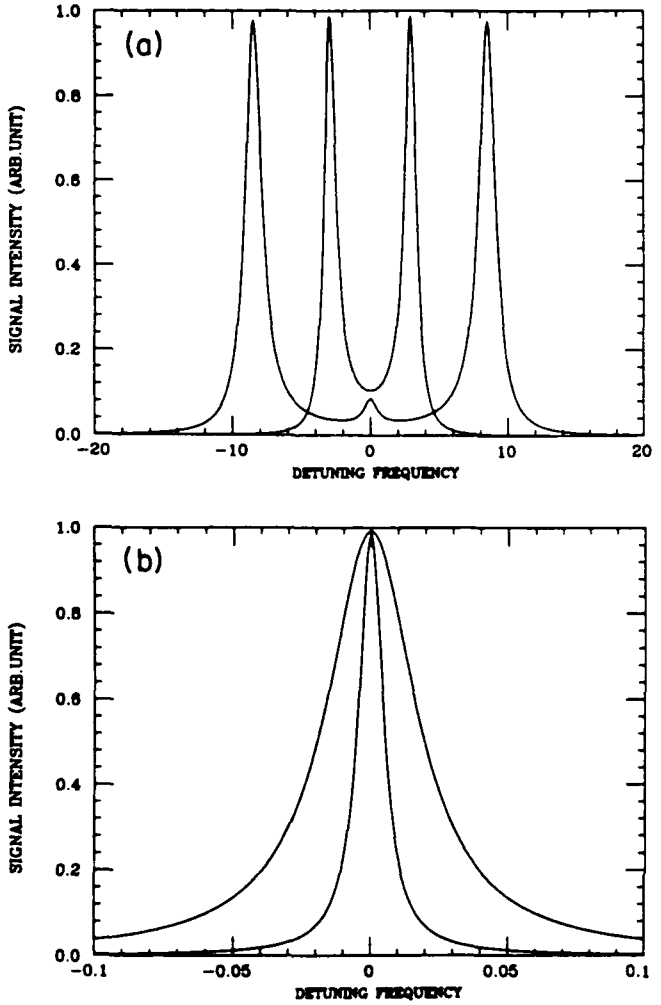

Fig. 6. (a) The NDFWM response for a closed two-level system. The curve with two resonances is the low-intensity ($\chi_R{}^T = 0$) response, similar to Fig. 2(a). The three-peaked structure is the strong field response, showing the ac-Stark splitting and a central resonance ($\chi_R{}^T = 8$). (b) The NDFWM response for a closed three-level system. The narrow resonance is the low-intensity response ($\chi_R{}^T = 0$). The broader repsonse shows the expected power broadening ($\chi_R{}^T = 6.71$). For this calculation, $\gamma_{31} = 0.005$, $\gamma_{23} = 2$, $\gamma_{ph} = 10^{-4}$, and $\Delta = 0$.

3. SUMMARY

In summary, we have presented an analytical description of backward NDFWM to extract a physical understanding of the origin of the spectral response in relatively simple systems. The analysis included a model for state-specific reservoir coupling and spontaneous emission and showed that noncancellation of quantum-mechanical amplitudes dominated the experimental observations.

ACKNOWLEDGMENTS

This research was supported in part by the U.S. Air Force Office of Scientific Research under grant 85-0280 and by the U.S. Army Research Office under contract DAAL03-86-K-0057.

D. G. Steel, J. Remillard, and J. Liu are also with the Department of Electrical Engineering, University of Michigan.

* Present address, Department of Electrical Engineering, University of Michigan, EECS Building, Ann Arbor, Michigan 48109.

REFERENCES AND NOTES

1. W. E. Lamb, Jr., Phys. Rev. A **134**, 1429 (1964).
2. B. H. Soffer and B. B. McFarland, Appl. Phys. Lett. **8**, 166 (1966).
3. S. E. Schwarz and T. Y. Tan, Appl. Phys. Lett. **10**, 4 (1967).
4. M. Sargent III, Phys. Rep. **43**, 223 (1978).
5. L. W. Hillman, R. W. Boyd, J. Krasinski, and C. R. Stroud, Jr., Opt. Commun. **45**, 416 (1983).
6. M. S. Malcuit, R. W. Boyd, L. W. Hillman, J. Krasinski, and C. R. Stroud, Jr., J. Opt. Soc. Am. B **1**, 73 (1984).
7. M. A. Kramer, W. R. Tompkin, and R. W. Boyd, Phys. Rev. A **34**, 2026 (1986).
8. R. W. Boyd and S. Mukamel, Phys. Rev. A **29**, 1973 (1984).
9. M. A. Kramer, R. W. Boyd, L. W. Hillman, and C. R. Stroud, Jr., J. Opt. Soc. Am. B **2**, 1444 (1985).
10. For a review, see *Optical Phase Conjugation*, R. A. Fisher, ed. (Academic, New York, 1983); B. Ya. Zel'dovich, N. F. Pilipetsky, and V. V. Schkunov, *Principles of Phase Conjugation* (Springer-Verlag, Berlin, 1985).
11. R. L. Abrams and R. C. Lind, Opt. Lett. **2**, 94, 3205 (1978).
12. F. Y. Wu, R. E. Grove, and S. Ezekiel, Phys. Rev. Lett. **35**, 1426 (1975).
13. T.-Y. Fu and M. Sargent III, Opt. Lett. **4**, 366 (1979).
14. D. J. Harter and R. W. Boyd, IEEE J. Quantum Electron. **QE-16**, 1126 (1980).
15. D. G. Steel and R. C. Lind, Opt. Lett. **6**, 587 (1981).
16. D. G. Steel and S. C. Rand, Phys. Rev. Lett. **55**, 2285 (1985); D. G. Steel, S. C. Rand, and J. Liu, J. Opt. Soc. Am. B **4**, 1794 (1987).
17. N. Bloembergen and Y. R. Shen, Phys. Rev. A **37**, 133 (1964).
18. See, for example, M. Sargent III, M. O. Scully, and W. E. Lamb, Jr., *Laser Physics* (Addison-Wesley, Reading, Mass., 1974), Chap. 16.
19. P. R. Berman, Phys. Rev. A **5**, 927 (1972).
20. P. R. Berman, J. Opt. Soc. Am. B **3**, 562 (1986).
21. J. F. Lam, D. G. Steel, and R. A. McFarlane, Phys. Rev. Lett. **49**, 1628 (1982).
22. J. F. Lam, D. G. Steel, and R. A. McFarlane, Phys. Rev. Lett. **56**, 1679 (1986).
23. S. Y. Yee and T. K. Gustafson, Phys. Rev. A **18**, 1597 (1978).
24. J. R. Andrews and R. M. Hochstrasser, Chem. Phys. Lett. **83**, 427 (1987).
25. N. Bloembergen, H. Lotem, and R. T. Lynch, Ind. J. Pure Appl. Phys. **16**, 151 (1978).
26. N. Bloembergen, A. R. Bogdan, and M. W. Downer, in *Laser Spectroscopy V*, A. R. W. McKellar, T. Oka, and B. P. Stoicheff, eds. (Springer-Verlag, Berlin, 1981), p. 157.
27. Y. Prior, A. R. Bogdan, M. Dagenais, and N. Bloembergen, Phys. Rev. Lett. **46**, 111 (1981).
28. A. R. Bogdan, Y. Prior, and N. Bloembergen, Opt. Lett. **6**, 82 (1981).
29. A. R. Bogdan, M. W. Downer, and N. Bloembergen, Opt. Lett. **6**, 348 (1981).
30. The plasma-dispersion function that results from velocity or frequency integrals has the limiting value $Z(a + ib) = i\sqrt{\pi}$ for $b > 0$. For $b > 0$, the plasma-dispersion function is defined as

$$Z(a + ib) = (\pi)^{-1/2} \int_{-\infty}^{\infty} dx \frac{\exp(-x^2)}{[x - (a + ib)]}$$

and

$$(\pi)^{-1/2} \int_{-\infty}^{\infty} dx \frac{\exp(-x^2)}{[x - (a - ib)]} = -Z(-a + ib).$$

31. J. F. Lam and R. L. Abrams, Phys. Rev. A **26**, 147 (1982).
32. In the presence of magnetic substates, a simple two-level system may be closed with respect to population, but alignment and orientation are not necessarily conserved. In this case, a narrow

feature can still be observed in the four-wave mixing response at $\delta = 0$. However, the decay of the excited-state alignment and orientation can create a ground-state alignment and orientation in excess of those produced by the optical field alone, resulting in a narrow dip in the $\delta = 0$ resonance. Such effects have been discussed in detail by G. Khitrova, Ph.D. dissertation (New York University, New York, 1986). These effects can be observed when the pump–probe angle is small enough to reduce the residual Doppler width to a few megahertz. Experiments and theory are discussed by P. R. Berman, D. G Steel, G. Khitrova, and J. Liu, "Effects of radiative decay in four-wave mixing spectroscopy: narrow resonances produced by nonconservation of population, alignment and orientation," in *Laser Spectroscopy VIII*, S. Svanberg, ed. (Springer-Verlag, Berlin, 1987).

33. J. Nilsen and A. Yariv, J. Opt. Soc. Am **71**, 180 (1981).
34. Because of the finite angle between the pump and probe, the linewidth would not be expected to narrow below the residual Doppler limit as seen in the experiments discussed in Fig. 5. However, for the buffer-gas pressure used in these measurements, Dicke narrowing eliminates the contribution of the residual linewidth.
35. J. Liu, J. T. Remillard, and D. G. Steel, Phys. Rev. Lett. **59**, 779 (1987).
36. G. J. Dunning and D. G. Steel, IEEE J. Quantum Electron. **QE-18**, 3 (1982).
37. R. L. Abrams, J. F. Lam, R. C. Lind, D. G. Steel, and P. F. Liao, in *Optical Phase Conjugation*, R. A. Fischer, ed. (Academic, New York, 1983) p. 211.

LASER SPECTROSCOPY IX

Proceedings of the Ninth International Conference on Laser Spectroscopy

Bretton Woods, New Hampshire
June 18–23, 1989

Edited by

Michael S. Feld
Department of Physics
Massachusetts Institute of Technology
Cambridge, Massachusetts

John E. Thomas
Department of Physics
Duke University
Durham, North Carolina

Aram Mooradian
MIT-Lincoln Laboratory
Lexington, Massachusetts

ACADEMIC PRESS, INC.
Harcourt Brace Jovanovich, Publishers
Boston San Diego New York
Berkeley London Sydney
Tokyo Toronto

High Resolution Nonlinear Laser Spectroscopy of Excitons in GaAs/AlGaAs Multiple Quantum Well Structures

J. G. Steel, H. Wang, J. T. Remillard, M.D. Webb
Departments of Physics and Electrical Engineering
University of Michigan, Ann Arbor, MI 48109 USA

P. K. Bhattacharya, J. Oh, J. Pamulapati
Department of Electrical Engineering and Computer Science
University of Michigan, Ann Arbor, MI 48109 USA

Frequency domain nonlinear laser spectroscopy is a powerful method for studying resonant optical excitation in solids. It provides a means for obtaining line shapes related purely to relaxation of optically excited states of the system. In addition, it often eliminates contributions from inhomogeneous broadening and enables studies of the homogeneous line shape and the effects of spectral diffusion.[1,2,3] In this paper, we discuss measurements of the exciton in a GaAs/AlGaAs multiple quantum well (MQW).

GaAs MQW's are semiconductor heterostructures of importance to electronic and optoelectronic devices[4]. They consist of a periodic structure of thin layers of GaAs and AlGaAs. The larger band gap of AlGaAs confines the optical excitation to the thin GaAs, resulting in quantum confinement of the exciton and an increase in the exciton binding energy. In this work, the MQW is grown by molecular beam epitaxy and consists of 65 periods of 96A wells of GaAs and 98A barriers of $Al_{.3}Ga_{.7}As$. The solid line in Fig. 1 shows the absorption spectrum at 5K. The two resonances are the heavy hole (HH1) and light hole (LH1) exciton which exhibit strong inhomogeneous broadening due to fluctuations in the well thickness.

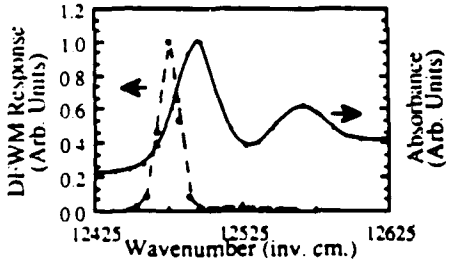

Figure 1. The absorption spectrum and the degenerate four-wave mixing response at 5K. The red shift in the nonlinear response shows the nonlinear response in this sample is due to localized excitons.

The primary backward four-wave mixing experimental configuration is discussed in reference 5. Two counter-propagating pump beams [identified by field amplitudes $\vec{\mathcal{E}}_f(\omega_f,\vec{k}_f)$ and $\vec{\mathcal{E}}_b(\omega_b,\vec{k}_b)$] interact with a third beam [$\vec{\mathcal{E}}_p(\omega_p,\vec{k}_p)$] through the third order susceptibility to produce a nonlinear polarization. The probe field k-vector $\vec{k}_p$ intersects the forward pump field k-vector, $\vec{k}_f$, at an angle θ. The signal field [designated, $\vec{\mathcal{E}}_s(\omega_s,\vec{k}_s)$], arises from the induced nonlinear response proportional to $\vec{\mathcal{E}}_f\vec{\mathcal{E}}_p^*\vec{\mathcal{E}}_b$. Since the frequencies are nearly degenerate, phase matching ensures that the signal is nearly counter-propagating with respect to the probe field. Physically, $\mathcal{E}_f\mathcal{E}_p$ form a traveling wave spatial grating asso-

ciated with the excitation of the system. $\mathcal{E}_b$ scatters from this grating to produce the signal. The nonlinear response in these systems is due to band filling and exchange effects[6].

For $\vec{\mathcal{E}}_b \| \vec{\mathcal{E}}_f \| \vec{\mathcal{E}}_p$, measurement of $|\mathcal{E}_s|^2$ as a function of $\omega_p-\omega_f=\delta$ (for $\omega_b-\omega_f$=constant), designated the FWMp response, gives a measure of the relaxation rates associated with the optical field induced perturbation of the excited states and the ground state, provided there is no orientation signal (i.e., E_s=0 if $\vec{\mathcal{E}}_b \| \vec{\mathcal{E}}_f \perp \vec{\mathcal{E}}_p$, which we have verified experimentally for low power cw excitation.) For fixed δ, measurement of $|\mathcal{E}_s|^2$ as a function of $\omega_b-\omega_f$ (designated the the FWMb response) gives the line shape associated with the nonlinear response in homogeneously broadened material, and a line shape related to the homogeneous line shape in inhomogeneously broadened material[5].

At 300K, the exciton is ionized by LO phonons on a time scale of 300fsec. The FWMp response measures dynamics associated with the electron-hole (e-h) plasma. Figure 2a shows a typical FWMp response. The solid curve is a fit of a Lorentzian. Dynamics are determined by e-h recombination and spatial diffusion. The spatial diffusion rate depends on the grating spacing ($\Delta K=|\vec{k}_f-\vec{k}_p|$) and hence the angle, θ. Figure 2b show the angle dependence. The solid curve is a fit of the form $\gamma_{rec}+D(\Delta K)^2$. The data gives γ_{rec} (=5nsec) and D (=18cm^2/sec). The measurements of the

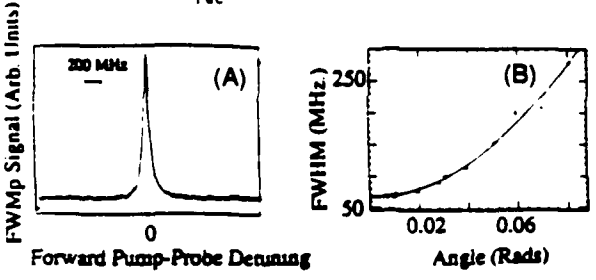

Figure 2. (a) The FWMp response at room temperature (b) The angle dependence of the FWMp response.

room temperature nonlinear response show the presence of a slow component. Figure 3a shows a high resolution display of the center of Fig. 2. The line shape shows a clear effect of interference in the scattering channel giving rise to the signal. Phenomenological modeling of the nonlinear response shows that the interference is likely due to a shift in the

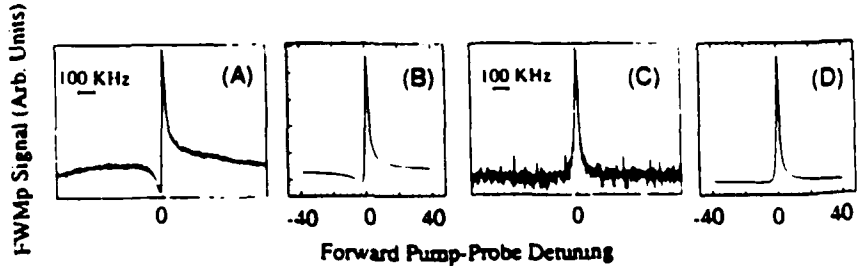

Figure 3. A high resolution scan of the FWMp response. (a) $\omega_b=\omega_f$ (c) $\omega_b<<\omega_f$ (b) and (d) are the results of the model.

resonance. Figure 3b shows the predicted behavior, in good agreement with the experiments. Further confirmation of the explanation is seen by comparing Fig 3c and the corresponding model in 3d. In this case, the back pump beam is detuned to the low energy side of the resonance, eliminating the interference effect. The origin of the shift may be due to a renormalization of the exciton energy or a shift in the exciton energy due to thermal effects.

At low temperature, the exciton is stable against ionization, and the dashed line in Fig 1 shows the nonlinear response (measured by degenerate FWM) is red shifted with respect to the absorption spectrum. The recombination time of the exciton is 1.5 nsec, so the FWMp response would be expected to give a line shape with a width determined by the inverse life time. Figure 4a shows a much more complex structure. The line shape shows the presence of two clear decay channels, corresponding to 100 psec and 15 nsec. In addition, a high resolution scan of the center shows a narrow resonance similar to Fig. 3a. Figure 4b shows an expanded scan of

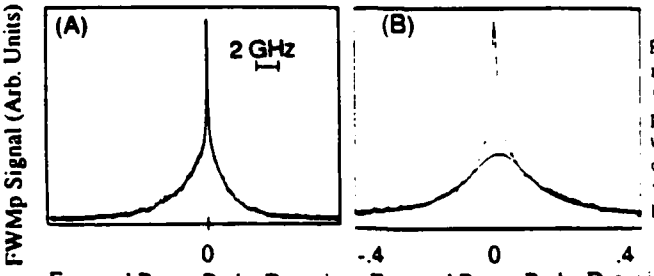

Figure 4. (a) FWMp response at 5K. (b) shows an expanded range along with a curve fit corresponding to the 1.5 nsec recombination time.

the intermediate region along with a curve fit corresponding to 1.5 nsec. We believe the 1.5 nsec decay is due to radiative recombination and the 100 psec decay corresponds to the decay due to spectral diffusion. Solutions of the optical Bloch equations for the FWMp response modified to describe spectral diffusion (MOSE)[3] show the FWMp response would have the form described by Fig 4b and the base of 4a. The origin of the 15nsec component is possibly due to the presence of residual electric fields which can result in an increase in the exciton lifetime.

Further evidence for spectral diffusion is seen in the FWMb response which eliminates inhomogeneous broadening and provides a line shape related to the homogeneous line shape along with contributions from spectral diffusion. Figure 5a shows the FWMb response obtained 28 cm^{-1} below the

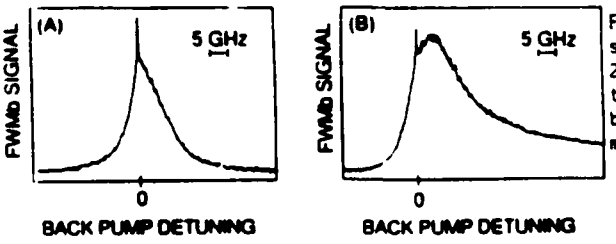

Figure 5. The FWMb response at 5K. (a) 28cm^{-1} below the absorption maximum. (b) 5cm^{-1} below the absorption maximum.

absorption maximum. This curve shows slight asymmetry on the high energy side. The asymmetry becomes more dramatic as the forward pump and probe frequency approach the absorption resonance, as seen 5b. It can be shown that in the absence of spectral diffusion, the FWMb response is symmetric

about $\omega_b - \omega_f (\approx \omega_p)$. The presence of asymmetry is consistent with excitation diffusion to other resonant frequencies, and such line shapes can easily be obtained from MOBE. A possible origin of the spectral diffusion is variable range hopping. Recent work has identified phonon assisted tunneling and thermal activation as two possible mechanisms. Figure 6 shows a comparison of the measured temperature dependence of the line width in Fig. 5a to a theory based on phonon assisted tunneling. The curve varies as $\Gamma \exp(B/kT^{-1.7})$ and is in general agreement with theoret-

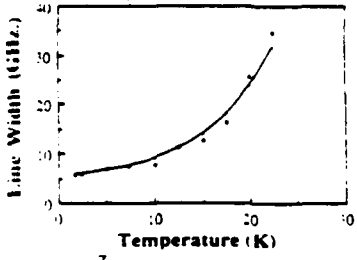

Figure 6. The FWMb line width in Fig. 5a as a function of temperature. The solid curve is a fit of the theory for phonon assisted tunneling.

ical expectations[7]. Finally the effects of spectral diffusion which we have observed are more clearly seen at higher temperatures. Figure 7a shows the FWMb response at 5K similar to Fig. 5b with an increase in scan

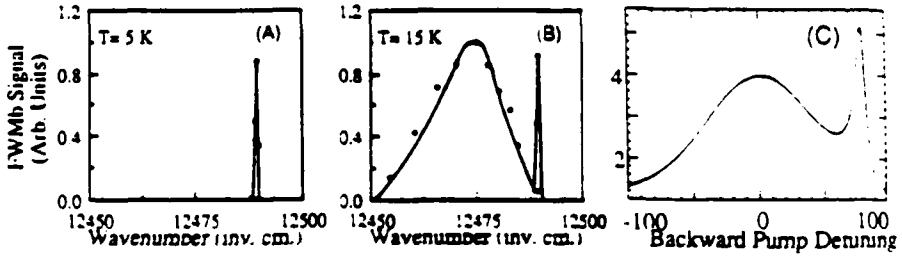

Figure 7. The FWMb response as a function of temperature. (a) 5K. (b) 15K. (c) Solution to MOBE.

At 15 K, we clearly observe the decay of the excitation to lower energy. In these measurements, we see that while the exciting radiation is centered at the peak of the absorption spectrum, the excitation clearly decays to the region of the localized exciton. The large broad peak is centered at the same wavelength as the peak of the nonlinear response shown in Fig. 1 and also corresponds to the peak in photoluminescence emission. Fig. 7c is a solution of the MOBE for the FWMb response in the presence of decay to a lower lying state.

This work is supported by the AFOSR and the ARO.

1 D. G. Steel and J.T. Remillard, Phys. Rev. A36, 4330 (1987).
2 P. R. Berman et al., Phys. Rev. A38, 252 (1988).
3 P. R. Berman, J. Opt. Soc. Am. B3, 564 (1986).
4 D. S. Chemla and D. A.B. Miller, "Physics and Applications of Excitons Confined in Semiconductor Quantum Wells," in Heterojunctions Band Discontinuities and Device Applications, F. Capasso and G. Margaritondo, eds., Elsevier Science Publisher B.V. 1987.
5 J. T. Remillard et al., Phys. Rev. Lett.
6 H. Haug and S. Schmitt-Rink, J. Opt. Soc. Am. B2, 1135 (1985).
7 T. Takagahara, Phys. Rev. B32, 7013 (1985).

High-resolution nonlinear laser spectroscopy of room-temperature GaAs quantum-well structures: observation of interference effects

J. T. Remillard, H. Wang, M. D. Webb, and D. G. Steel

Harrison M. Randall Laboratory, The University of Michigan, Ann Arbor, Michigan 48109

J. Oh, J. Pamulapati, and P. K. Bhattacharya

Department of Electrical Engineering and Computer Science, EECS Building, The University of Michigan, Ann Arbor, Michigan 48109

Received December 5, 1988; accepted July 6, 1989

We describe frequency-domain four-wave mixing spectroscopy measurements near the fundamental band edge in room-temperature GaAs multiple quantum wells. The line-shape information gives a measure of the dynamical behavior of the material and what is to our knowledge the first observation of an interference line shape due to a dominant slow contribution to the nonlinear response.

Using frequency-domain four-wave mixing (FWM), we report nonlinear laser spectroscopy studies of room-temperature in GaAs/AlGaAs multiple-quantum-well (MQW) structures in the vicinity of the $n = 1$ exciton features. These materials have been studied in recent years because of their large nonlinear response, which is of importance to optoelectronic applications.[1] These studies are also of fundamental interest since the optical properties reflect the effects of quantum confinement.

Experimental and theoretical research suggests that the origin of the room-temperature nonlinear response near the exciton resonances is due to band filling and exchange effects caused by the electron–hole (e–h) plasma produced by the rapid thermal ionization of the exciton. In a simple picture the linear-optical polarization is proportional to $\sum_n f_n/(\omega - \omega_n + i\gamma_n)$, where the sum is over all exciton states.[2] The parameters ω_n, γ_n, and f_n represent the frequency, width, and oscillator strength, respectively. When the exciton is formed, it ionizes on a time scale of 300 fsec, and theory has shown that the resultant e–h plasma significantly modifies the exciton oscillator strength. Earlier experimental work on differential transmission[3] resulted in a phenomenological description of the nonlinear response that described the experimental measurements if the e–h plasma modified not only the oscillator strength but also the linewidth due to collisions. A small shift in the resonance frequency was also required to produce a good fit. A shift of this resonance has been predicted theoretically as a result of renormalization of the exciton resonance frequency.[4]

In such a phenomenological model the fundamental parameters are taken to be the value in the absence of the optical field plus a term that is linearly dependent on the induced e–h plasma density. The optical response can then be expanded about the zero-field value to obtain a third-order polarization at frequency ω that has the general form $\sum_{ijk}\chi^{(3)}_{ijk}$ $(\omega = \omega_i - \omega_j + \omega_k)\mathcal{E}_i\mathcal{E}_j^*\mathcal{E}_k \exp[i(\mathbf{k}_i - \mathbf{k}_j + \mathbf{k}_k)\cdot\mathbf{r} - i(\omega_i - \omega_j + \omega_k)t]$, where $\chi^{(3)}_{ijk}$ is the third-order susceptibility. Physically for $\omega_i \approx \omega_j$ near an exciton resonance, $\mathcal{E}_i\mathcal{E}_j^*$ creates the e–h plasma modifying the optical response that is sensed by the third field $\mathcal{E}_k$. Spectroscopic measurements are made as a function of any of the three input frequencies. Information can be obtained about specific energy-level structure as well as relaxation rates (i.e., dynamical behavior) associated with states involved in the transition. In this Letter we describe measurements of the line shapes associated with the room-temperature susceptibility that provide information on e–h recombination, ambipolar diffusion, and heavy- and light-hole (hh) and (lh) line shapes. We also show what is to our knowledge the first observation of a narrow interference line shape, which is evidence of a shift in the exciton resonance frequency.

The FWM experimental configuration is discussed in Ref. 5. Two counterpropagating pump beams [identified by field amplitudes $\mathcal{E}_f(\omega_f, \mathbf{k}_f)$ and $\mathcal{E}_b(\omega_b, \mathbf{k}_b)$] interact with a third beam $[\mathcal{E}_p(\omega_p, \mathbf{k}_p)]$ through the third-order susceptibility to produce a nonlinear polarization. The probe field k vector $\mathbf{k}_p$ intersects the forward pump field k vector $\mathbf{k}_f$ at an angle θ. The signal field [designated $\mathcal{E}_s(\omega_s, \mathbf{k}_s)$] arises from the induced nonlinear response proportional to $\mathcal{E}_f\mathcal{E}_p^*\mathcal{E}_b$.

For $\mathcal{E}_b \perp \mathcal{E}_f \parallel \mathcal{E}_p$, measurement of $|\mathcal{E}_s|^2$ as a function of $\omega_p - \omega_f = \delta$ (for $\omega_f = \omega_b$ = constant), designated the FWMp response, gives a measure of the relaxation rates associated with the optical-field-induced perturbation of the excited states and the ground state,[6] provided that there is no orientation signal[7] (i.e., $E_s = 0$ if $\mathcal{E}_b \parallel \mathcal{E}_f \perp \mathcal{E}_p$, which we have verified experimentally for low-power cw excitation). Experimentally, one dye laser is used to provide the pump beams, and a second dye laser provides the probe beam. For measurement of line shapes narrower than 2 MHz, the interlaser jitter is too large, and FWMp measurements are made with one laser and two acousto-optic modulators using the method of correlated optical fields.[8] For a fixed δ, measurement of $|\mathcal{E}_s|^2$ as a function of $\omega_b - \omega_f$ (designated the FWMb response) gives the line shape associated with the nonlinear response in homo-

0146-9592/89/201131-03$2.00/0

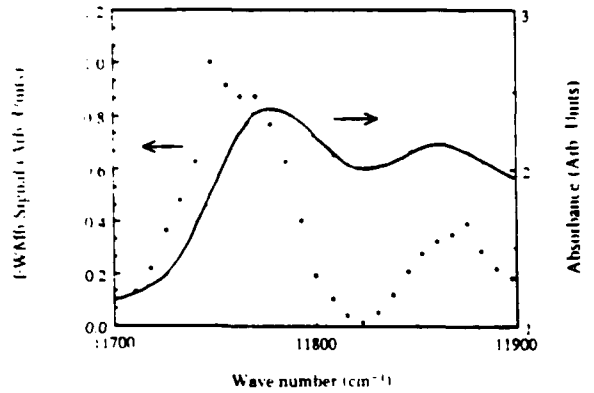

Fig. 1. Comparison of the room-temperature linear absorption (solid curve) and the FWMb response (points).

geneously broadened material and gives the line shape related to the homogeneous line shape in inhomogeneously broadened material.[5] Experimentally, one laser provides the forward pump and probe beams and a second laser provides the back pump beam. Acousto-optic modulators are used to control of δ.

The MQW well was grown by molecular beam epitaxy on a GaAs substrate and consists of alternate layers of 9.6-nm GaAs wells and 9.8-nm $Al_{0.3}Ga_{0.7}As$ barriers with a total of 65 periods. The incident optical beams are nearly normal to the growth direction. All measurements were done at low power (1–5 W/cm^2), corresponding to an exciton density in the well region of the order of 10^5 cm^{-2} and a carrier density of the order of 10^9 cm^{-2}.

In the first measurements, we obtained the FWMb response. As shown below, by adjusting δ, it is possible to control the relative contributions of different states involved in the nonlinear interaction because these states are characterized by different excitation-relaxation rates. To reduce contributions from slow terms in the nonlinear response, we set δ = 500 kHz. Figure 1 shows the room-temperature absorption spectrum (the solid curve) characterized by the usual hh and lh features and the interband transitions contributing to the background. Superimposed onto Fig. 1 is the FWMb response (the points). The spectrum clearly shows the hh and lh features with no background contribution from interband transitions. Such measurements are similar to the first measurements of degenerate FWM ($\omega_f = \omega_b = \omega_p$) in a MQW at low temperature[9] and at room temperature[10]; however, by tuning only the back beam, the relative signal strengths in optically thin material (normalized, e.g., to the response at the hh) are proportional to the magnitude squared of the optical response functions of the hh and lh excitons rather than the more complex dependence in degenerate FWM. Physically, the origin of the behavior is qualitatively understood. The forward pump and probe fields interact to produce a spatial modulation of excitons that quickly ionize, producing a spatial modulation (and for finite δ, a traveling modulation) of the e–h plasma. $\mathbf{E}_b$ scatters from this grating, and scanning of the backward beam frequency measures the basic frequency response of the linear exciton susceptibility.

In the next measurements, we examined the FWMp response, which measures the decay rate of the excitation. The decay of the spatial modulation is determined by e–h recombination and spatial diffusion. The spatial diffusion in the grating is determined by ambipolar diffusion $D_a = 2D_h$, where the electron mobility is much greater than the hole mobility.[3,11] In this limit the nonlinear polarization is given by

$$P^{\mathrm{NL}} = \zeta \mathcal{E}_f \mathcal{E}_p^* \mathcal{E}_b (i\delta + \gamma + D_a|\Delta\mathbf{k}|^2)^{-1} \times \exp(i\delta t + i\Delta\mathbf{k}\cdot\mathbf{x})\exp(-i\omega_b t + i\mathbf{k}_b\cdot\mathbf{x}) + \text{c.c.},$$

where ζ is a constant, γ is the decay rate due to carrier recombination, $|\Delta\mathbf{k}|^2 = |\mathbf{k}_f - \mathbf{k}_p|^2 = (2k)^2 \sin^2(\theta_{\mathrm{int}}/2)$, with θ_{int} the internal angle between the forward pump and probe beams, and we have taken $|k_f| \cong |k_p| = k$. Tuning δ provides information on the relaxation of these states, and the dependence of the FWMp spectral response on D_a and θ gives a way to measure D_a and γ. A corresponding method in the time domain has been used for exciton delocalization studies.[12]

There are two regimes for this experiment, corresponding to $\delta = \omega_p - \omega > 1$ MHz and $\delta < 1$ MHz ($\omega = \omega_f = \omega_b$). For the large detuning range, we find line shapes similar to that shown in Fig. 2. The solid curve is a fit of a Lorentzian curve, showing that the line shape associated with the decay is clearly Lorentzian. As anticipated above, this line shape is angle dependent as shown in Fig. 3. The functional form of the curve is given by $\gamma + D_a(2k)^2 \sin^2(\theta_{\mathrm{int}}/2)$. The solid curve is a fit of this equation, from which we determine the ambipolar diffusion coefficient and the recombination time of the e–h plasma. In this case, we find that D_a = 18 cm^2/sec and $\gamma^{-1} = \tau_R$ = 5 nsec. D_a is in reasonable agreement with that expected from the measured hole mobility,[11] and both D_a and τ_R are in agreement with those values reported by Chemla *et al.*[3] using time-domain methods.

For $\delta < 1$ MHz, the FWMp spectrum was obtained

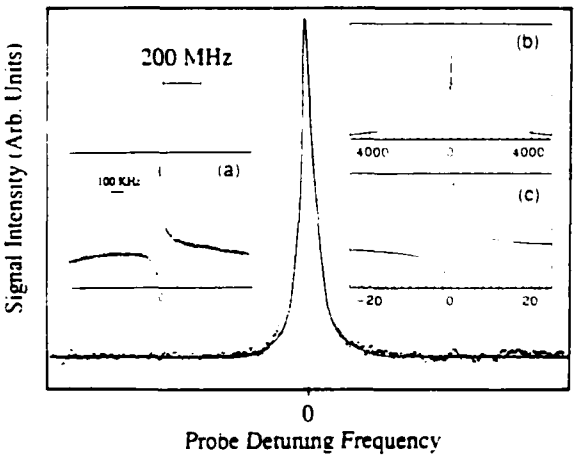

Fig. 2. FWMp response. The solid curve is a least-squares fit of a simple Lorentzian. Inset (a) is a high-resolution spectrum of the tip of the primary curve showing an interference profile. Insets (b) and (c) show that such profiles can be seen in MOBE's, which are phenomenologially modified to account for the nonlinear-optical response in semiconductors. Inset (c) is an enlargement of the central region of inset (b).

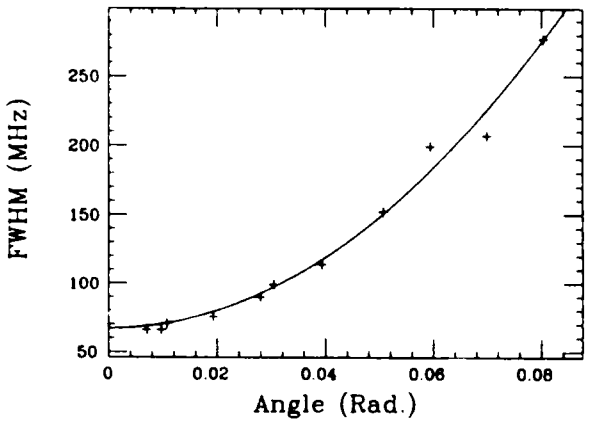

Fig. 3. Linewidth in Fig. 2 as a function of the angle between the forward pump and probe beams. The solid curve is a least-squares fit of the linewidth described by recombination and ambipolar diffusion.

using the method of correlated optical fields. Inset (a) of Fig. 2 shows the response, a profile associated with interference effects. The relaxation time associated with this profile is of the order of 10 μsec. We interpret these data as being the result of interference between multiple scattering channels in the nonlinear interaction, where at least one of the channels is associated with a long-lived excitation of the system.

Existing theoretical descriptions have not described such behavior, and the origin is likely to be complex. However, there have been recent discussions of effective optical Bloch equations, (EOBE's)[13] which resemble typical density-matrix equations describing optical interactions [the modified optical Bloch equations[14] (MOBE's)]. Without solving the EOBE's it is instructive to solve the MOBE's, where these equations are further *phenomenologically* modified to account for the nonlinearity in semiconductors. Recalling that the origin of the room-temperature nonlinear response is due to the presence of an e–h plasma that modifies the fundamental parameters ω_n, γ_n, and f_n, we assume that these different terms are modified according to the prescription $\xi_n \rightarrow \xi_n(1 + \alpha_n \sum_{ij} \mathcal{E}_i \mathcal{E}_j^*)$, where α_n is a constant that describes the linear dependence of a given parameter, ξ_n ($=\gamma_n$, ω_n, or f_n), on the electron and hole density. If we assume that either the electron or the hole is trapped in a long-lived state such as an interface state, then there exists a long-lived effect on the modified parameters.

Solving the corresponding equation for the FWMp response, we obtain the profile shown in inset (b) of Fig. 2, where the δ is normalized to the inverse lifetime of the long-lived state. Inset (c) of Fig. 2 is an enlargement of the interference region. The interference effect arises between the e–h-modified γ or f and a small but *necessary* modified exciton frequency ω. Without the shift in the resonant frequency (owing to carriers or some other laser-induced mechanism), the model shows just a narrow resonance with no interference dip. The interference results because the contribution of the frequency shift to the nonlinearity is shifted in phase by 90° from the contributions to the nonlinearity due to shifts in f_n and γ_n. In a direct measurement of the FWM response, the sign of the shift cannot be determined because the signal is proportional to the square of the difference between the f_n (and γ_n) term and the frequency-shift term. Current research is based on use of a heterodyne-detection measurement, which should resolve this ambiguity. Furthermore, in this material (as in other samples that we have examined) the cw nonlinear response is dominated by the slow component. The slow component gives rise to a signal which is four times the strength of the fast response. [This was determined from the one laser FWMp measurement shown in inset (a) of Fig. 2 by taking the ratio of the signal at the peak to the signal in the wings of the narrow resonance.] This component is most likely electronic in origin since it persists (with the same width) when the sample is immersed in liquid helium.[5] Note, however, that the room-temperature behavior could also be the result of a contribution from a spatially modulated temperature-induced shift in the resonance. The phenomenological calculation shown in the inset of Fig. 2 would be similar for a thermal effect.

This resarch was supported by the U.S. Air Force Office of Scientific Research. M. D. Webb was partially supported by a U.S. Army Research Office University Research Initiative Fellowship, and J. T. Remillard received partial support from a Howard Hughes Doctoral Fellowship.

References

1. See, e.g., the recent review by D. S. Chemla, S. Schmitt-Rink, and D. A. B. Miller, in *Nonlinear Effects and Instabilities in Semiconductors*, H. Haug, ed. (Academic, Orlando, Fla., 1988).
2. S. Schmitt-Rink, D. S. Chemla, and D. A. B. Miller, Phys. Rev. B **32,** 6601 (1985).
3. D. S. Chemla, D. A. B. Miller, P. W. Smith, A. C. Gossard, and W. Wiegmann, IEEE J. Quantum Electron. **QE-20,** 265 (1984).
4. S. Schmitt-Rink and C. Ell, J. Lumin. **30,** 585 (1985).
5. J. T. Remillard, H. Wang, D. G. Steel, J. Oh, J. Pamulapati, and P. K. Bhattacharya, Phys. Rev. Lett. **62,** 2861 (1989).
6. D. G. Steel and J. Remillard, Phys. Rev. A **36,** 4330 (1987).
7. B. S. Wherrett, A. L. Smirl, and T. F. Boggess, IEEE J. Quantum Electron. **QE-19,** 680 (1983).
8. D. G. Steel and S. C. Rand, Phys. Rev. Lett. **55,** 2285 (1985).
9. J. Hegarty, M. D. Sturge, A. C. Gossard, and W. Wiegmann, Appl. Phys. Lett. **40,** 132 (1982).
10. D. A. B. Miller, D. S. Chemla, D. J. Eilenberger, P. W. Smith, A. C. Gossard, and W. Wiegmann, Appl. Phys. Lett. **42,** 925 (1983).
11. J. D. Wiley, in *Semiconductors and Semimetals*, R. K. Willardson and A. C. Beer, eds. (Academic, New York, 1975), Vol. 10, p. 91.
12. J. Hegarty, L. Goldner, and M. D. Sturge, Phys. Rev. B **30,** 7346 (1984).
13. H. Haug, J. Lumin. **30,** 171 (1985); J. F. Müller, R. Mewis, and H. Haug, Z. Phys. B **69,** 231 (1987); S. Schmitt-Rink, D. S. Chemla, and H. Haug, Phys. Rev. B **37,** 941 (1988); M. Lindberg and S. W. Koch, Phys. Rev. B **38,** 3342 (1988).
14. P. R. Berman, J. Opt. Soc. Am. B **3,** 564 (1986).

QUANTUM WELLS FOR OPTICS AND OPTOELECTRONICS

1989 TECHNICAL DIGEST SERIES, VOLUME 10

CONFERENCE EDITION

Summaries of papers presented at the
Quantum Wells for Optics and Optoelectronics
Topical Meeting

March 6–8, 1989

Salt Lake City, Utah

Cosponsored by the

Air Force Office of Scientific Research
Lasers and Electro-Optics Society of IEEE
Optical Society of America

in Cooperation with

Quantum Electronics Group of the
Japan Society of Applied Physics

Optical Society of America
1816 Jefferson Place, N.W.
Washington, D.C. 20036
(202) 223-8130

High Resolution Nonlinear Laser Spectroscopy of Excitation and Relaxation Near the Band Edge in GaAs Quantum Well Structures

D.G. Steel, P.K. Bhattacharya, J.T. Remillard,
Hailin Wang, M.D. Webb, J. Pamulapati, J. Oh

Departments of Electrical Engineering and Physics
Harrison M. Randall Laboratory of Physics
The University of Michigan, Ann Arbor, Michigan 48109

The linear and nonlinear optical properties near the fundamental band edge of GaAs quantum well structures are important for applications of these materials to devices as well as providing new insight into the effects of quantum confinement. Excitons dominate the optical spectrum in this region, however, the coupling of excitons to the applied radiation field is modified by dynamical interactions due to the coupling of the exciton to the surrounding crystal lattice and the vacuum radiation field. At room temperature, the exciton is quickly ionized by phonons resulting in an electron-hole plasma which modifies the optical properties due to the effects of bandfilling and exchange that lead to strong optical nonlinearities.[1] At low temperature, the exciton is more stable and other effects such as *spontaneous emission, tunneling, diffusion,* and scattering from phonons and defects modify the optical properties. These processes can result in decay of the excitation as well as decay of the coherence or induced polarization between the initial and the excited state. In this paper, we describe the use of high resolution nonlinear laser spectroscopy based on four-wave mixing (FWM) to obtain lineshapes associated with the nonlinear susceptibility. The measurements provide new understanding of the physical processes associated with the relaxation of the exciton and the dynamics of the optical response. At low temperatures, FWM can often eliminate inhomogeneous broadening leading to a direct measurement of the exciton homogeneous lineshape.

The experimental configuration for these measurements is based on backward four-wave mixing using frequency stabilized tunable cw dye lasers. Two counterpropagating pump beams with fields $\vec{E}_f(\omega_f)$ and $\vec{E}_b(\omega_b)$ interact with a probe beam $\vec{E}_p(\omega_p)$ in the sample. The angle between the forward pump and probe beams is θ. The three beams interact through the nonlinear response to produce a signal field ($\vec{E}_s$) arising from a polarization proportional to $\chi^{(3)}(\vec{E}_f \cdot \vec{E}^*_p)\vec{E}_b$. For these measurements, $\vec{E}_f \| \vec{E}_p \perp \vec{E}_b$ (no signal is obtained for $\vec{E}_f \| \vec{E}_b \perp \vec{E}_p$ for low power cw excitation), and the signal arises from the coherent scattering of $\vec{E}_b$ from the traveling wave grating of excitation produced by

$\vec{E}_f \cdot \vec{E}_p^*$. By measuring $|E_s|^2$ as a function of $\omega_b - \omega_f$ for fixed $\delta = \omega_p - \omega_f$ (the FWMb response,) we obtain a lineshape associated with the fundamental excitation. By measuring $|E_s|^2$ as a function of δ for fixed ω_b (the FWMp response,) we obtain a lineshape related to relaxation rates associated with the excitation produced by the forward pump and probe.

The degenerate FWM response (DFWM where $\omega_f = \omega_b = \omega_p$) using cw excitation has been reported for both low temperature and room temperature[2,3]. For comparison, Fig. 1 shows the room temperature linear absorption and FWMb

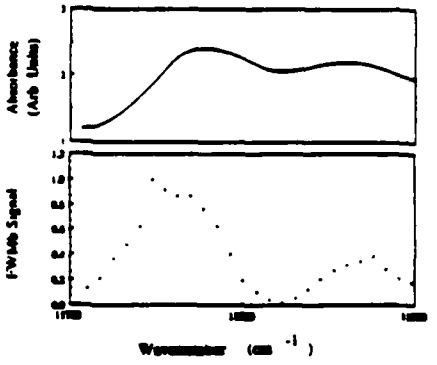

Figure 1. A comparison of the linear absorption spectrum and the FWMb reponse.

response showing two features corresponding to the heavy hole (HH1) and light hole (LH1). The ratio of the HH1 to LH1 FWMb response is expected to vary as the oscillator strength squared, in contrast to the more complex dependence in DFWM. In these measurememts, δ is fixed at 500kHz which reduces contributions from slow terms in the nonlinear response that (as shown below) dominate the cw nonlinear response and affect the ratio of the HH1 to LH1 response.

At room temperature, the exciton is ionized by LO phonons and the resultant e-h plasma modifies the fundamental parameters of the exciton such as the oscillator strength, resulting in the nonlinear response. A measurement of the FWMp response provides a linewidth determined by the dynamics of the e-h plasma. Figure 2 shows a typical FWMp spectrum, obtained at a forward pump-probe angle of $\theta = 10^{-2}$rad. The solid line is an excellent least squares fit of a simple Lorentzian. The width of the Lorentzian is given by the funtion $\gamma + D_a |\vec{k}_f - \vec{k}_p|^2$ where γ is the carrier recombination rate and D_a is the ambipolar diffusion coefficient. Because of ambipolar diffusion, the linewidth depends on angle, as seen in the inset [A]. The solid line is a fit of the above function where γ and D_a are adjusted to fit the data. We find $\gamma = 5$nsec and $D_a = 18 cm^2/sec$.

Using the method of correlated optical fields to eliminate interlaser jitter, we examined the FWMp response at the peak of the main curve in Fig. 2. The inset [B] shows the observed spectrum. The feature is extremely narrow

(≈30kHz) corresponding to a relaxation time of 10μsec and shows a clear interference feature associated with this profile. We note further that *the amplitude associated with the slow feature provides a nonlinear signal which is a factor of four above the "normal" faster component.* Hence, the importance of setting δ to be large in the FWMb response of Fig. 1b is now

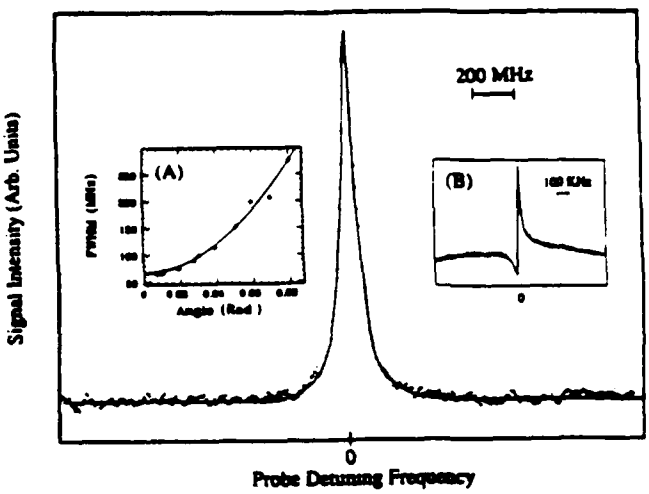

Figure 2. The FWMp response. The solid line is a Lorentzian. Inset [A] shows the angle dependence along with a fit of the expected response. Inset [B] shows the FWMp reponse obtained at the top of the main curve.

clear. It is also interesting to note that this slow component persists down to liquid helium temperatures and is clearly electronic in origin. Finally, we observe that the modified optical Bloch equations can predict such behavior,[4] though the physical origin of the structure is not understood.

At low temperature, the lineshapes and physical meaning change significantly, since the exciton is more stable. Figure 3 compares two FWMb

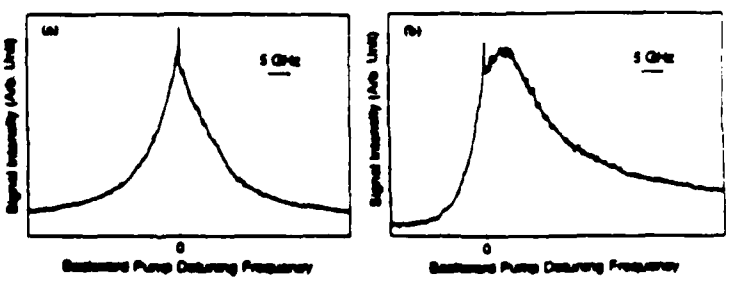

Figure 3. The FWMb response at two different excitation wavelengths at 5 K. (a) is 20cm^{-1} below the HH1 absorption maximum. (b) is at the HH1 aborption maximum.

lineshapes obtained at 5K, where the material is inhomogeneously broadened due to static fluctuations in well thickness. The FWMb response yields a spectral response given by the convolution of the *homogeneous lineshape* with itself. Figure 3a shows the FWMb response obtained 20cm^{-1} below the HH1 absorption peak (δ=500kHz) and Fig. 3b shows the response at the peak of the HH1 absorption. The data shows the evolution of a high energy tail due to

contributions from slow excitation decay terms in the nonlinear response, shown below. We believe this data represents a direct measurement of the homogeneous lineshape of the exciton. The data also indicates that the common assumption that the homogeneous lineshape of the exciton is Lorentzian may not always be appropriate.

The FWMp response also shows complex structure. Figure 4 shows the spectrum is clearly characterized by two resonances situated about δ=0. In fact, more careful study shows additional structure is present, consistent with at least 2 additional resonances within the bandwidth of the above spectrum, plus another resonance which is observed using the method of

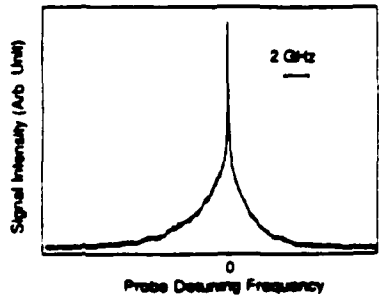

Figure 4. The FWMp response at 5 K.

correlated optical fields. Based on other work, we assign the broad resonance at the base of Fig. 4 as arising from radiative recombination, corresponding to a radiative recombination time of order 100psec. This number is consistent with other recent reports obtained at comparable optical intensity[5].

This work is supported by the U.S. Army Research Office, the Air Force Office of Scientific Research, and the National Science Foundation.

References:

1. D.S. Chemla and D.A.B. Miller, "Physics and Applications of Excitons Confined in Semiconductor Quantum Wells," in Heterojunctions: Band Discontinuities and Device Applications, F. Capasso and G. Margaritondo, eds., Elsevier Science Publisher B.V., 1987. D.S. Chemla, S. Schmitt-Rink, and D.A.B. Miller, "Nonlinear Optical Properties of Semiconductor Quantum Wells," in Nonlinear Effects and Instabilities in Semiconductors, H. Haug, ed., Academic Press, 1988.
2. J. Hegarty, M.D. Sturge, A.C. Gossard, and W. Wiegmann, App. Phys. Let. 40, 132 (1982)
3. D.A.B. Miller, D.S. Chemla, D.J. Eilenberger, P.W. Smith, A.C. Gossard, and W. Wiegmann, Appl. Phys. Lett. 42, 925 (1983).
4. J.T. Remillard, H. Wang, M.D. Webb, D.G. Steel, J. Oh, J. Pamulapati, and P.K. Bhattacharya, "High Resolution Nonlinear Laser Spectroscopy of Room Temperature GaAs Quantum Well Structures: Observation of Interference Effects," submitted for publication.
5. A. Honold, L Schultheis, J. Kuhl, C.W. Tu, XVI Int. Conf. Quan. Elec., Tech. Digest, Tokyo, p624 (1988).

Optical Phase Conjugation and Nonlinear Optical Bandpass Filter Characteristics in CdSSe Microcrystallite-Doped Glass

J. T. REMILLARD, H. WANG, M. D. WEBB, AND D. G. STEEL

Abstract—**This paper describes experimental measurements of the backward CW four-wave mixing response in semiconductor-doped glass in a regime important to applications. In particular, we show that lowering the operating temperature to 125 K yields a $\chi^{(3)} \approx 2 \times 10^{-4}$ esu. Aberration correction through optical phase conjugation is demonstrated with a phase conjugate reflectivity of 0.3 percent along with a wide-angle field-of-view response. In addition, we report on the nearly-degenerate four-wave mixing response of importance to tunable bandpass optical filters.**

SEMICONDUCTOR-DOPED glasses (SDG) have been the subject of considerable recent research because of their potential importance to new nonlinear optical devices and because they provide a material for the study of quantum confinement effects. These glasses are doped with microcrystallites of $CdS_{1-x}Se_x$ and are commercially available as sharp-cut color glass filters [1]. The commercial material is characterized by a wide distribution in microcrystallite size [2] (typically 100 Å in diameter with a FWHM size distribution of 50 Å) resulting in a featureless absorption edge at room temperature. (At low temperature, i.e., 5.4 K, these materials have shown spectral features attributed to quantum confinement in the luminescence [3].) However, special preparation procedures have enabled one group [4] to produce structures as small as 12 Å in CdS, CdSe, and CuCl and another group [2] has made glasses doped with microcrystallites where the size distribution is controlled by a heat treatment process and microcrystallites as small as 25 Å have been observed. These materials show clear structure in the room temperature optical absorption edge, believed to be due to the effects of quantum confinement [2], [4], [5].

The importance of SDG to device applications for optical switches and integrated optics has been recognized by numerous groups. Very early, the material was used to demonstrate a Q switch in a laser [6]. Optical bistability was demonstrated by McCall and Gibbs [7] and Gibbs et al. [8]; however the slow response suggested the nonlinearity was thermal in origin [9]. Using a Q-switched laser, Jain and Lind [10] demonstrated optical phase conjugation and showed that a large nonlinear optical susceptibility was observable ($\chi^{(3)} \approx 10^{-8}$ esu) using transient excitation. They determined that the relaxation time was faster than 8 ns (determined as an upper limit.) The model for the nonlinear response proposed by Jain and Lind was based on the production of a short-lived electron-hole plasma. This work was followed by numerous other experimental [11]–[20] and theoretical [21]–[23] reports of the nonlinear response using pulsed excitation. Included in these observations have been several measurements of the dynamical behavior [24]–[27] of key importance to high-speed applications. These measurements show carrier relaxation times are in the picosecond time domain. More recently, using the methods of ultrafast laser spectroscopy, measurements of transient absorption have shown relaxation processes occurring on the time scale of a few hundred femtoseconds [28], [29].

The large nonlinear optical susceptibility and fast response times have been important for several recent applications. In particular, 25 ps switching in optical bistability has been reported [30]. In addition, the use of this material for nonlinear wave guides [31]–[34], of importance to optical processing [35]–[37] has been examined.

In this paper, we examine the application of a slower but much larger nonthermal contribution to the nonlinear optical response obtained under CW excitation. The first indication of the possibility of a large CW nonlinear response was provided by the observation of low-frequency dynamical behavior leading to subharmonic generation and near chaotic behavior in SDG observed at low temperatures (140 K) by Zhedulev *et al.* [38]. The room temperature CW nonlinear response was measured by our group using DFWM and found to have $\chi^{(3)} \approx 10^{-7}$ esu and a narrow resonance (4.4 kHz) in the nearly-degenerate four-wave mixing (NDFWM) response corresponding to a 72 μs excitation relaxation time. The origin of the nonlinear dynamics is attributed to contributions from traps and is the subject of a more detailed experimental study to be presented elsewhere [40] which emphasizes the physics of the nonlinear process and the effect on trap dynamics of temperature, intensity, and energy transport. However, in the present paper, we show that reducing the

Manuscript received June 21, 1988; revised July 29, 1988. This work was supported in part by the Air force Office of Scientific Research under Grant 85-0280 and by the Office of Naval Research under Grant N 00014-86-0124. The work of M. D. Webb was supported by a University Research Initiative Fellowship from the Army Research Office.

The authors are with the Harrison M. Randall Physics Laboratory, University of Michigan, Ann Arbor, MI 48109.

IEEE Log Number 8825886.

temperatur to 125 K has a dramatic effect on $\chi^{(3)}$, increasing the value to 2×10^{-4} esu. Based on this result, we demonstrate behavior important to optical phase conjugation [41], including wide-angle field-of-view reflectivities as large as 0.3 percent, sufficient for self-pumped ring resonators [42], and tunable optical filtering [43], [44] with bandwidths (measured below saturation) on the order of a few hundred hertz.

The experimental configuration consists of two counterpropagating pump beams E_f and E_b and a probe beam E_p, which interact with the two pump beams in the glass. The glass is a standard 3 mm thick commercial sample (RG630 from Schott, with similar results observed in Corning material [45]). The angle between the forward pump and probe is small enough to ensure that there is complete overlap between the three beams. All three beams are focused by a 1 m focal length lens with a spot area of approximately 8×10^{-3} cm^2. The signal is produced by the induced nonlinear polarization proportional to $\chi^{(NL)}(E)\ E_f E_p^* E_b$ where the field dependencce of $\chi^{NL}(E)$ is intended to represent the possibility of saturation of the four-wave mixing nonlinear response due to higher order effects. (Clearly, under saturation conditions, the susceptibility is no longer third order.) As is well known, the phase-matching conditions result in a signal which is counterpropagating with respect to the probe beam. The signal was detected by either a PMT or an ordinary power meter (e.g., Coherent 212). Physically, the signal is a result of the scattering of the backward (forward) pump beam from the spatial modulation of the absorption and dispersion produced by the forward (backward) pump and probe beam.

The effect of temperature on the strength of the nonlinear response is shown in Fig. 1, where the phase conjugate reflectivity is given as a function of incident pump intensity (below saturation) for two different temperatures. The phase conjugate reflectivity is defined as the ratio of the signal power to the probe power. Corrections have been made for the losses at the windows of the dewar and the reflection loss of the sample. The solid line in the figure has a slope of two, corresponding to a quadratic dependence on pump intensity. The nonlinear response saturates as a function of inverse temperature below 125 K. As is evident in Fig. 1, the decrease in temperature results in a considerable increase in the nonlinear response as is evident by comparing the reflectivities and corresponding pump intensities in Fig. 1(a) to the much higher reflectivities and lower pump intensities of Fig. 1(b). The corresponding values for $\chi^{(3)}$ can be obtained using the expression [46] (in CGS units) $R = [(2\pi\omega/cn)\chi^{(3)}]^2 (8\pi/cn)^2 L^2 I_f I_b$, where R is the reflectivity, L is the interaction length, n is the index of refraction, c is the speed of light, ω is the frequency of the optical field (rad/s), and I_α is the intensity (erg/cm^2/s) of the α pump beam (no local field corrections are made and this susceptibility value includes the degeneracy factor.) We find that Fig. 1(a) corresponds to $\chi^{(3)} \approx 10^{-7}$ esu and Fig. 1(b) corresponds to $\chi^{(3)} \approx 10^{-4}$ esu.

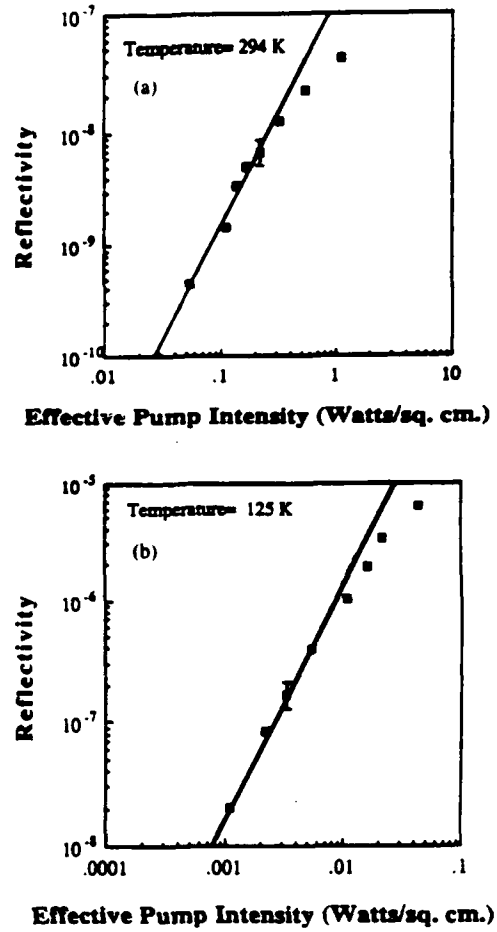

Fig. 1. The OPC reflectivity as a function of incident pump intensity. (a) 294 K. (b) 125 K. The solid lines have a slope of 2, corresponding to the unsaturated third-order response.

The model discussed for the CW nonlinear response [39] provides a physical explanation for this strong temperature dependence. Namely, the forward (backward) pump and probe couple a valence band to conduction band transition and produce a spatial modulation in the conduction band. Some fraction of this excitation decays to a deep-level trap, resulting in a spatial modulation of the absorption and dispersion associated with the populated trap. The strength of the spatial modulation of the trap is determined by the rate of filling of the trap and the trap lifetime. The trap lifetime is determined by thermal activation, hence, at lower temperatures the trap lifetime is longer, resulting in a stronger spatial modulation of the traps and a higher scattering efficiency of the backward (forward) pump.

However, the nonlinear response saturates at high pump intensity, as shown in Fig. 2. Currently, we believe that the onset of this saturation is the result of photoionization of the optically-excited trap. This conclusion is suggested because we have demonstrated that the NDFWM bandwidth, which is determined by the excitation relaxation rate, increases linearly with pump intensity due to photoionization of the trap. At low intensity, the NDFWM bandwidth (obtained by measuring the phase conjugate reflectivity as a function of the detuning of the probe beam

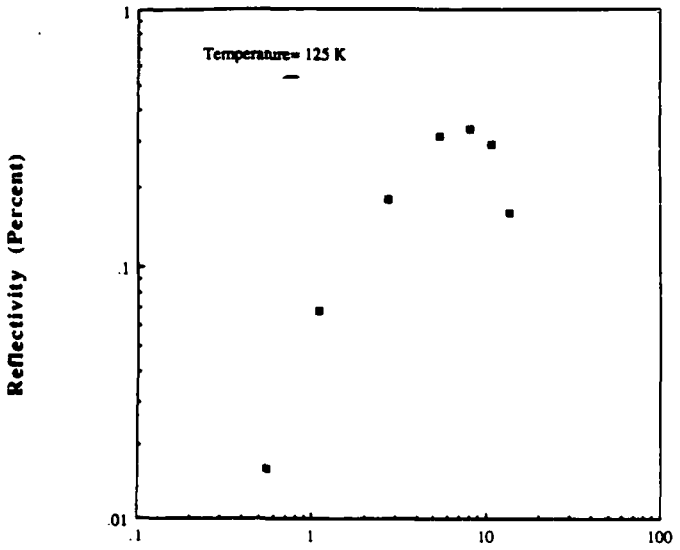

Fig. 2. The OPC reflectivity obtained at 125 K at high pump intensity. The data show the saturation of the nonlinear response.

frequency with respect to the fixed pump beam frequencies) is determined by the intrinsic trap lifetime. However, at high intensity, the trap lifetime is shortened by photoionization. In RG630, we see that the maximum reflectivity at this temperature is of order 0.3 percent but is limited by this saturation. It is possible that engineering of the microcrystallites may be able to decrease the photoionization cross section, thus enabling larger reflectivities.

Operating at the high reflectivity, a simple qualitative demonstration of optical phase conjugation was made using a thermally-distorted piece of glass as an aberrator. In the usual procedure, the far field of the probe beam was obtained at the focus of a 2 m focal length lens. Fig. 3(a) shows the expected near-diffraction-limited spot. A single pass through the aberrator results in the far-field pattern shown in Fig. 3(b). However, Fig. 3(c) shows the corrected beam obtained by allowing the phase conjugate signal produced by the aberrated probe beam to retrace its path back through the aberrator.

In addition to aberration correction, it was suggested very early that based on optical phase conjugation, the NDFWM response could be used for a bandpass optical filter [43]. The filtering action occurs because the phase conjugate reflectivity depends on the detuning of the probe frequency with respect to the pump frequency. In the original proposal, the material was assumed to have an instantaneous excitation relaxation rate and the filter bandwidth was determined by phase-matching restrictions on the detuning. However, the first demonstration of a filter was based on atomic sodium [44] and the filter bandwidth was determined by the excitation relaxation rate set by spontaneous emission. Unfortunately, for CW applications, the field of view of devices based on collisionless gas phase systems is limited by thermal motion. Optical

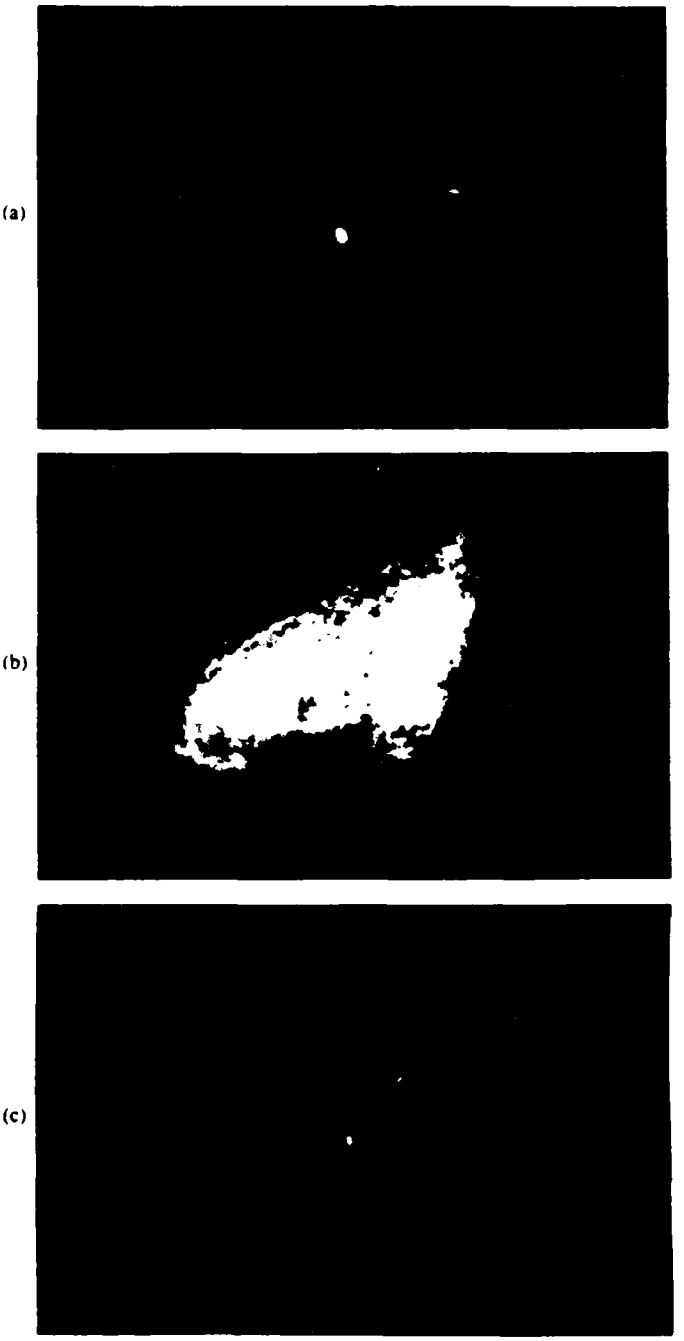

Fig. 3. A qualitative demonstration of aberration correction though CW OPC in semiconductor-doped glass. (a) Far-field intensity distribution of the incident probe beam. (b) Far-field intensity distribution of the probe beam after a single pass through the aberrator. (c) Demonstration of the correction of the aberration in (b) after reflection from the OPC and passing back through the aberrator.

filter characteristics in materials such as $Cr:YAlO_3$ [47] also have limited field of view because of energy diffusion. The field of view is determined by the decrease in the signal as the angle between the forward pump and probe increases.

To understand why thermal motion and energy diffusion limit the field of view of any device based on optical phase conjugation (including phase conjugate mirrors,) we note that as the angle increases, the period of spatial mod-

ulation decreases. In collisionless gas phase systems, if the transit time (determined by the spatial period spacing divided by the thermal velocity) is comparable to or smaller than the spontaneous emission lifetime, the spatial modulation "washes out," resulting in a decrease in the scattering efficiency. For small angles, the spacing is large and the transit time is long compared to the spontaneous emission lifetime, and there are no washout effects. However, for large angles, the transit time is reduced considerably and washout occurs, lowering the signal. Alternatively, for solid-state systems, the rate of energy diffusion depends on the gradient of the spatial modulation of the excitation. As in the gas phase system, if the energy diffusion time is comparable to the state lifetimes, the strength of the spatial modulation is reduced, again reducing the scattering efficiency. For small angles, this is usually not important. But for large angles, the gradient increases and the energy diffusion time decreases, again resulting in washout and reduced scattering efficiency. Hence, for optical phase conjugate mirror applications, these effects limit the field of view. However, in addition, thermal motion and energy diffusion both contribute to the rate of excitation relaxation. Hence, the NDFWM response and the corresponding filter properties also become angle dependent, with the NDFWM bandwidth increasing with larger angles. It is interesting to note that optical phase conjugation based on photorefractive properties in insulators are not characterized by large diffusion coefficients and therefore have a wide field of view and high efficiency [48], but are often limited by extremely-small bandwidths (e.g., 1 Hz).

In the semiconductor-doped glass, our earlier room temperature measurements show that the NDFWM bandwidth, obtained by measuring the reflectivity as a function of pump-probe detuning, provided a useful bandwidth on the order of 4.4 kHz, which is determined by the inverse trap lifetime. In addition, because the microcrystallites are surrounded by glass insulator and the microcrystallites are much smaller than the grating spacing associated with the nonlinear response, it was pointed out [10] that there should be no energy diffusion and no angle dependence in the nonlinear response, a result confirmed by our room temperature measurements.

To study the optical filter properties of SDG we first note that as the temperature is decreased, the NDFWM bandwidth decreases, which as we indicated earlier, is due to the fact that the trap lifetime increases. The physical reason for this is that when the probe frequency is detuned from the pump frequency, the fringes move through the medium. The time for the spatial modulation to move a half period is of order δ^{-1} (δ is the pump-probe detuning frequency.) If that time is long compared to the excitation relaxation time (trap lifetime), then there is no loss of scattering efficiency for the pump beam. However, if δ is large compared to the inverse relaxation time, the spatial modulation is washed out by the moving fringes, thus reducing the strength of the spatial modulation and the scattering efficiency. Note if the excitation decay rate is γ, then the NDFWM bandwidth (in hertz) is (γ/π). Therefore, the NDFWM bandwidth provides a measure of the real time response capability of the material.

To study the filter properties, we measured the NDFWM bandwidth using the method of correlated optical fields, a technique useful when the bandwidth is less than the interlaser jitter in a two laser measurement [47]. In this measurement, the pump beams and the probe beam are the first-order Bragg-scattered beams from two separate acoustooptic modulators driven by two phase-locked frequency synthesizers. In this way, the frequency of the probe beam can be independently varied with respect to the pump beams. The detuning is given by $\delta = \omega_{\text{probe}} - \omega_{\text{pump}}$. By using two modulators (one for the pumps and one for the probe) it is possible to scan through zero detuning.

The low intensity (unsaturated) NDFWM bandwidth is shown in Fig. 4 as a function of excitation frequency. The plot shows that at 125 K, narrow bandwidths (ranging from 215 to 430 Hz) can be obtained over a wide range of excitation frequencies. The excitation tuning bandwidth (100 Å) is determined by the slope of the filter absorption edge. The roll-off on the long wavelength end is due to decreased optical coupling in the material while the roll-off on the short wavelength end is due to pump absorption. The large bandwidth and narrow NDFWM response suggests that a tunable filter based on this material could have over 10^9 channels. Alternatively, such properties may be important to phase locking of narrow-band diode lasers. Larger bandwidths are obtained at higher pump powers, due to the decrease in trap lifetime by photoionization. At this time, the variation of the NDFWM response with excitation frequency is not completely understood.

Finally, for application to either OPC or optical filtering, we need to determine the angle dependence and thus field of view at low temperature. As discussed above, in SDG, the microcrystallites are small compared to an optical wavelength and surrounded by insulator, hence we would expect no excitation diffusion. For reasons which we do not completely understand at this point, we do observe an angle dependence at 125 K. Fig. 5 shows the NDFWM bandwidth of the grating produced by the forward pump and probe as a function of the forward pump-probe angle. For these measurements, the backward pump polarization was orthogonal to the copolarized forward pump and probe in order to eliminate the contribution from the grating produced by the backward pump and probe. For all beams copolarized, the angle dependence would be weaker since the back grating contribution would dominate for large angles with a bandwidth and efficiency similar to the forward grating at small angles. At low temperatures, the data suggest that even though the microcrystallites are surrounded by insulator, there is still energy transfer taking place, although the angle dependence is far from the predictions of simple diffusion. We should note, however, that even though the bandwidth variation is a factor of 4 over a field of view in the plane

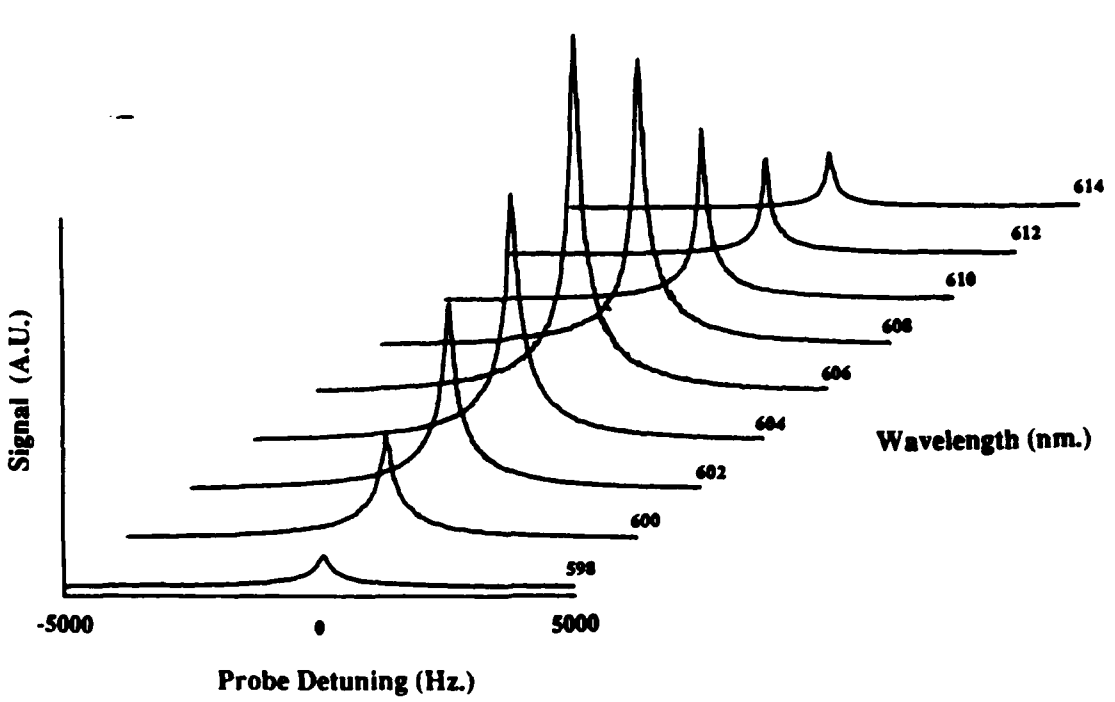

Fig. 4. The narrow bandpass optical filter characteristics of semiconductor-doped glass. The x axis is the pump probe detuning. The y axis is the signal magnitude. The z axis is the optical excitation frequency (note the pump-probe detuning is very small compared to the frequency of the optical excitation.) This data were obtained at pump intensity below saturation of the response.

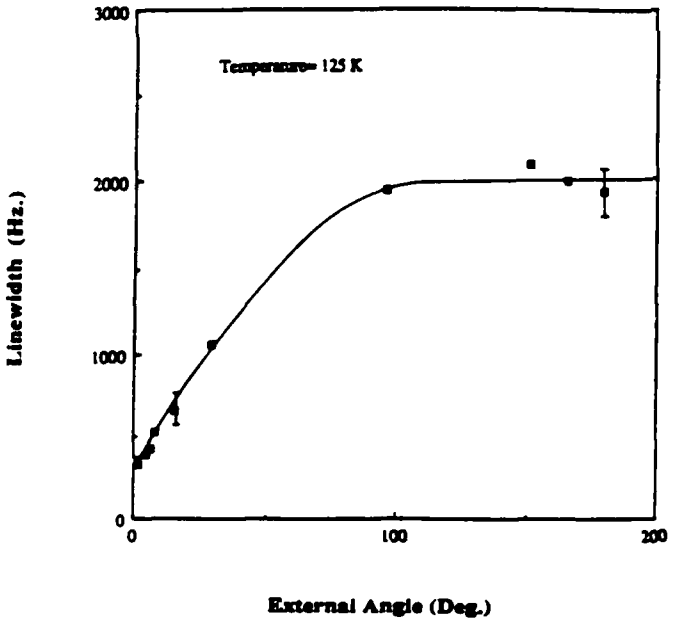

Fig. 5. The NDFWM bandwidth of the forward pump-probe grating as a function of angle between the forward pump and probe. The solid line is intended to guide the eye.

of π when the back pump beam is orthogonally polarized, this is quite small compared to many diffusion-limited materials. In addition, in the case that all beams are copolarized, the reflectivity and NDFWM bandwidth variations are less than a factor of 3 over 2π.

In summary, we have described the large third-order nonlinear optical response in CdSSE-doped glass. The optical phase conjugation reflectivities are limited to about 0.34 percent at 125 K (1 percent at 5 K) although the efficiency is certainly large enough to permit laboratory studies of real time aberration correction, for instance in studies of imaging through some forms of biological systems. Furthermore, the high efficiencies are obtainable with low-power lasers. In addition, we have described the behavior of this material as it might be important to tunable narrow-band optical filters. This latter example is interesting in that it might provide a convenient material to test filtering properties when the probe beam is a quasi-white light source.

References

[1] For example, Corning, Schott, Hoya, and Toshiba.

[2] N. F. Borrelli, D. W. Hall, H. J. Holland, and D. W. Smith, "Quantum confinement effects of semiconducting microcrystallites in glass," *J. Appl. Phys.*, vol. 61, pp. 5399-5409, 1987.

[3] J. Warnock and D. D. Awschalom, "Quantum size effects in simple colored glass," *Phys. Rev. B*, vol. 32, pp. 5529-5531, 1985.

[4] A. I. Ekimov and A. A. Onushchenko, "Size quantization of the electron energy spectrum in microscopic semiconductor crystal," *Pis'ma Zh. Eksp. Teor. Fiz.*, vol. 40, pp. 337-340, 1984 (*JETP Lett.*, vol. 40, pp. 1136-1139, 1984); ——, "Quantum size effect in three-dimensional microscopic semiconductor crystals," *Pis'ma Zh. Eksp. Teor. Fiz.*, vol. 34, pp. 363-366, 1981 (*JETP Lett.*, vol. 34, pp. 343-349, 1981); A. I. Ekimov, Al. L. Efros, and A. A. Onushchenka, "Quantum size effect in semiconductor microcrystals," *Solid State Commun.*, vol. 56, pp. 921-924, 1985.

[5] L. Banyai and S. W. Koch, "Absorption blue shift in laser-excited semiconductor microspheres," *Phys. Rev. Lett.*, vol. 57, pp. 2722-2724, 1986. See also, "Comment" by S. Schmitt-Rink, *Phys. Rev.*

Lett., vol. 60, p. 1205, and "Reply" by L. Banyai and S. W. Koch, p. 1206, 1988.
[6] G. Bret and F. Gires, "Giant-pulse laser and light amplifier using variable transmission coefficient glasses light switches," *Appl. Phys. Lett.*, vol. 4, pp. 175-176, 1964.
[7] S. L. McCall and H. M. Gibbs, "Optical bistability via thermal effects in a glass filter," *J. Opt. Soc. Amer. A*, vol. 68, p. 1378, 1978.
[8] H. M. Gibbs, G. K. Olbright, N. Peyghambarian, H. E. Schmidt, S W. Koch, and H. Haug, "Kinks: Longitudinal excitation discontinuities in increasing absorption optical bistability," *Phys. Rev. A*, vol. 32, pp. 692-694, 1985; see also, H. Gibbs, *Optical Bistability, Controlling Light with Light*. Orlando, FL: Academic, 1985.
[9] G. Thibault and M.-M. Denariez-Roberge, "Thermooptical effects observed in CdS,Se_{1-x} semiconductor doped glasses," *Can J. Phys.*, vol. 63, pp. 198-201, 1985.
[10] R. K. Jain and R. C. Lind, "Degenerate four-wave mixing in semiconductor-doped glasses," *J. Opt. Soc. Amer.*, vol. 73, pp. 647-653, 1983.
[11] S. S. Yao, C. Karaguleff, A. Gabel, R. Fortenbuery, C. T. Seaton, and G. Stegeman, "Ultrafast carrier and grating lifetimes in semiconductor-doped glasses," *Appl. Phys. Lett.*, vol. 46, pp. 801-802, 1985.
[12] P. Roussignol, D. Ricard, K. C. Rustagi, and C. Flytzanis, "Optical phase conjugation in semiconductor-doped glasses," *Opt. Commun.*, vol. 55, pp. 143-148, 1985.
[13] B. Danielzik, K. Nattermann, and D. von der Linde, "Nanosecond optical pulse shaping in cadmium-sulfide-selenide glasses," *Appl. Phys. B*, vol. 38, pp. 31-36, 1985.
[14] G. R. Olbright and N. Peyghanbarian, "Interferometric measurement of the nonlinear index of refraction, n_2, of CdS_xSe_{1-x}-doped glasses," *Appl. Phys. Lett.*, vol. 48, pp. 1184-1186, 1986.
[15] D. Cotter, "High-contrast ultrafast phase conjugation in semiconductor-doped glass," in *Proc. XIV Int. Quantum Electron. Conf.*, San Francisco, CA, postdeadline paper PD19-1, 1986.
[16] G. R. Olbright, N. Peyghambarian, S. W. Koch, and L. Banyai, "Optical nonlinearities in glasses doped with semiconductor microcrystallites," *Opt. Lett.*, vol. 12, pp. 413-415, 1987.
[17] F. Hache, P. Roussignol, D. Ricard, and C. Flytzanis, "Measuring the phase of slow Kerr-type nonlinearities: The role of phase modulation," *Opt. Commun.*, vol. 64, pp. 200-204, 1987.
[18] F. de Rougemont, R. Frey, P. Roussignol, D. Ricard, and C. Flytzanis, "Evidence of strong Auger recombination in semiconductor in semiconductor-doped glasses," *Appl. Phys. Lett.*, vol. 50, pp. 1619-1621, 1987.
[19] P. Roussignol, M. Kull, D. Ricard, F. de Rougemont, R. Frey, and C. Flytzanis, "Time-resolved direct observation of Auger recombination in semicondcutor doped glasses," *Appl. Phys. Lett.*, vol. 51, pp. 1882-1884, 1987.
[20] P. Roussignol, D. Ricard, J. Lukasik, and C. Flytzanis, "New results on optical phase conjugation in semiconductor-doped glasses," *J. Opt. Soc. Amer. B*, vol. 4, pp. 5-13, 1987.
[21] K. C. Rustagi and C. Flytzanis, "Optical nonlinearities in semiconductor-doped glasses," *Opt. Lett.*, vol. 9, pp. 344-345, 1984.
[22] C. Flytzanis, F. Hache, D. Ricard, and Ph. Roussignol, "Optical nonlinearities in small particles and composite materials," in *The Physics and Fabrication of Microstructures and Microdevices*, M. J. Kelly and C. Weisbuch, Eds. Berlin, West Germany: Springer, 1986.
[23] E. Hanamura, "Very large optical nonlinearity of semiconductor microcrystallites," *Phys. Rev. B*, vol. 37, pp. 1273-1279, 1988.
[24] J. Warnock and D. D. Awschalom, "Picosecond studies of electron confinement in simple colored glasses," *Appl. Phys. Lett.*, vol. 48, pp. 425-427, 1986.
[25] S. C. Hsu and H. S. Kwok, "Picosecond carrier recombination dynamics of semiconductor-doped glasses," *Appl. Phys. Lett.*, vol. 50, pp. 1782-1784, 1987.
[26] K. Shum, G. C. Tang, M. R. Junnarkar, and R. R. Alfano, "Electron-hole recombination lifetimes in a quasi-zero dimensional electron system in CdS_xSe_{1-x}," *Appl. Phys. Lett.*, vol. 51, pp. 1839-1841, 1987.
[27] M. Tomita, T. Matsumoto, and M. Jatsuoka, "Ultrafast optical nonlinearity in semiconductor-doped glasses controlled through the trapping state," *Proceedings of the Conference on Ultrafast Phenomena*, Berlin, West Germany: Springer, 1988.
[28] M. C. Nuss, W. Zinch, and W. Kaiser, "Femtosecond carrier relaxation in semiconductor-doped glasses," *Appl. Phys. Lett.*, vol. 49, pp. 1717-1719, 1986.
[29] N. Peyghambarian and S. W. Koch, "Femtosecond and coherent effects in bulk CdSe and $CdSe_xSe_{1-x}$ doped glasses," *Revue Phys. Appl.*, vol. 22, pp. 1711-1715, 1987.
[30] J. Yumoto, S. Fukushima, and K.-I. Kubodera, "Observation of optical bistability in CdS_xSe_{1-x}-doped glasses with 25-psec switching time," *Opt. Lett.*, vol. 12, pp. 832-834, 1987.
[31] S. Patela, H. Jerominek, C. Delisle, and R. Tremblay, "Nonlinear optical properties of thin-film waveguides deposited onto semiconductor-doped glasses," *J. Appl. Phys.*, vol. 60, pp. 1591-1594, 1986.
[32] T. J. Cullen, C. N. Ironside, C. T. Seaton, and G. I. Stegeman, "Semiconductor-doped glass ion-exchanged waveguides," *Appl. Phys. Lett.*, vol. 49, pp. 1403-1405, 1986.
[33] Z. Jakubczyk, J. Jerominek, S. Patela, R. Tremblay, and C. Delisle, "Power-transfer effects in monomode optical nonlinear waveguiding structures," *Opt. Lett.*, vol. 12, pp. 750-752, 1987.
[34] A. Gabel, K. W. DeLong, C. T. Seaton, and G. I. Stegeman, "Efficient degenerate four-wave mixing in an ion-exchanged semiconductor-doped glass waveguide," *Appl. Phys. Lett.*, vol. 51, pp. 1682-1684, 1987.
[35] C. T. Seaton, X. Mai, G. I. Stegeman, and H. G. Winful, "Nonlinear guided wave applications," *Opt. Eng.*, vol. 24, pp. 593-599, 1985.
[36] G. I. Stegeman and C. T. Seaton, "Nonlinear integrated optics," *J. Appl. Phys.*, vol. 58, pp. R57-R78, 1985.
[37] C. T. Seaton, J. D. Valera, R. L. Shoemaker, G. I. Stegeman, J. T. Chiwell, and S. D. Smith, "Calculations of nonlinear TE waves guided by thin dielectric films bounded by nonlinear media," *IEEE J. Quantum Electron.*, vol. QE 21, pp. 774-783, 1985.
[38] N. I. Zheludev, I. S. Ruddock, and R. Illingworth, "Generation and amplification of subharmonics in semiconductor-doped glass by a modulated argon-ion laser," *J. Mod. Opt.*, vol. 34, pp. 1257-1262, 1987.
[39] J. T. Remillard and D. G. Steel, "Narrow nonlinear-optical resonances in CdSSE-doped glass," *Opt. Lett.*, vol. 13, pp. 30-32, 1988.
[40] J. T. Remillard, H. Wang, M. D. Webb, and D. G. Steel, "High resolution nonlinear laser spectroscopy of temperature, optical intensity and angle dependent relaxation in CdSSe microcrystallite doped glass," to be published, 1989.
[41] R. A. Fisher, Ed., *Optical Phase Conjugation*. New York: Academic, 1983; B. Ya. Zel'dovich, N. F. Pilipetsky, and V. V. Shkumov, *Principles of Phase Conjugation*. Berlin, West Germany: Springer, 1985; D. M. Pepper, "Nonlinear optical phase conjugation," in *Laser Handbook, Vol. 4*, M. L. Stitch and M. Bass, Eds. Amsterdam, The Netherlands: North-Holland, 1985.
[42] A ring resonator operated with even lower reflectivities was recently reported by G. Grynberg and M. Pinard: "Four-wave mixing oscillation in a ring cavity: A new type of optical gyro," *Tech. Dig. IQEC'88*, 1988, paper Tuf-1, pp. 264-265.
[43] D. M. Pepper and R. L. Abrams, "Narrow optical bandpass filter via nearly degenerate four-wave mixing," *Opt. Lett.*, vol. 3, pp. 212-214, 1978.
[44] J. Nilsen, N. S. Gluck, and A. Yariv, "Narrow-band optical filter through phase conjugation by nondegenerate four-wave mixing in sodium vapor," *Opt. Lett.*, vol. 6, pp. 380-382, 1981.
[45] We note that in thin material (< 1 mm), the absorption edge is closer to the band edge and we have observed different behavior in this regime.
[46] A. Yariv and D. M. Pepper, "Amplified reflection, phase conjugation and oscillation in degenerate four-wave mixing," *Opt. Lett.*, vol. 1, pp. 16-18, 1977.
[47] D. G. Steel and S. C. Rand, "Ultranarrow nonlinear optical resonances in solids," *Phys. Rev. Lett.*, vol. 55, pp. 2285-2288, 1985.
[48] *J. Opt. Soc. Amer. B*, Special issue on Photorefractive Materials vol. 5, 1988.

J. T. Remillard, photograph and biography not available at the time of publication.

H. Wang, photograph and biography not available at the time of publication.

M. D. Webb, photograph and biography not available at the time of publication.

D. G. Steel, photograph and biography not available at the time of publication

To be published in Surface Science, 1990

High Resolution Laser Spectroscopy of Relaxation and the Excitation Line Shape of Excitons in GaAs Quantum Well Structures

Hailin Wang, J.T. Remillard, M.D. Webb and D.G. Steel
J. Pamulapati, J. Oh and P.K. Bhattacharya
Departments of Physics and Electrical Engineering
Harrison M. Randall Physics Laboratory
University of Michigan, Ann Arbor, MI 48109

ABSTRACT

A new class of measurements on GaAs quantum well structures based on frequency domain nonlinear laser spectroscopy is described. Room temperature measurements of the excitation relaxation show an interference effect in the line shape which is interpreted as a shift in exciton frequency. Low temperature measurements on the localized exciton provide an excitation line shape which eliminates the effects of inhomogeneous broadening and shows the presence of spectral diffusion.

The room temperature nonlinear optical response near the band edge in GaAs quantum wells has resulted in considerable interest in these materials because of their potential importance to optoelectronic devices.[1] Studies of these materials have also resulted in new understanding of the fundamental physics of excitons.[2,3,4] In this paper, we describe a new class of measurements based on high resolution frequency domain nonlinear laser spectroscopy which are distinguished from earlier measurements because of the ability to report on excitation line shapes as well as the ability to provide greater sensitivity in measurements of excitation relaxation. The measurements of the excitation line shape are significant because this spectroscopy eliminates the contribution of inhomogeneous broadening which characterizes low temperature absorption measurements.

The basic experimental configuration for these experiments is based on backward four wave mixing.[5] In these experiments, two optical beams

intersect each other at a small angle. One beam is designated the probe beam with field amplitude $\vec{E}_p(\omega_p,\vec{k}_p)$ while the remaining beam is the forward pump beam with field amplitude $\vec{E}_f(\omega_f,\vec{k}_f)$. The beams are nearly normal to the growth direction of the quantum well and produce an interference pattern which results in a spatial and temporal modulation of excitation proportional to $\vec{E}_f(\omega_f,\vec{k}_f)\circ\vec{E}^*_p(\omega_p,\vec{k}_p)$. A coherent signal, $\vec{E}_s(\omega_s,\vec{k}_s)$, is produced by the scattering of a back beam with field amplitude $\vec{E}_b(\omega_b,\vec{k}_b)$. Spectroscopic information is obtained by varying any one frequency with respect to the remaining two frequencies. In particular, the FWMp response is obtained by varying ω_p holding $\omega_f=\omega_b$ while the FWMb response is obtained by varying ω_b, holding $\omega_p-\omega_f$=constant. The FWMp response provides a line shape related to the excitation decay rate and contains contributions such as inelastic scattering and carrier or excitonic recombination in addition to the contribution of nonradiating states. The FWMb response provides a measure of the excitation line shape without contributions from inhomogeneous broadening.[5,6]

At room temperature, the exciton absorption line shape is dominated by homogeneous broadening due to the rapid LO phonon ionization rate. Hence, a study of the FWMb response provides little additional information. However, the nonlinear response arises because the electron-hole plasma generated from the ionization of the exciton results in band filling and exchange effects which lead to a modification of the optical properties of the exciton including the oscillator strength, dephasing rate, and resonance frequency. Hence, a grating produced by the interference of the forward pump and probe has a decay rate determined by the e-h recombination time and the time it takes carriers to spatially diffuse across the grating. Figure 1a shows the FWMp response at room temperature along with a fit of a Lorentzian. The line width is given by $\gamma_{e-h} + D|\Delta\vec{k}|^2$ where γ_{e-h} is the e-h

recombination rate, D is the ambipolar diffusion coefficient, and $|\Delta\vec{K}| = |\vec{k}_f - \vec{k}_p|$. Figure 1b shows the angle dependence of the FWMp line width as a function of angle and the solid line is a fit of the above line width expression. From the shape of the curve, we can obtain the ambipolar diffusion coefficient (18 cm^2/sec) and from the y-intercept, we can obtain the e-h recombination rate (5 nsec.)

Using the method of correlated optical fields[7] to eliminate interlaser jitter contributions to the line shape, we examined the FWMp response near $\omega_p - \omega_f = 0$. Figure 2a shows the line shape. There are two important observations which can be drawn from Fig. 2a. First, there exists a strong (dominant) contribution to the room temperature nonlinear response which is slow (10μsec). Secondly, the line shape is characterized by a shape which is typical of interference effects.[8] We believe this line shape is due to a shift in the exciton resonance. Solutions to the optical Bloch type equations which have been phenomenologically modified to account for bandfilling and exchange effects show that this interference profile results when the Bloch equations are further modified to account for a shift in the exciton resonance.[9] The curve in Fig. 2b is the calculated FWMp response, showing the interference line shape. It is important to stress that the solutions of the modified Bloch equations only show interference effects when the exciton resonance is allowed to shift due to the presence of the e-h plasma or some other laser induced mechanism. We also note that the shape of the FWMp response is dependent on the wavelength of the back pump. Figure 2c shows the FWMp line shape measured when the back pump is tuned red of the peak of the heavy hole exciton. (The forward pump and probe beams remained tuned on the peak of the heavy hole exciton.) Figure 2d shows the line shape calculated from the modified Bloch equations when the back pump is shifted red of the exciton resonance.

At low temperatures, the excitons are stable against phonon ionization. Hence, studies of relaxation provide information on the exciton dynamics. In addition, because the exciton is now stable, data obtained from the FWMb response provide information on the excitation line shape. At 5 K, the absorption line shape is inhomogeneously broadened due to fluctuations in the well thickness. The HH1 absorption line width in this sample is 3.7 meV. The sample was further characterized by performing luminescence measurements as well as obtaining a degenerate four wave mixing (DFWM) spectrum. (A DFWM spectrum is obtained by using one laser for all beams in the nonlinear interaction and observing the change in intensity of the signal as the frequency of the laser is tuned across the exciton resonance.) The peak of the luminescence from the excitons is shifted 2.8 meV to the red of the HH1 absorption maximum. The red shifted luminescence is interpreted as being due to the recombination of excitons which have become localized due to fluctuations in well thickness. The DFWM measurements show a peak which coincides exactly with the luminescence peak, suggesting the nonlinear response is also due to localized excitons.

In the first set of measurements, we examined the FWMp response to determine the excitation relaxation dynamics. In the simple picture of the exciton undergoing a single relaxation due to radiative decay, the line shape would be a single Lorentzian. Figure 3 shows the FWMp line width obtained at 5 K. The curve shows clear evidence of multiple decay processes rather than a single decay. In particular, three decay channels are observed in Fig. 3. The fastest and slowest channels having relaxation times of 100 psec and 15 nsec are clearly observed in this figure. However a third component to the line shape corresponding to a relaxation time of 1.5 nsec is observable upon expansion of the center portion of the figure. The 1.5 nsec feature corresponds to the expected radiative decay time for a

well of thickness of 98A.[10] The origin of the 100 psec feature is most likely due to decay of the excitation by spectral diffusion via phonon assisted tunneling. Similar behavior has been reported in transient pump-probe measurements.[4] Further evidence for this is given below. The origin of the 15 nsec decay rate is due possibly to the presence of electric fields in the material which are known to extend the life time of the exciton.

FWMb experiments were then conducted to determine the line shape of the excitation. Note that the energies at which the following FWMb line shapes were recorded are referenced with respect to the position of the peak of the absorption. Figure 4a shows the FWMb line shape obtained 3.45 meV to the low energy side of the absorption maximum. The line shape is slightly asymmetric on the high energy side. This asymmetry becomes much clearer in the FWMb spectra recorded at the absorption line center as seen in Fig. 4b. The presence of asymmetry in the FWMb response is highly significant, since it can be shown[6] that if we are measuring just the homogeneous line shape, the FWMb response should be symmetric about $\omega_b-\omega_f=0$, even if the homogeneous line shape is asymmetric. However, such asymmetric line shapes can be observed in the FWMb response in the presence of spectral diffusion. Hence we believe these measurements show directly that excitons are spectrally diffusing, as suggested by earlier work.[4] Figure 4c shows a comparison of the measured temperature dependence of the line width in 4a to a theory based on phonon assisted tunnelling. The curve varies as $e^{\beta T^{1.6}}$ and is in general agreement with theoretical expectations.[11]

Further evidence for spectral diffusion is shown in Fig. 5. Figure 5a is an extended scan of the data shown in Fig. 4b at 5 K. Figure 5b shows the same data taken at 15 K illustrating the spectral diffusion of excitons to lower energies, the peak of the response occuring at the same energy as

the peak of the luminescence. As in the case of the luminescence peak, the wide resonance in the FWMb spectra shown in figure 5b represents the energy distribution of the localized excitons. Theoretical results of the FWMb line shape obtained from optical Bloch type equations, modified to include spectral diffusion, show similar behavior. It is interesting to note that while we obtain clear evidence for energy diffusion, there is no evidence in the data to suggest that the excitons are spatially diffusing.

In summary, we have used high resolution frequency domain nonlinear spectroscopy to study relaxation and excitation line shapes in GaAs multiple quantum wells. At room temperature, we have measured the ambipolar diffusion coefficient and the free carrier recombination time. In addition, we have observed an interference effect in the FWMp line shape which we believe is due to a shift in the exciton resonance. At low temperatures, we have identified contributions to the relaxation of the exciton population due to spectral diffusion and exciton recombination. Using FWMb spectroscopy, we have obtained measurements of the line shape of the excitation. The observation of asymmetric FWMb line shapes and the measured temperature dependence of the line width provide evidence that the excitons are spectrally diffusing via phonon assisted tunnelling.

This work is supported by the AFOSR, U.S. ARO and the U.S. ARO URI.

References

1. D.S. Chemla, S. Schmitt-Rink, and D.A.B. Miller, "Nonlinear Optical Properties of Semiconductor Quantum Wells," in Nonlinear Effects and Instabilities in Semiconductors, H. Haug, ed., Academic Press, 1988.

2. S. Schmitt-Rink, D.S. Chemla, and D.A.B Miller, Phys. Rev. B, 32, 6601 (1985).

3. D.S. Chemla and D.A.B. Miller, JOSA B 2, 1155 (1985).

4. J. Hegarty and M.D. Sturge, J. Opt. Soc. Am. B 2, 1143 (1985).

5. D.G. Steel and J.T. Remillard, Phys. Rev. A 36, 4330 (1987).

6. J.T. Remillard, H. Wang, D.G. Steel, J. Oh, J. Pamulapati, and P.K. Bhattacharya, Phys. Rev. Lett 62, 2861 (1989).

7. D.G. Steel and S. Rand, Phys. Rev. Lett. 55, 2285 (1985).

8. Interference effects are common in nonlinear laser spectroscopy as discussed in M.D. Levenson and S. Kano in Introduction to Nonlinear Laser Spectroscopy, revised edition,Academic Press Inc. 1988 p. 156. However, the origin of the interference effects in this paper is new and distinct.

9. J.T. Remillard, H. Wang, M.D. Webb, D.G. Steel, J. Oh, J. Pamulapati, and P.K. Bhattacharya," High Resolution Nonlinear Laser Spectroscopy of Room Temperature GaAs Quantum Well Structures: Observation of Interference Effects",accepted for publication in Opt. Lett, 1989.

10. J. Feldmann, G. Peter, E.O. Gobel, P. Dawson, K. Moore, C. Foxxon, and R.J. Elliot, Phys. Rev. Lett. 59, 2337 (1987).

11. T. Takagahara, Phys. Rev. B. 32, 7013 (1985).

Figure Captions

Figure 1. Figure 1a shows the room temperature FWMp line shape. Figure 2a shows the angle dependence of the FWMp line width.

Figure 2. The FWMp line shape using the technique of correlated fields. Figure 2a shows the interference profile when the back beam wavelength is on the exciton peak. Figure 2c shows the line shape when the back beam is tuned red of the exciton peak. Figures 2b and 2d show the calculated line shapes using modified Bloch equations.

Figure 3. The FWMp line shape at 5 K showing the presence of multiple relaxation mechanisms.

Figure 4. The FWMb line shape at 5 K. Figure 4a shows the line shape red of the absorption maximum. Figure 4b shows the line shape measured at the peak of the exciton absorption. Figure 4c shows the temperature dependence of the line width in figure 4a.

Figure 5. FWMb response shown for 2 temperatures. Figure 5a shows the response at 5 K. Figure 5b shows the response at 15 K illustrating the spectral diffusion of the excitation to lower energies.

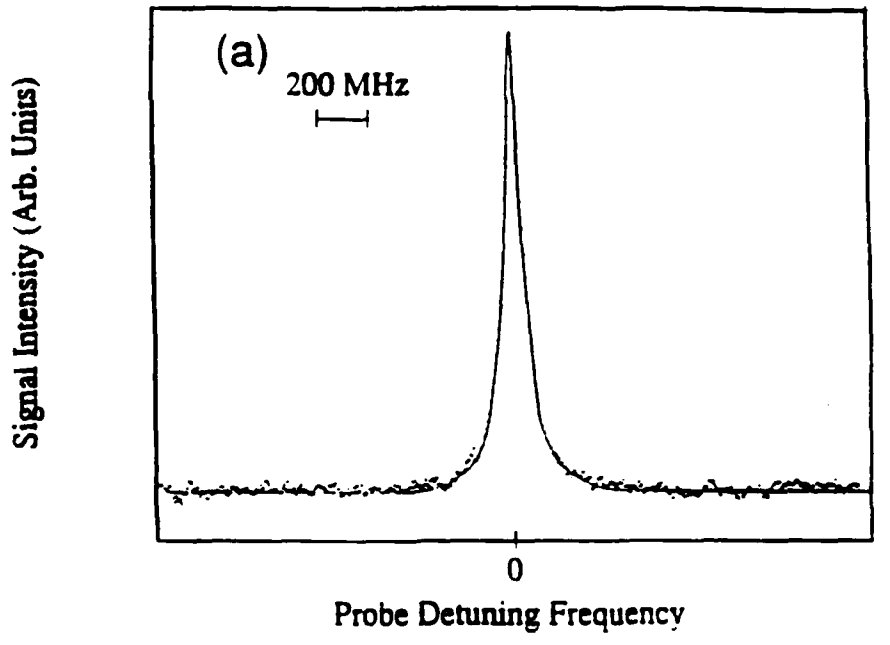
(a)
200 MHz
Signal Intensity (Arb. Units)
0
Probe Detuning Frequency

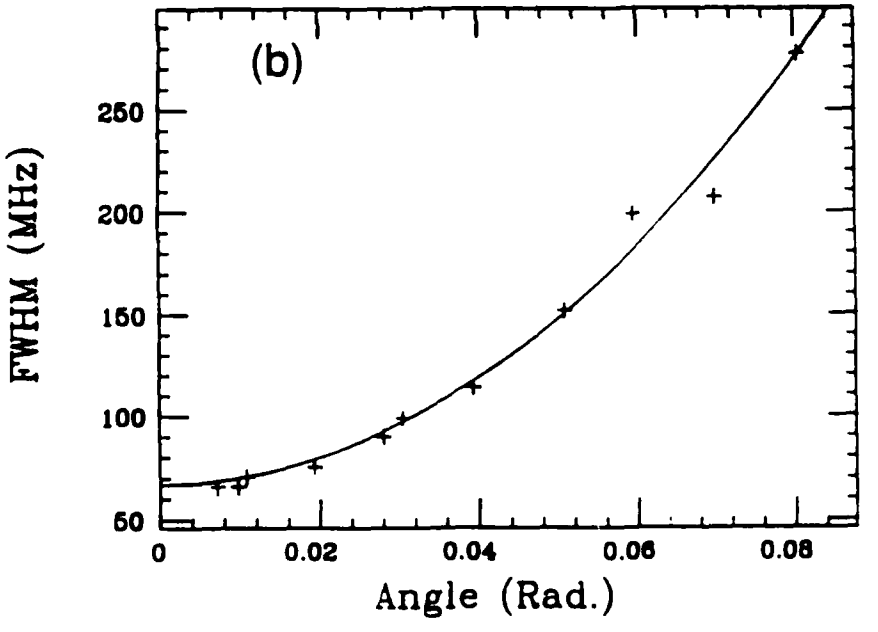
(b)
FWHM (MHz)
250
200
150
100
50
0
0.02
0.04
0.06
0.08
Angle (Rad.)

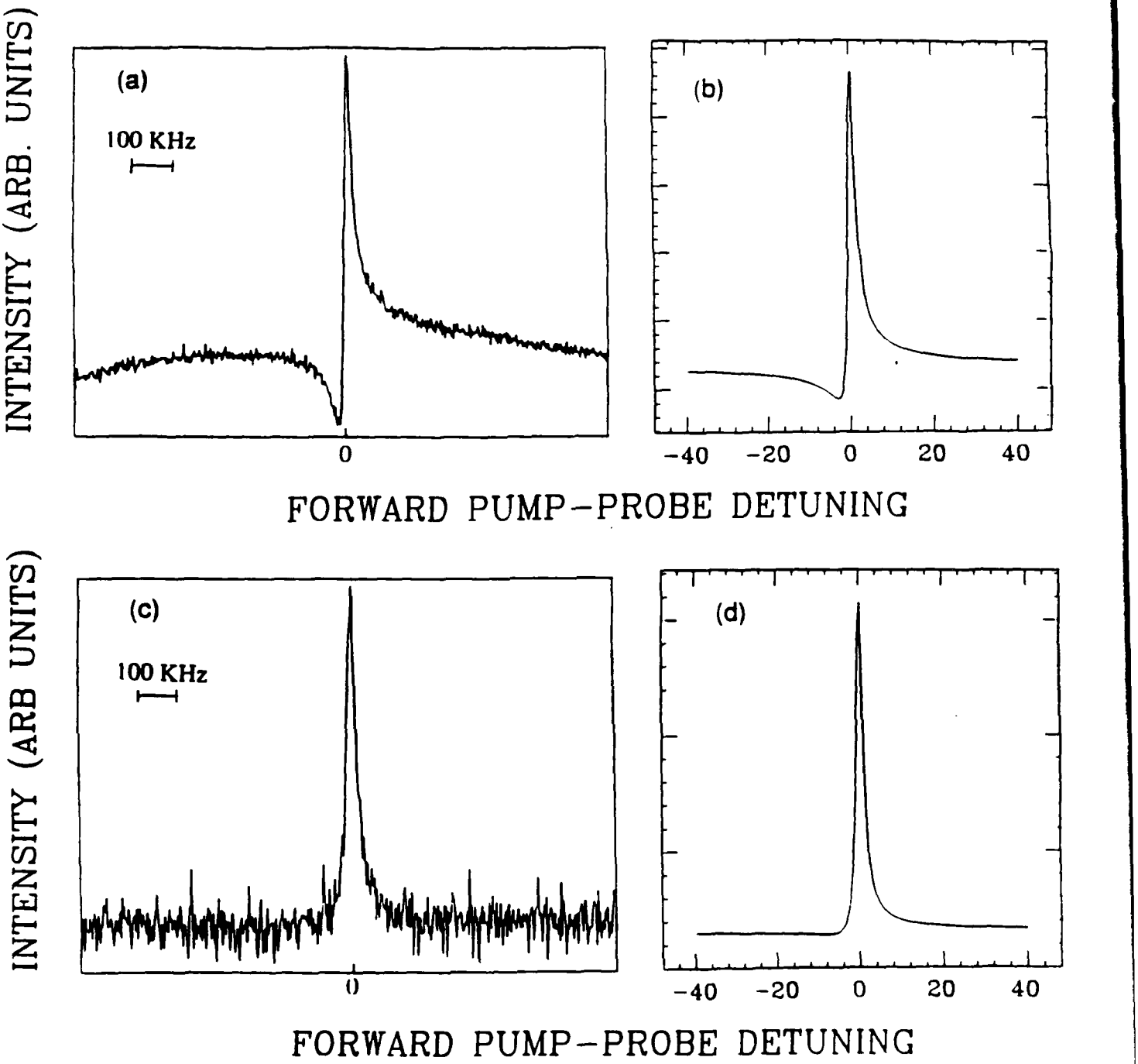
INTENSITY (ARB. UNITS)
(a)
100 KHz
0
(b)
-40
-20
0
20
40
FORWARD PUMP-PROBE DETUNING
INTENSITY (ARB UNITS)
(c)
100 KHz
0
(d)
-40
-20
0
20
40
FORWARD PUMP-PROBE DETUNING

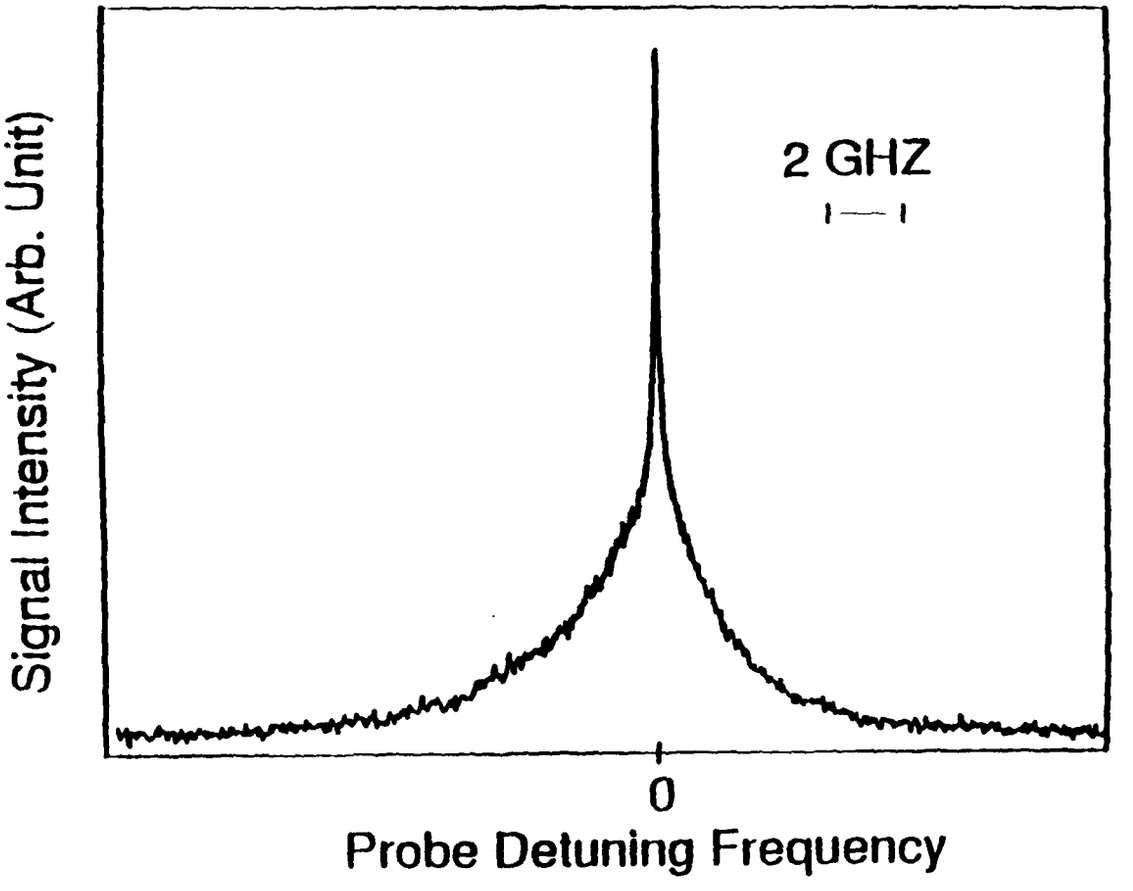
Signal Intensity (Arb. Unit)
2 GHZ
0
Probe Detuning Frequency

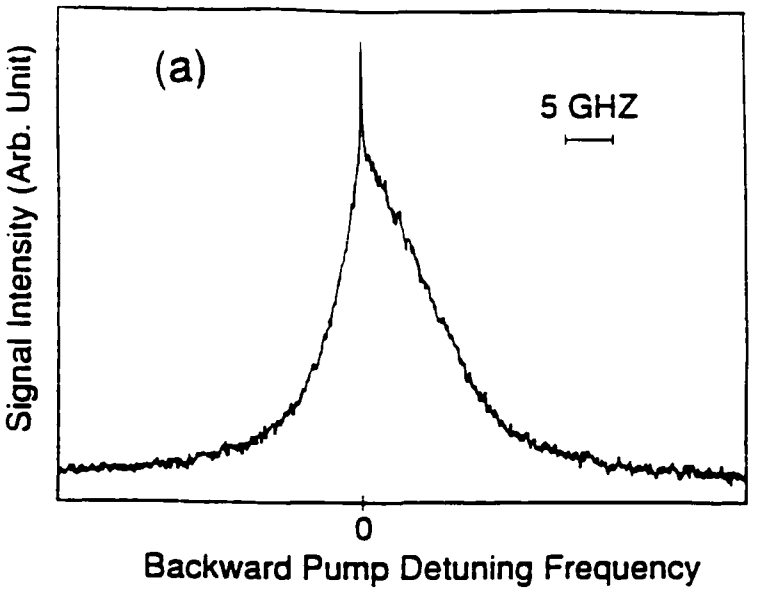
(a)
5 GHZ
Signal Intensity (Arb. Unit)
0
Backward Pump Detuning Frequency

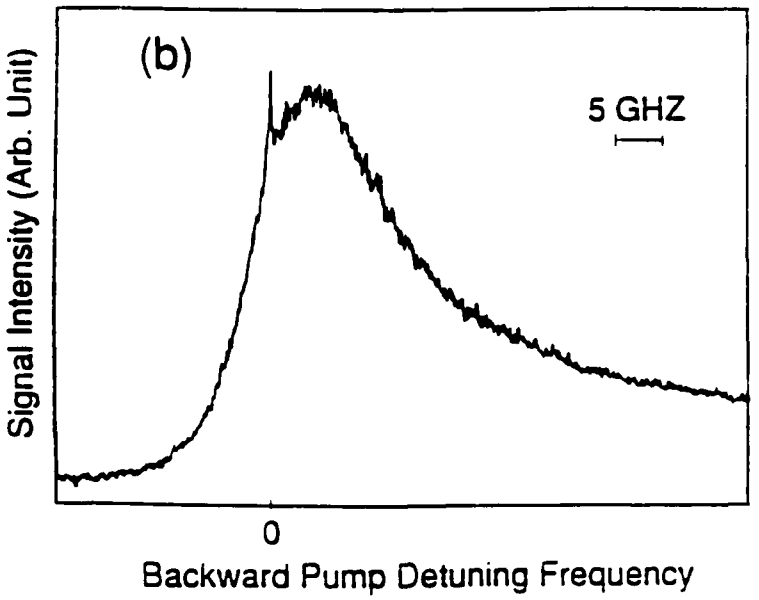
(b)
5 GHZ
Signal Intensity (Arb. Unit)
0
Backward Pump Detuning Frequency

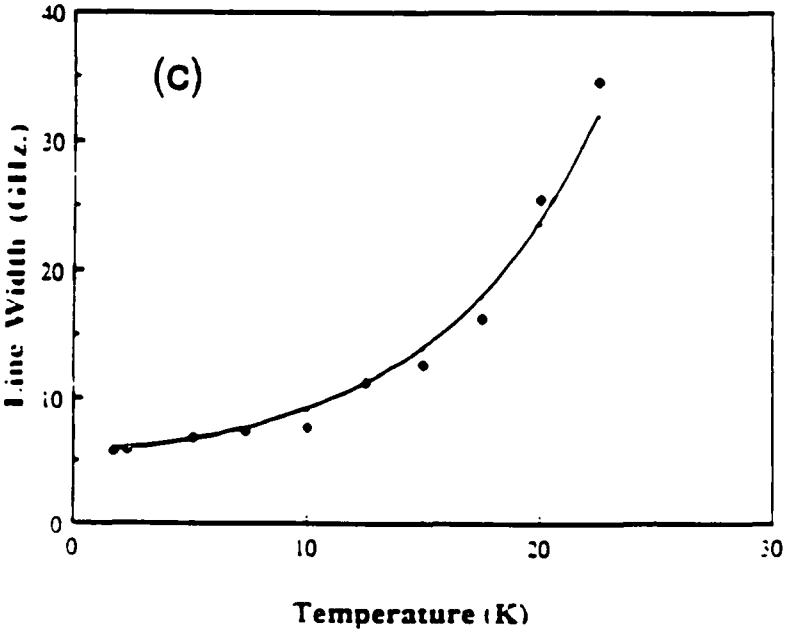
(c)
40
30
20
10
0
0
10
20
30
Temperature (K)

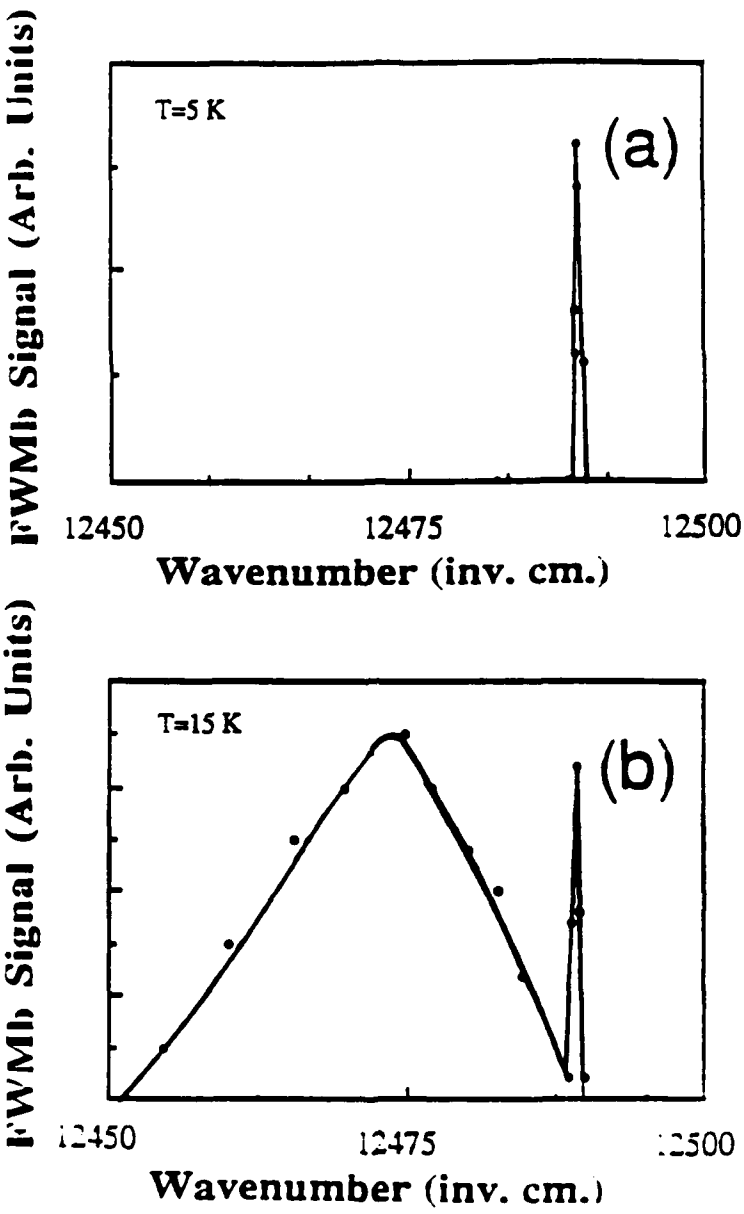
T=5 K
(a)
FWMb Signal (Arb. Units)
12450
12475
12500
Wavenumber (inv. cm.)
T=15 K
(b)
FWMb Signal (Arb. Units)
12450
12475
12500
Wavenumber (inv. cm.)

To be published in JOSA-B, 1990

Frequency Domain Four Wave Mixing Spectroscopy of Temperature and Optical Intensity Dependent Relaxation in CdSSe Microcrystallite Doped Glass

J.T. Remillard, H. Wang, M.D. Webb, D.G. Steel
Departments of Physics and Electrical Engineering
Randall Laboratory of Physics
University of Michigan
Ann Arbor, MI 48109

ABSTRACT

This paper describes cw frequency domain nonlinear laser spectroscopy results obtained in the study of relaxation in glasses doped with microcrystallites of CdSSe. Measurements are made as a function of temperature and optical intensity using low intensity cw optical excitation. The results are interpreted based on the assumption that the dynamics of the nonlinear response in this material are controlled by traps.

Applications to nonlinear optical problems and the possibility of learning about the physics of quantum size effects has lead to considerable recent interest in glasses doped with semiconductor microcrystallites. These glasses are doped with $CdS_{1-x}Se_x$ and are commercially available as sharp-cut color glass filters[1].

In the commercial material, the microcrystallites have an average diameter typically of 100A with a FWHM distribution of 50A, as determined by electron microscopy (obtained for Corning material[2]), resulting in a relatively featureless room temperature absorption edge. At low temperature, these materials have been reported to exhibit structure in the luminescence spectrum attributed to quantum confinement[3] and more recent results have shown the existence of structure in the modulated absorption spectrum[4]. More careful material processing methods have produced material with a uniform size distribution showing clear structure in the room temperature linear absorption spectrum which have been attributed to quantum size effects[5]. One group[6] has produced structures as small as 12A in CdS, CdSe, and CuCl. Another group has made glasses doped with microcrystallites where the size distribution is controlled by a heat treatment process and microcrystallites as small as 25A have been observed.[2]

Because of the relative ease of fabrication, the large fast nonlinear optical response, and the fact that the host material is a glass, the applications of these materials to optical switches and integrated optics have been studied by

numerous groups. In addition, there have been several studies discussing the physics of these materials. Very early, the material was used to demonstrate a Q-switch in a laser[7]. Optical bistability was demonstrated by McCall and Gibbs[8] and Gibbs et al.[9], however the slow response suggested the nonlinearity was thermal in origin[10]. Using a Q-switched laser, Jain and Lind[11] demonstrated optical phase conjugation and showed that a large nonlinear optical susceptibility was observable ($\chi^{(3)} \approx 10^{-8}$ esu) using transient excitation. They determined that the relaxation time was faster than 8 nsec (determined as an upper limit.) The model for the nonlinear response proposed by Jain and Lind was based on the production of a short-lived electron-hole plasma. This work was followed by numerous other experimental[12-22] and theoretical[23-25] reports of the nonlinear response using pulsed excitation. Included in these observations have been several measurements of the dynamical behavior[26-29] of key importance to high speed applications. These measurements show carrier relaxation times are in the picosecond time domain. The range of fast relaxation times reported in the literature has been attributed to defects which decrease the relaxation time and which are induced by high power optical irradiation (photo-darkening)[21]. More recently, using the methods of ultrafast laser spectroscopy, measurements of transient absorption have shown relaxation processes occurring on the time scale of a few hundred femtoseconds[30,31]. Measurements on CdSSe glasses in which quantum confinement effects dominate have demonstrated

the importance of phonon broadening and have shown evidence for spectral hole burning at low temperature.[32] Other measurements of hole burning in small (35-55A) microcrystallites of CdSe clusters suspended in a polystyrene film have resulted in measurements of the contributions of homogeneous and inhomogeneous broadening to the electronic absorption spectra.[33] A discussion of the recent applications is given in reference 34.

In this paper, we examine the physical behavior of a slower but much larger nonthermal contribution to the nonlinear optical response obtained under *cw excitation*. The first indication of the possibility of a large cw nonlinear response was provided by the observation of low frequency dynamical behavior leading to subharmonic generation and near chaotic behavior in SDG observed at low temperature (140K) by Zheludev et al.[35] This work was followed by measurements in our laboratory of the room temperature cw nonlinear response using DFWM which showed a nonlinear response much larger but slower than the response obtained based on pulsed excitation.[36] The results showed $\chi^{(3)} \approx 10^{-7}$ esu. Using four-wave mixing spectroscopy methods, a narrow resonance (4.4kHz) was found in the nonlinear susceptibility corresponding to a 72μsec excitation relaxation time. In that work, we attributed the origin of the nonlinear dynamics to contributions from traps, a result suggested by earlier measurements[3,13] and confirmed in more recent work[29,37].

This paper extends the earlier measurements to show the

temperature and optical intensity dependence of the nonlinear response. These results are discussed based on the assumption that the dynamics of the nonlinear response are controlled by traps. As a result of this work, we have demonstrated[34] that a large third order susceptibility ($\chi^{(3)} \approx 2\text{x}10^{-4}$ esu) can be obtained at 125K. In addition, the current work provides a measure of an effective thermal activation energy and a model is discussed which suggests that the saturation of the nonlinear response reported in our earlier work is due to saturation of the available traps. The large nonlinear response has been used to demonstrate efficient optical phase conjugation, and the narrow bandwidth and near angle independent response has been used to demonstrate a tunable optical filter[34].

The experimental configuration for these measurements is based on backward four-wave mixing using a frequency stabilized tunable cw dye laser. Two counter propagating pump beams with fields $\vec{E}_f(\omega)$ and $\vec{E}_b(\omega)$ interact with a probe beam $\vec{E}_p(\omega_p=\omega+\delta)$ in the sample which is contained in a variable temperature cryostat. The angle between the forward pump and probe beams is θ. The three beams interact through the nonlinear response to produce a signal field ($\vec{E}_s$) arising from a polarization proportional to $\chi^{(3)}(\vec{E}_f \circ \vec{E}_p^*)\vec{E}_b$. For these measurements, $\vec{E}_f \| \vec{E}_p \perp \vec{E}_b$ (no signal is obtained for $\vec{E}_f \| \vec{E}_b \perp \vec{E}_p$ for low power cw excitation), and the signal arises from the coherent scattering of $\vec{E}_b$ from the traveling wave grating of excitation produced by $\vec{E}_f \circ \vec{E}_p^*$. In the limit where the dephasing rate is large compared

to the excitation relaxation rates, a measurement of $|E_s|^2$ as a function of δ for fixed ω (the FWMp response,) gives a line shape related to relaxation rates associated with the excitation grating produced by the forward pump and probe. (If the dephasing rate is not large, the FWMp response may include interference effects arising from the induced dipole.[38]) A simple physical understanding of the FWMp response can be obtained by considering the response in the limit of small and large δ. For δ small compared to the excitation relaxation rate, the spatial modulation of the excitation is in phase with the intensity pattern formed by $E_f E_p^*$, and a strong signal is produced by the scattering of the backward pump beam from the grating. However, for δ large compared to the excitation relaxation rates, the spatial modulation of the excitation is washed out and there is no grating to produce a coherent signal.[39]

In this system, we assume that the nonlinear response is due to phase space filling effects due to the free carriers produced by the forward pump and probe which result in a modulation of the transition oscillator strength[40]. As indicated above, because of the slow response, it is believed that the dynamics of the nonlinear response are dominated by the presence of traps.[41] If an electron (or hole) decays to a long lived trap, the remaining hole (or electron) can still contribute to the bandfilling. Thus a component of the bandfilling relaxation rate will be determined by the effective decay time of the carriers from the traps. The line width of a

FWMp measurement is thus related to the effective trap relaxation rate.

A detailed study of the FWMp line width was performed using the experimental setup described in reference 36. Since the line widths were much smaller than the interlaser jitter associated with a measurement based on one stabilized dye laser providing the pump beams and a second dye laser providing the probe beam, we used the method of correlated optical fields using two acoustooptic modulators driven by two phase locked frequency synthesizers. In this approach, the first order Bragg scattered beam from the first modulator provided the pump beams while the second AO cell provided the probe beam. The first AO modulator was operated at a fixed drive frequency of 40 MHz. The second driver could be varied about the 40 MHz drive frequency. In this way, we could vary δ over the range needed for the measurement to obtain line shapes without contributions from laser jitter.

Figure 1 shows the FWMp line width obtained at 125K in RG630. The data shows that the profile is not a pure Lorentzian, suggesting that if trap dynamics are responsible for the behavior, then most likely, the response is an average over a distribution of traps, a possibility supported by additional data below. The inset on the left shows the FWMp profile as a function of excitation wavelength around the filter absorption edge. There is a dependence on excitation wavelength with the line width varying from 214 Hz to 429 Hz at this temperature as the wavelength is varied from 600 nm to 614

nm. The inset on the right shows this dependence with a linear fit of the data. In addition, the strength of the nonlinear response also varies. On the blue side of the data, the incident beams are strongly absorbed by the material, while on the red side, there is a decrease in the optical coupling. For the remaining data below, all measurement were made at the peak of the response.

The FWMp response was studied as a function of temperature. Figure 2 shows the log of the FWMp line width as a function of 1/T. All line widths were observed to have a linear dependence on optical intensity. The data used for Fig. 2 corresponds to the zero intensity intercept. (Further discussion is given below regarding intensity dependent effects.) The general form of the data in Fig. 2 suggests a functional form for the effective trap decay rate given by: $\gamma(0) + \Gamma e^{-(\mathcal{E}_b/kT)}$ where $\gamma(0)$ is the zero temperature decay rate, and $\Gamma\exp(-\mathcal{E}_b/kT)$ is the probability per unit time for the electron or hole to escape from a thermally activated trap ($\mathcal{E}_b$ is the activation energy). The solid line shown in Fig. 2 is the best fit of the functional form for the effective trap decay rate given above. The asymptotic value of the curve gives the zero temperature decay rate. The slope of the curve gives the activation energy, determined to be 137 meV. The decay parameter, Γ, is 0.7 MHz and the zero temperature decay rate, $\gamma(0)$ is 43 Hz.

It is most likely that at these powers, the excitation is in near equilibrium with the crystal lattice imbedded in the

glass material and the actual details of decay are most likely far more complex than indicated by such a simple description. Experiments have been reported in colloidal suspensions of CdS clusters[42] where luminescence decay is interpreted based on a theory for multiphonon assisted excitation transfer[43]. For our measurements, we are unable to distinguish between these different decay mechanisms.

We also observe that the FWMp line width is intensity dependent as shown in Fig. 3, showing a linear dependence on intensity at low powers. Additionally, as reported in reference 34, we observed a roll off in the nonlinear response at high pump intensities. (At 125 K, saturation of the nonlinear response occurred around $10W/cm^2$). A qualitative understanding of the saturation behavior reported in reference 34 and the results obtained in the FWMp measurements can be obtained by considering a simple model of the nonlinear response based on the energy level diagram shown in figure 4. In this model, optical radiation induces a transition from the valence band to the conduction band, producing an electron-hole (e-h) pair. The electron in the conduction band can decay back to the valence band with decay rate γ_{cv} or to a trap with decay rate KN_t in the limit that the traps are unsaturated where N_t is the total trap density. (For this discussion, we consider only electron traps.) The trapped electron can then be thermally activated from the trap and return to the conduction band with rate γ_{tc} or recombine with a hole in the valence band with rate γ_{rec}.

In the absence of traps, the FWMp line shape would have a width determined by the carrier recombination rate (decay of the induced grating by spatial diffusion of the carriers is not included since the size of microcrystallites is small compared to the grating spacing and they are surrounded by insulating glass.) However, if electrons (or holes) can be trapped, the remaining electrons and holes can still contribute to bandfilling. The time constant for the decay of this system would have a fast component due to free carrier recombination and a slow component determined by the rate of electron (or hole) escape from the trap.

In the limit that the dynamics of the nonlinear response are determined by trap kinetics, this simplified model can be used to obtain a more quantitative understanding by considering the rate equations for the electron density, n, and trap density, n_t:

$$\dot{n} = \Phi - \gamma_{cv} n - K(N_t - n_t) n + \gamma_{tc} n_t \qquad (1)$$

$$\dot{n}_t = K(N_t - n_t) n - \gamma_{tc} n_t - \gamma_{rec} n_t \qquad (2)$$

where Φ represent the optical generation rate of e-h pairs. The possibility of trap saturation is included through the term $K(N_t - n_t)$. The nonlinear response of this material is the result of bandfilling so that we take the nonlinear susceptibility to be proportional to the density of free electrons and holes[40]. However, since experimentally we detect only a slow component of the nonlinear response due to the

presence of holes that persist because of the presence of electron traps, we take the dominant term in the nonlinear susceptibility to be proportional to the filled trap density. The above set of rate equations can be solved in the presence of strong pumps. However, the essential features of importance to spectroscopy can be seen from the solution obtained in the limit of perturbation theory and in the absence of trap saturation. (Trap saturation effects are discussed below.) Taking $\Phi = \frac{\alpha_{abs}}{\hbar\omega} I$ where $I=\frac{c}{4\pi}\left\langle [\sum_i E_i \cos(k_i x-\omega_i t+\phi_i)]^2 \right\rangle_t$, we obtain an expression for the nonlinear polarization for the FWMp response for the interaction described above in the limit $\delta=\omega_f-\omega_p << \gamma_{cv}$, KN_t:

$$P^{NL}=\xi \mathcal{E}_f \mathcal{E}_p^* \mathcal{E}_b e^{i(k_f-k_p+k_b)x-i(\delta+\omega_b)t} \frac{N_t}{i\delta+\gamma_{rec}+\gamma_{tc}\left(\frac{\gamma_{cv}}{\gamma_{cv}+KN_t}\right)} + c.c \qquad (3)$$

where ξ is a constant and $E_i \cos(k_i x-\omega_i t+\phi_i)=\frac{1}{2}\mathcal{E}_i e^{i(k_i x-\omega_i t)}+c.c.$ Thus, in the case of a single trap (i.e., no distribution of trap lifetimes) the line width at zero intensity measured in a FWMp experiment is given by an effective trap lifetime given by $\gamma_{eff} = \gamma_{rec}+\gamma_{tc}\left(\frac{\gamma_{cv}}{\gamma_{cv}+KN_t}\right)$.

When the effects of trap saturation are included, the model predicts a roll off in the nonlinear response at high pump intensities, as well as a linear increase in the line width with pump intensity in the low pump intensity limit. In

particular, the above equations can be solved in the presence of strong pumps (standing wave effects are ignored since the pump polarizations are orthogonal.) In the limit that the dominate decay channel from the trap is γ_{tc}, the above polarization describes the intensity dependent nonlinear response if we replace N_t with $N_t - n_{t(dc)}$ and replace γ_{tc} with $\gamma_{tc} + Kn_{(dc)}$ where

$$n_{t(dc)} = \frac{Kn_{(dc)}N_t}{\gamma_{tc}+Kn_{(dc)}} \tag{4}$$

$$n_{(dc)} = \frac{\alpha_{abs}I_o}{\hbar\omega}\frac{1}{\gamma_{cv}} \tag{5}$$

and I_o is the pump intensity. These equations do show the linear dependence of the line width on intensity, and the roll over at high intensity, however using the single trap level model presented above, it is not possible to reconcile the low intensity line width broadening rate with the observed saturation intensity. Estimation of the saturation intensity from the low intensity line width broadening rate predicts a value of saturation intensity much lower than what was observed experimentally. Currently, we believe the explanation for this difference is that this material is characterized by a range of trap lifetimes with correspondingly different concentrations and positions within the band-gap. As the intensity of the pumps is increased, the traps begin to fill and different groups of traps in the distribution then contribute to the response. Thus at low pump intensities, the response most

likely results from one group of traps and the values of trap relaxation time and activation energy thus pertain only to this group of traps. However at the higher intensities, different parts of the trap distribution contribute to the signal resulting in an effective saturation intensity that will differ from the prediction based on assuming a single trap and using the measured low intensity line width broadening rate. Such an interpretation is supported by recent measurements by Tomita et al[37] which have shown nonexponential decays in luminescence lifetimes with time constants ranging from 2μsec up to lifetimes beyond 20μsec at liquid nitrogen temperature. These multiple exponential decays are consistent with our non-Lorentzian line shapes.

In summary, these measurements provide further insight into the nature of the nonlinear response obtained in CdSSe doped glass using cw excitation. Using frequency domain nonlinear laser spectroscopy methods, we have determined the effects of temperature and pump intensity on the dynamical behavior of the nonlinear response. There is strong evidence that traps are responsible for the dynamics of the cw nonlinear response and that trap saturation is responsible for the observed roll off of the response.

This work was supported by AFOSR, Grant No. 85-0280. In addition, M.D. Webb was supported by an Army Research Office Fellowship from the University Research Initiative program.

REFERENCES

1. For example, Corning, Schott, Hoya, and Toshiba.

2. N.F. Borrelli, D.W. Hall, H.J. Holland, and D.W. Smith, Jr. Appl. Phys. 61, 5399 (1987).

3. J. Warnock and D.D. Awschalom, Phys. Rev. B 32, 5529 (1985).

4. F. Moshary and S.R. Hartmann, private communication.

5. L. Banyai and S.W. Koch, Phys. Rev. Lett. 57, 2722 (1986). See also "Comment" by S. Schmitt-Rink, Phys. Rev. Lett. 60, 1205 (1988) and "Reply" by L Banyai and S.W. Koch, 1206.

6. A.I. Ekimov and A.A. Onushchenko, Pis'ma Zh. Eksp. Teor. Fiz.40, 337 (1984) (JETP Lett. 40, 1136 (1984)). A.I. Ekimov and A.A. Onushchenko, Pis'ma Zh. Eksp. Teor. Fiz. 34, 363 (1981) (JETP Lett. 34, pp343-349 (1981)). A.I. Ekimov, Al.L. Efros, and A.A. Onushchenka, Solid State Comm. 56, 921 (1985).

7. G. Bret, and F. Gires, Appl. Phys. Lett. 4, 175(1964).

8. S.L. McCall and H.M. Gibbs, J. Opt. Soc. Am. 68, 1378 (A) (1978).

9. H.M. Gibbs, G.R. Olbright, N. Peyghambarian, H.E. Schmidt,

S.W. Koch, and H. Haug, Phys. Rev. A 32, 692 (1985). See also H. Gibbs, Academic Press, Optical Bistability, Controlling Light with Light",Orlando, (1985).

10. G. Thibault and M.-M. Denariez-Roberge, Can. J. Phys. 63, 198 (1985).

11. R.K. Jain and R.C. Lind, J. Opt. Soc. Am. 73, 647(1983).

12. S.S. Yao, C. Karaguleff, A. Gabel, R. Fortenbuery, C.T. Seaton, and G. Stegeman, Appl. Phys. Lett. 46, 801 (1985).

13. P. Roussignol, D. Ricard, K.C. Rustagi, and C. Flytzanis, Optics Comm. 55, 143 (1985).

14. B. Danielzik, K. Nattermann, and D. von der Linde, Appl. Phys. B 38, 31 (1985).

15. G.R. Olbright and N. Peyghanbarian, Appl. Phys. Lett. 48, 1184 (1986).

16. D. Cotter, XIV International Quantum Electronic Conference, San Francisco, CA post deadline paper PD19-1 (1986).

17. G.R. Olbright, N. Peyghambarian, S.W. Koch, and L. Banyai, Opt. Lett. 12, 413 (1987).

18. F. Hache, P. Roussignol, D. Ricard, and C. Flytzanis, Opt. Comm. 64, 200 (1987).

19. F. de Rougemont, R. Frey, P. Roussignol, D. Ricard, and C. Flytzanis, Appl. Phys. Lett. 50, 1619 (1987).

20. P. Roussignol, M. Kull, D. Ricard, F. de Rougemont, R. Frey, and C. Flytzanis, Appl. Phys. Lett. 51, 1882 (1987).

21. P.Roussignol, D. Ricard, J. Lukasik, and C. Flytzanis. J. Opt. Soc. Am. B, 4, 5 (1987).

22. D.W. Hall and N.F. Borrelli, J. Opt. Soc. Am. B 5, 1650 (1988).

23. K.C. Rustagi and C. Flytzanis, Opt. Lett. 9, 344(1984).

24. C. Flytzanis, F. Hache, D. Ricard, and Ph. Roussignol, "Optical nonlinearities in small particles and composite materials," in The Physics and Fabrication of Microstructures and Microdevices, M.J. Kelly, and C. Weisbuch, Ed., Springer-Verlag, Berlin (1986).

25. Eiichi Hanamura, Phys. Rev. B 37, 1273 (1988).

26. J. Warnock and D.D. Awschalom, Appl. Phys. Lett. 48, 425

1986).

27. S.C. Hsu and H.S. Kwok, Appl. Phys. Lett. 50 1782 (1987).

28. Kai Shum, G.C. Tang, Mahesh R. Junnarkar, and R.R. Alfano, Appl. Phys. Lett., 51, 1839 (1987).

29. Makoto Tomita, Takahiro Matsumoto, and Masahiro Jatsuoka, "Ultrafast optical nonlinearity in semiconductor-doped glasses controlled through the trapping state," Proceedings of the Conference on Ultrafast Phenomena, to be published by Springer-Verlag, Berlin, 1988.

30. M.C. Nuss, W. Zinch, and W. Kaiser, Appl Phys. Lett. 49, 1717 (1986).

31. N. Peyghambarian and S.W. Koch, Revue. Phys. Appl. 22, 1711 (1987).

32. P. Roussignol, D.Ricard, C. Flytzanis, and N Neuroth, Phys. Rev. Lett. 62, 312 (1989).

33. Alivisatos, Harris, Levinos, Steigerwald, and Brus, J. Chem. Phys 89, 4001 (1988).

34. J.T. Remillard, H. Wang, M.D. Webb, D.G. Steel, IEEE Journal of Quantum ELectronics 25, 408 (1989).

35. N.I. Zheludev, I.S. Ruddock, and R. Illingworth, Jr. Mod. Opt. 34, 1257 (1987).

36. J.T. Remillard and D.G. Steel, Opt. Let. 13, 30 (1988).

37. M. Tomita, T. Matsumoto, and M. Maysuoka, J. Opt. Sci. Am. B 6, 165 (1989).

38. Duncan G. Steel and J.T. Remillard, Phys. Rev. A 36, 4330 (1987).

39. Jing Liu, Ph.D. thesis, University of Michigan.

40. H. Haug, J. Lumin 30, 171 (1985), J.F. Müller, R. Mewis, H. Haug, Z. Phys. B 69, 231 (1987), S. Schmitt-Rink, D.A.B. Miller, D.S. Chemla, Phys. Rev. B 35, 8113 (1987), S. Schmitt-Rink, D.S. Chemla, H. Haug, Phys. Rev. B 37, 941 (1988), M. Lindberg and S.W. Koch, Phys. Rev. B 38, 3342 (1988).

41. Contributions from thermal effects have been eliminated for two reasons: 1. An estimate of the signal strength expected from thermal effects can be obtained from a knowledge of the temperature dependence of the refractive index and absorption coefficient (i.e., from dn/dt and dα/dt.) At temperatures of order 125 K (corresponding to the data in

Figure 1,) the change in absorption with temperature was measured along with the corresponding change in index of refraction. (Our measured values of dn/dt ($\approx 8 \times 10^{-6}$) and $d\alpha/dt$ (≈ 0.055 $cm^{-1}K^{-1}$) at 125 K do not differ appreciably from the reported values at room temperature. See G. Thibault and M.-M. Denariez-Roberge, Can J. Phys 63, 198 (1985) and Schott Glass Technologies Inc. catalog for optical glass filters.) Using these results, we determined that the nonlinear signal due to thermal effects is of order 10^{-8} times weaker than the measured response. 2. A second reason to rule out thermal effects is that thermal lateral thermal diffusion would result in a four wave mixing line width which would have a $\sin^2\theta$ dependence (θ represents the angle between the forward pump and probe beams) which is not observed.

42. N. Chestnoy, T.D. Harris, R. Hull, and L.W. Brus, J. Phys. Chem, 90, 3393 (1986).

43. J. Jortner, J. Chem. Phys. 64, 4860 (1976).

FIGURE CAPTIONS

Figure 1. The FWMp spectrum obtained using the method of correlated optical fields. The inset on the left shows the FWMp line shape obtained for different excitation wavelengths at a constant temperature. The inset on the right shows the dependence of line width on wavelength.

Figure 2. The FWMp line width as a function of inverse temperature.

Figure 3. The FWMp line width as a function of pump intensity.

Figure 4. Energy level diagram describing the optical interaction believed responsible for the nonlinear response in CdSSe doped glass.

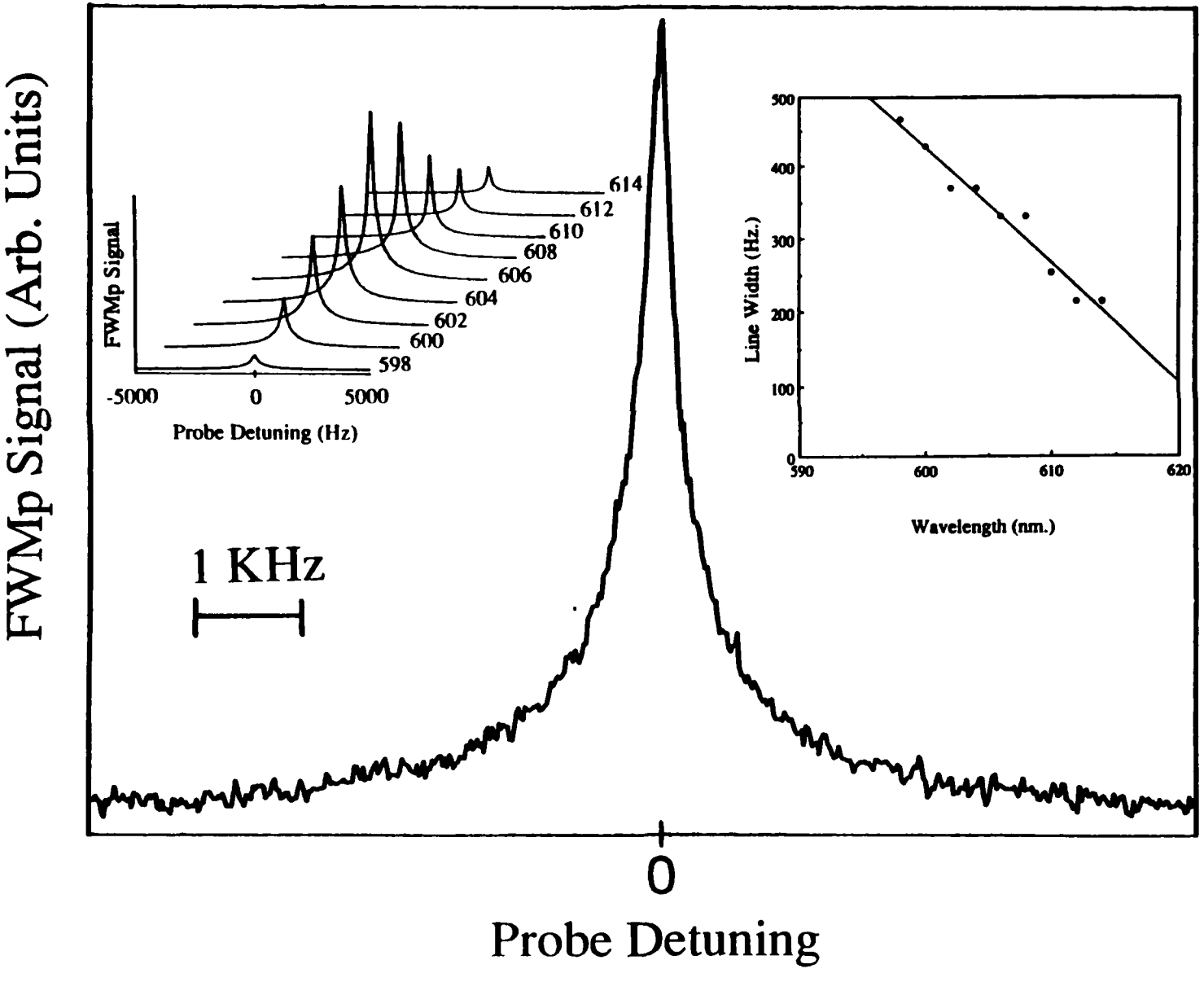
FWMp Signal (Arb. Units)
FWMp Signal
614
612
610
608
606
604
602
600
598
-5000
0
5000
Probe Detuning (Hz)
1 KHz
Line Width (Hz.)
500
400
300
200
100
0
590
600
610
620
Wavelength (nm.)
0
Probe Detuning

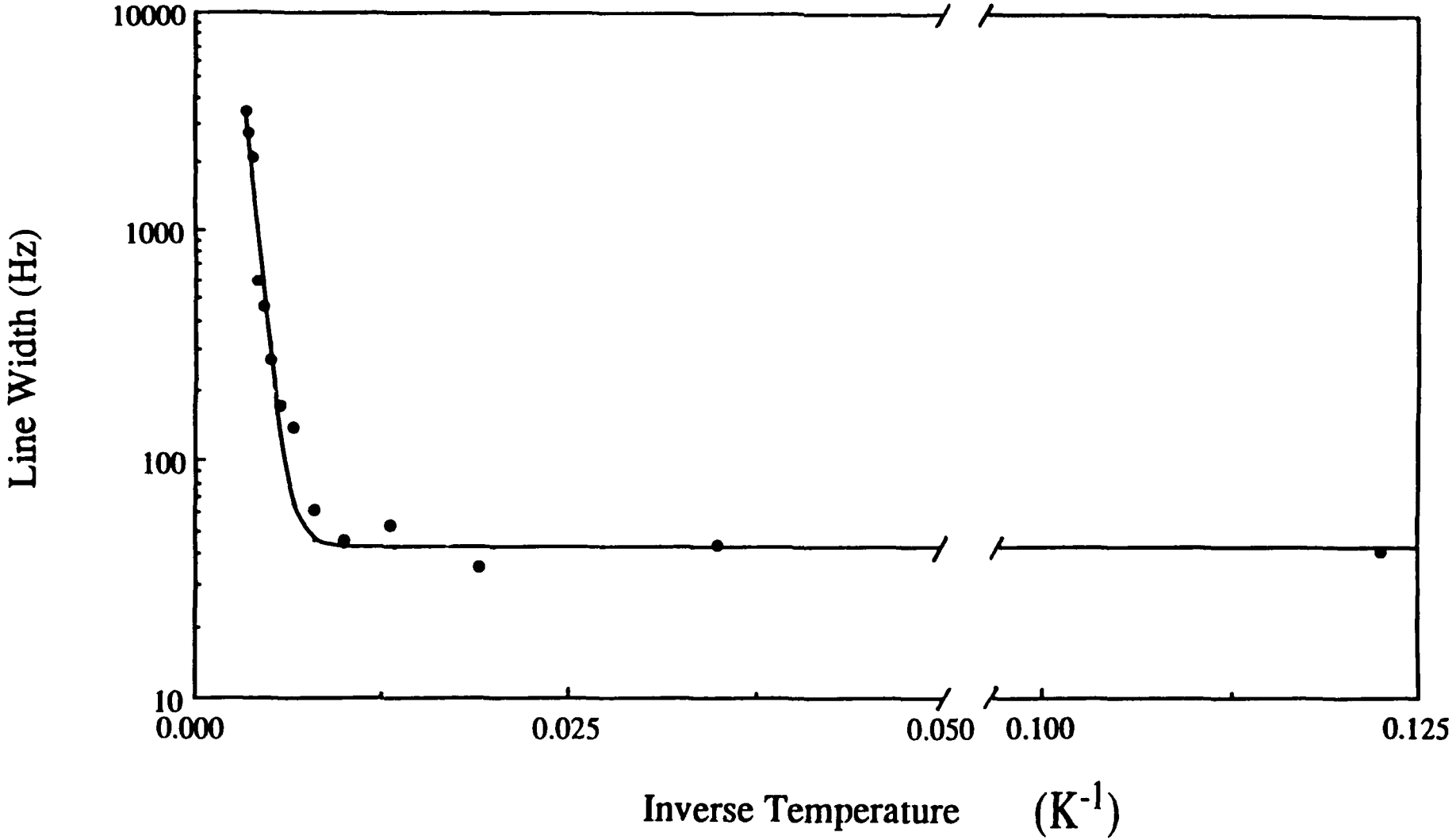
10000
1000
100
10
Line Width (Hz)
0.000
0.025
0.050
0.100
0.125
Inverse Temperature (K-1)

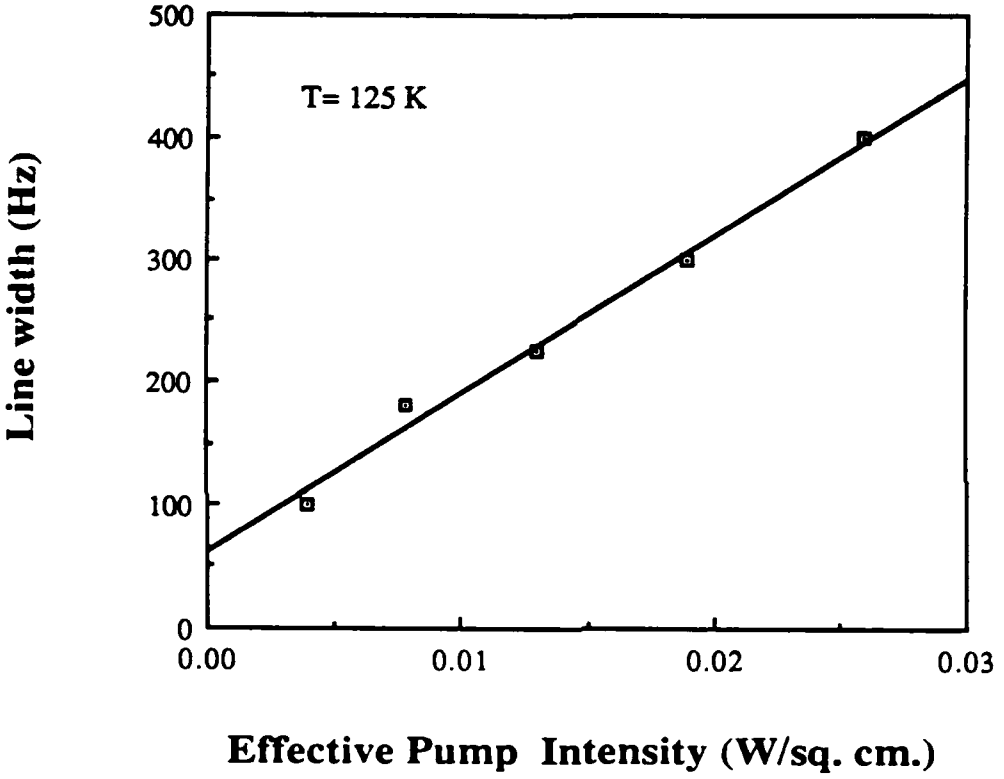
T= 125 K
Line width (Hz)
500
400
300
200
100
0
0.00
0.01
0.02
0.03
Effective Pump Intensity (W/sq. cm.)

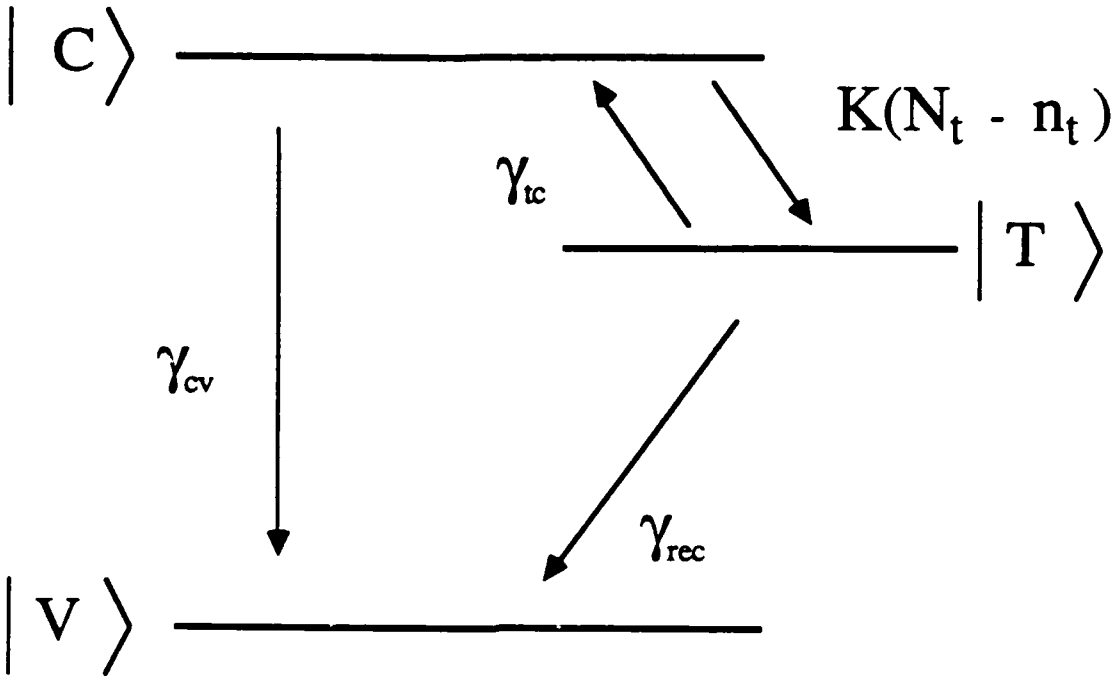
| C ⟩
K(N_t - n_t)
γ_tc
| T ⟩
γ_cv
γ_rec
| V ⟩

Submitted to The Physical Review

Measurement of phonon assisted migration of localized excitons in GaAs/AlGaAs multiple quantum well structures

H. Wang, M. Jiang, and D.G. Steel

Harrison M. Randall Laboratory of Physics

The University of Michigan, Ann Arbor, Michigan 48109

Abstract

We report high resolution nonlinear laser spectroscopy measurements of relaxation of lowest energy heavy hole excitons in GaAs/AlGaAs multiple quantum well structures. We show that excitons below the absorption line center are spatially localized, and migrate among localized sites with a time scale of order 100 ps. The measurement also gives the resultant quasi-equilibrium energy distribution of the scattered excitons, and based on the temperatur dependence of the migration rate confirms the theoretical model for the phonon assisted migration.

Optical resonant excitation of excitons with nearly monochromatic light of energy E leads to an optically induced polarization (coherence) and a population of excitons within ΔE of E where $\Delta E \sim \hbar\Gamma_h$ (Γ_h is the homogeneous width of the exciton). The decay of this excitation must be characterized by decay of the polarization (often called dephasing) as well as decay of the population about energy E. In a perfect quantum well , quasi two dimensional excitons are described by a Bloch type of wave function and are free to move in the well plane. At low excitation density, decay of the excitation is then expected to be predominantly due to exciton-phonon scattering along with exciton recombination. In practice, however, the problem becomes more complicated due to nonideal growth processes. Recent transport and chemical lattice imaging measurements[1,2] have shown the interface of GaAs/AlGaAs multiple quantum well (MQW) samples exhibits island-like structures with a height of one monolayer and a lateral size of order 50 Å. For an exciton confined to a thin GaAs layer in a MQW, its energy depends strongly on the well thickness. For example, well width fluctuations of one monolayer in a 100 Å $GaAs/Al_{0.3}Ga_{0.7}As$ MQW can result in a change of exciton energy on the order of several meV. Therefore, at low temperature in the low energy region of the heavy hole exciton (HH1) absorption spectrum, excitons can be localized in the well with an energy determined by the local environment[3] leading to inhomogeneous broadening of the linear absorption spectrum. Excitons in the high energy region may still be delocalized[3]. These excitons are expected to experience additional dephasing due to elastic scattering from potential fluctuations in addition to the decay due to exciton phonon scattering and exciton recombination.

Localized excitons are in local minimum in energy, and at very low temperature, decay of the localized exciton is dominated by migration between localization sites. The migration is accompanied by absorption or emission of acoustic phonons to compensate for the energy difference. Indeed, phonon assisted migration was proposed to explain the slow

and non-exponential energy relaxation observed in time resolved luminescence measurements in a GaAs MQW[4]. Furthermore, the migration is primarily due to the inersite dipole-dipole interaction when the intersite distance is much greater than the exciton Bohr radius and localization length[5]. Furthermore, the migration is primarily due to the inersite dipole-dipole interaction when the intersite distance is much greater than the exciton Bohr radius and localization length[5]. Migration due to the overlap of the exciton wave functions between different sites also becomes important when the intersite distance is comparable with the exciton Bohr radius or the localization length. It is estimated[5] that the typical magnitude of participating phonon wave vectors is within a few times of the inverse of the localization length, which indicates the energy of participating phonons is on the order of 0.01 to 0.1 meV. At higher temperature (>10K), thermal activation of localized excitons to delocalized states becomes important. This process is associated with phonon absorption, and has been observed in GaAs MQW structures using resonant Rayleigh scattering[3]. The estimated activation energy indicates that the onset for the delocalized exciton is near the absorption line center.

A distinctive signature for phonon assisted migration is the temperature dependence. Recent work by Takagahara[6] has shown the temperature dependence of the migration rate in MQW structures has a form given by $\exp(BT^{\alpha})$, and has been observed in transient hole burning experiments in an InGaAs/InP MQW[7]. In this expression, B is positive and independent of temperature but is expected to increase with the exciton energy, and α is estimated to be between 1.6 and 1.7. The predicted temperature dependence is quite different from that of variable range hopping used by Mott to interpret electronic conduction in the localized regime[8], and is attributed to the role of the long-range dipole-dipole interaction involved in the migration of the localized exciton[5].

In this paper, we present results of high resolution nonlinear laser spectroscopy of lowest energy heavy hole excitons in a GaAs/AlGaAs MQW at temperatures between 2.5 K

and 15 K. Using frequency domain four wave mixing, we are able to obtain relaxation rates for the exciton population at a given energy E, and to measure directly the steady state exciton redistribution under narrow band CW excitation. The measurement shows excitons below the absorption line center are localized, and migrate among localization sites in a time scale of order 100 ps. The predicated temperature dependence of the migration rate is also confirmed.

The experimental configuration is discussed elsewhere[9], and is based on the use of two frequency stabilized tunable CW dye lasers. Three incident beams $\mathbf{E}_f(\omega_f, \mathbf{k}_f)$, $\mathbf{E}_b(\omega_b, \mathbf{k}_b)$ and $\mathbf{E}_p(\omega_p, \mathbf{k}_p)$ (f, b, and p stand for forward, backward and probe respectively) with $\mathbf{E}_f \| \mathbf{E}_p \perp \mathbf{E}_b$ interact in the sample through the third order susceptibility. A signal beam $\mathbf{E}_s(\omega_s, \mathbf{k}_s)$ with frequency $\omega_s=\omega_f+\omega_b-\omega_p$ is generated and is proportional to $\chi^{(3)}\mathbf{E}_f\mathbf{E}_p^*\mathbf{E}_b$. Physically, $\mathbf{E}_f\mathbf{E}_p^*$ results in a modulation of the exciton population[10]. The modulation further modifies the optical response of the sample through exciton phase space filling and exchange effects[11]. The signal arises from coherent scattering of the backward beam from the modulation. Because of the resonant enhancement which occurs when the emission dipole is resonant with the signal beam[12], only excitons that are resonant with $\omega_s=\omega_f+\omega_b-\omega_p$ contribute significantly to the nonlinear response.

In general, spectroscopic information related to the energy level structure and relaxation of the system is obtained by measuring the nonlinear response as a function of the frequency of any of the three input beams. We further designate the line shape obtained as FWMi where i stands for f, b, or p depending on which frequency is tuned. The measurement can be understood in the following simplified picture with a more rigorous analysis based on the effective optical Bloch equations to be discussed elsewhere[13].

In the FWMb measurement, $\mathbf{E}_f$ and $\mathbf{E}_p$ ($|\omega_f-\omega_p| << \Gamma_h$) create an exciton population in a narrow spectral hole with a width $\Delta E=\hbar\Gamma_h$ within the inhomogeneous width. Scanning

ω_b while keeping ω_f and ω_p fixed effectively changes ω_s. The resultant line shape reflects a direct measure of the steady state spectral redistribution of excitons that have a nonzero emission dipole moment. Hence, in the case of localized excitons, scattering to other energy states can then be directly measured in the FWMb response. However, while delocalized excitons can also be scattered to other energies by inelastic processes such as exciton-phonon interactions, delocalized excitons in these states have nonzero momentum, and as a result, a zero emission dipole moment. In this case, the FWMb line shape simply provides a measure of the exciton homogeneous line shape.

In the FWMf and FWMp measurement, detuning the probe or forward pump generates a traveling wave modulation oscillating in time at a fixed point in space with the detuning frequency $\delta=\omega_f-\omega_p$. The nonlinear response as a function of δ then measures the decay rate of the modulation formed by *excitons that are resonant with the signal beam*. The rate obtained includes contributions from exciton recombination as well as scattering of excitons from energy E to E' where $|E-E'| > \Gamma_h$. Spatial diffusion of the exciton also contribute to the decay of the modulation and manifests itself as the dependence of the decay rate on the grating period[14]. Note that tuning ω_f or ω_p will also change ω_s since $\omega_s=\omega_f+\omega_b-\omega_p$. Complications may arise when the exciton energy relaxation rate is comparable with Γ_h. However, such complications are reduced by choosing to tune ω_f instead of ω_p[13, 15], and introduce only an overall correction factor (close to 1) for decay rates measured by the FWMf response. In the limit that Γ_h is much larger than the energy relaxation rate, tuning ω_f or ω_p gives the same line shape.

The MQW sample used for our measurement consists of 65 periods of 96 Å GaAs wells and 98 Å $Al_{0.3}Ga_{0.7}As$ barriers grown by molecular-beam-epitaxy. The sample is mounted on a sapphire disk (c axis normal) with the substrate removed. All the experiments are carried out on the HH1 exciton with an exciton density on the order of $10^7/cm^2$.

The complex decay dynamics of the exciton population is seen in the FWMf response. A typical line shape below the absorption line center is shown in Fig. 1a. The FWHM corresponds to a relaxation time of 60 ps, which is too slow to be due to phonon scattering of the delocalized exciton (typically in a time scale of several ps[16]), and is over an order of magnitude faster than the exciton recombination time. Furthermore, the FWHM is independent of the grating period, indicating the contribution from exciton diffusion is negligible and that excitons are localized in this spectral region. Hence, the data suggest that the decay is due to spectral diffusion as a result of scattering of localized excitons from energy E to E' ($|E-E'|>\Gamma_h$). In fact, the decay rate is in agreement with the recent calculation based on phonon assisted migration of the localized exciton[5]. In addition, excitons that are scattered from E to E' can later be scattered back and establish a quasi-equilibrium exciton population about E before they eventually recombine. This quasi-equilibrium population contributes to the FWMf response with a decay rate characterized by the exciton recombination[13]. The FWMf response shown in Fig. 1a indeed shows a small and narrow feature at the top of the line shape. The narrow feature becomes more pronounced at higher temperature due to faster exciton migration as shown in Fig. 1b. The width associated with the feature corresponds to a decay time of 1.2 ns, consistent with the exciton recombination rate[17].

We further examine the relaxation mechanism of the localized exciton by studying the temperature dependence of the exciton relaxation rate. Fig. 2a shows the temperature dependence of the exciton relaxation rate obtained at 0.6 meV and 1.5 meV below the absorption line center using the FWMf response. The data is in good agreement with the theory of phonon assisted migration discussed above with $\alpha=1.6$. The measurement indicates that the dominant contribution to relaxation of the localized exciton is phonon assisted migration up to a temperature of 15 K. Note that earlier measurements using resonant Rayleigh scattering have reported observations of activation type of temperature

dependence for the localized exciton at temperatures between 7 and 20 K, indicating that in this temperature region relaxation for the localized exciton is dominated by thermal activation to delocalized states. It has been suggested that depending on details of quantum well interface roughness, the effective activation energy can be much higher than simply the energy difference between the mobility edge and the localized exciton[18]. Therefore it is possible that at relatively low temperature (e.g. below 15 K), the thermal activation rate is much smaller than the phonon assisted migration rate.

The energy dependence of the decay of the exciton population below the absorption line center is shown in Fig. 2b. For exciton energies less than 1.5 meV below the absorption line center, the decay rate depends very weakly on the energy . The rate increases rapidly when the exciton energy approaches the absorption line center, suggesting a transition from localized to delocalized excitons[3].

If we imagine that localized excitons are optically excited at energy E and then migrate among localized sites to different energies, a quasi-equilibrium exciton population over a broad spectral range can be established assuming the exciton migration rate is large compared with the recombination rate. As indicated earlier, indeed, it is the decay of this quasi-equilibrium distribution that gives rise to the narrow feature in Fig. 1a, b. The spectral distribution of the population can be directly measured in the FWMb response by scanning ω_b while keeping ω_f and ω_p fixed at E. Fig. 3 shows a FWMb line shape where excitons are optically excited at 1.5 meV below the absorption line center. The nonlinear response is corrected for sample absorption, and is proportional to the quasi-equilibrium exciton population assuming all excitons in the spectral region concerned give rise to the same CW nonlinear response.

To quantitatively describe the exciton migration process, we introduce a distribution kernel f(E, E'), the rate for a exciton to migrate from energy E to E'. f(E, E') is analogous

to collision kernels which are used to describe velocity changing collisions in atomic vapor[19]. Decay of the exciton population can then be described by the following transport equation $\dot{\rho}(E) = -(\gamma + \Gamma_E)\rho(E) + \int f(E',\ E)\rho(E')dE'$, where $\rho(E)$ is the density of the exciton at E, γ is the recombination rate, $\Gamma_E = \int f(E,\ E')dE'$ is the overall rate at which excitons migrate out of states with energy E. In principle, the transport equation, together with the equation for the nonlinear polarization[11, 20], can provide a description for the FWMf and FWMb line shape, though in general, f(E, E') is unknown and has to be determined by experiments. However, by assuming f(E, E') to be independent of the initial state energy, analytical solutions[13] can be obtained for standard distributions and show that the FWMf response has an additional component with a width given by γ as anticipated based on physical arguments. The FWMb line shape in Fig. 3 can be described by a simple model which neglects migration to states above the excitation energy, and is based on the understanding of the solution to the above transport equation. The model assumes a Gaussian distribution for the quasi-equilibrium population of excitons that have migrated to states below the excitation energy. The result is plotted as the solid line in Fig. 3.

Finally, we note that earlier measurements have suggested that excitons above line center are weakly delocalized[3]. Indeed, our measurements of the FWMf response show a quadratic dependence[14] of the modulation decay rate on the inverse of the excitation grating period yielding a diffusion coeffificient on the order of 4 cm^2/s. More strikingly, for large grating spacing where there is negligible contribution from exciton spatial diffusion, the FWMf line shape is completely dominated by the recombination component due to the rapid exciton-phonon scattering (on the order of several ps[16]). A typical FWMf line shape in this case is shown in Fig. 1c. The FWHM of the line shape corresponds to an exciton recombination time of 1.2 ns. Using the FWMb response, we also determined the homogeneous width to be on the order 0.5 meV (corresponding to a dephasing time of 1.3 ps) at a temperature of 5 K, consistent with what is expected for the delocalized exciton[16].

In summary, using high resolution nonlinear laser spectroscopy, we have shown that lowest energy excitons are localized and migrate in energy by absorption or emission of acoustic phonons. The line shapes have enabled us to determine the migrating rate along with the temperature dependence and the resultant quasi-equilibrium energy distribution.

This work was supported by the Air force Office of Scientific Research.

References:

1. R. Gottinger, A. Gold, G. Abstreiter, G. Weiman, and W. Schlapp, Europhys. Lett. **6**, 183 (1988).

2. A. Ourmazd, D. W. Taylor, J. Cunningham, and C.W. Tu, Phys. Rev. Lett. **62**, 933 (1989).

3. J. Hegerty, L. Goldner, and M.D. Sturge, Phys. Rev. B**30**, 7346 (1984).

4. Yasuaki, Masumoto, Shigeo Shionoya, and Hitoshi Kawaguchi, Phys. Rev. B**29**, 2324 (1984).

5. T. Takagahara, J. Lumin. **44**, 347 (1989).

6. T. Takagahara, Phys. Rev. B**32**, 7013 (1985).

7. J. Hegarty, K. Tai, and W.T. Tsang, Phys. Rev. B**38**, 7843 (1988).

8. N.F. Mott, and E.A. Davis, Electronic Processes in Noncrystalline Materials, 2nd ed. (Oxford Univ. Press, New York, 1979).

9. J.T. Remillard, H. Wang, D.G. Steel, J. Oh, J. Pamulapati, and P.K. Bhattacharya, Phys. Rev. Lett. **62**, 2861 (1989).

10. For CW measurements, the orientational grating has not been observed.

11. S. Schmitt-Rink, D.S. Chemla, and D.A.B. Miller, Advan. in Phys. **38**, 89 (1989).

12. J.L. Oudar, and Y.R. Shen, Phys. Rev. A**22**, 1141 (1980).

13. H. Wang, and D.G. Steel, to be published.

14. J.T. Remillard, H. Wang, D.G. Steel, J. Oh, J. Pamulapati, and P.K. Bhattacharya, Opt. Lett. **14**, 1131 (1989).

15. D.G. Steel, and J.T. Remillard, Phys. Rev. A**36**, 4330 (1987).

16. L. Schultheis, A. Honold, J. Kuhl, K. Kohler, and C.W. Tu, Phys. Rev. B**34**, 9027 (1986).

17. J. Feldman, G. Peter, E.O. Gobel, P. Dawson, K. Moore, C. Foxon, and R.J. Elliott, Phys. Rev. Lett. **55**, 2337 (1987).

18. T. Takagahara, private communication.

19. Paul R. Berman, Phys. Rep. **43**, 102 (1978).

20. M. Lindberg, and S.W. Koch, Phys. Rev. B**38**, 3342 (1988).

Figure Captions:

Fig. 1. The FWMf responses. (a) at 1.5 meV below line center and at 2.5 K. (b) at 0.6 meV below line center and at 10 K. (c) at 2 meV above line center and at 10 K.

Fig. 2. (a) The temperature dependence of the exciton decay rate. Circles and crosses are data obtained at 1.5 meV and at 0.6 meV below line center respectively. Dashed lines are fit to the theory of phonon assisted migration. (b) The energy dependence of the exciton decay rate at 10 K. The dash line is only a guide to the eye.

Fig. 3. The FWMb response with the frequencies of the forward and probe beams at 1.5 meV below line center.

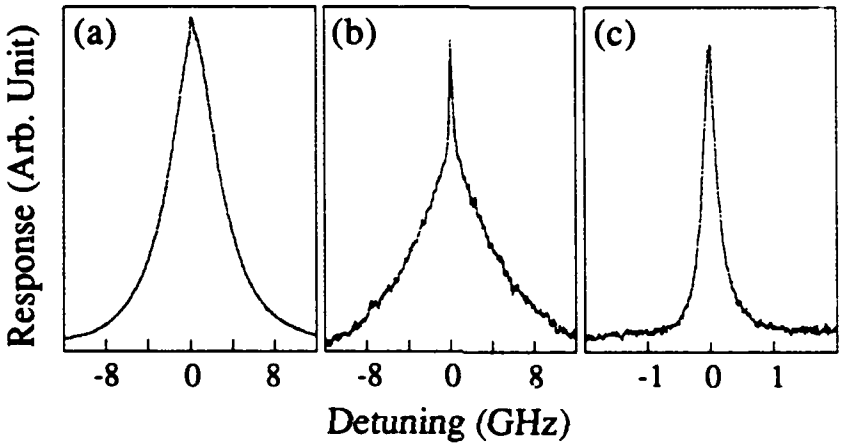

Fig. 1

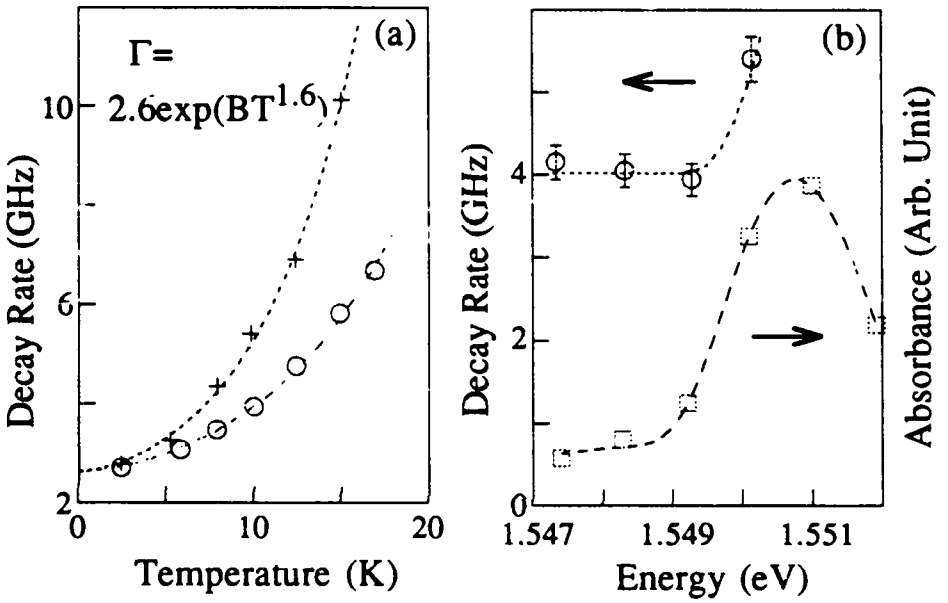
(a)
Γ=
2.6exp(BT^1.6)
Decay Rate (GHz)
Temperature (K)
(b)
Decay Rate (GHz)
Absorbance (Arb. Unit)
Energy (eV)

Fig. 2

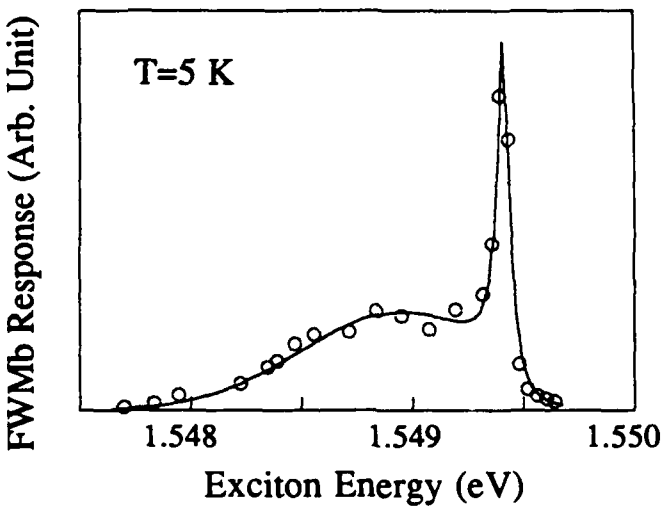

Fig. 3